EFFECT OF TETRAETHOXYSILANE AND TETRAMETHOXYSILANE (TEOS/TMOS) ON MELTING GEL BEHAVIOR

By

KUTAIBA HUSSEIN AL-MARZOKI

A Dissertation submitted to the

School of Graduate Studies

Rutgers, The State University of New Jersey

In partial fulfillment of the requirements

For the degree of

Doctor of Philosophy

Graduate Program in Materials Science and Engineering

Written under the direction of

Prof. Lisa C. Klein

And approved by

_____

_____

_____

_____

_____

New Brunswick, New Jersey

May, 2018

ABSTRACT OF THE DISSERTATION

Effect of Tetraethoxysilane and Tetramethoxysilane (TEOS/TMOS) on Melting Gel Behavior

by KUTAIBA HUSSEIN AL-MARZOKI

Dissertation Director:

Lisa C. Klein

Melting gels are silica-based organic–inorganic hybrid gels. A characteristic of so called melting gels is that the gels, which are rigid at room temperature, are able to soften and re-soften at temperatures around 110°C. However, after consolidation at a temperature higher than 150°C, the gels no longer re-soften. In hybrid gels, which show melting gel behavior, the system contains a di-substituted alkoxysilane and a mono-substituted alkoxysilane. Melting gels have many applications such as corrosion protection for metals, alternatives for low-melting sealing glasses, and hermetic packaging for electrochemical devices.

Melting gels with phenyltriethoxysilane (PhTES) and diphenyldiethoxysilane (DPhDES), as well as phenyltrimethoxysilane (PhTMS) and diphenyldimethoxysilane (DPhDMS), have been studied in the past. It is known that melting gels do not form when

PhTES or PhTMS is mixed with tetraethoxysilane (TEOS) or tetramethoxysilane (TMOS) alone. Nevertheless, it is possible to form melting gels when small amounts of TEOS or TMOS are added to PhTES/DPhDES and PhTMS/DPhDMS gels. This study was carried out to determine the limits of TEOS or TMOS additions, before melting gels lost the ability to soften.

The limit of TEOS or TMOS additions was determined for eight different mixtures. In all cases, the mole ratio of PhTES/DPhDES or PhTMS/DPhDMS was held constant at 1/0.25. The TEOS or TMOS addition was expected to give an increase in the number of bridging oxygens between silicons, -Si-O-Si-, during the hydrolysis and condensation polymerization stage. The miscibility limits were maximum for the gel containing PhTES and DPhDES in ethanol with 50% TEOS in methanol, and minimum for the gel containing PhTMS and DPhDMS in methanol with 5% TEOS in methanol.

An increase in the number of bridging oxygens that result when condensation polymerization is more complete was accompanied by a decrease in the total weight loss measured in thermal gravimetric studies, and to slight decreases in the consolidation temperature. The glass transition temperature recorded using differential scanning calorimetry increased for compositions with increasing TEOS in ethanol or TMOS in methanol. Different solvents, for example, TEOS in methanol, caused transesterification and trends that were not consistent. Helium pycnometer measurements showed that the density of all samples after consolidation increased with increasing the TEOS or TMOS additions. Those with TMOS had higher densities than those with TEOS, due to the higher reactivity and more complete hydrolysis of TMOS. Micro-hardness values for gels increased gradually with increasing TEOS in ethanol or TMOS in methanol. All

compositions produced coatings with hydrophobic surfaces, with methoxy substituted compositions being slightly more hydrophobic than ethoxy-substituted compositions.

FTIR spectra revealed the species present in the consolidated gels. The peaks in the spectra were assigned to hydroxyl groups, phenyl and other organic groups, and Si–O–Si bonds in the organically modified glass network. Si–C direct bonds from the substituted siloxanes were retained in the consolidated hybrid glasses. The general trend was that peaks were shifted to higher wavenumbers in systems with TEOS, while peaks were shifted to lower wavenumbers in systems with TMOS, reflecting the faster gelation in TMOS systems.

Acknowledgments

Firstly, I would like to thank Allah for everything and for allowing me to reach this point in my career and for giving me the strength to succeed.

Secondly, I would like to express my sincere gratitude to my advisor Prof. Lisa C. Klein for the continuous support of my Ph.D. study and related research, for her patience, motivation, and immense knowledge. Her guidance helped me in all the time of research and writing of this dissertation. I could not have imagined having a better advisor and mentor for my Ph.D. study.

My sincere gratitude also goes to Prof. Andrei Jitianu who provided me an opportunity to join his research team, and who gave me access to his laboratory and research facilities. Without his precious support and advice in research methods and life in general, it would not be possible to conduct this research. Also, many thanks go to Dr. Quentin Picard for helping me doing the SEM and Mrs. Gabriela Rodriguez who helped me with my thermal tests in Dr. Andrei Lab.

Besides my advisor, I would like to thank the rest of my thesis committee: Prof. Richard Lehman, Assistant Prof. Ashutosh Goel, and Associate Prof. Laura Fabris, for their insightful comments and encouragement, but also for the hard question which incented me to widen my research from various perspectives.

This work was also supported by NSF – DMR Award #1313544, Materials World Network, SusChEM: Hybrid Sol–Gel Route to Chromate-free Anticorrosive Coating.

Last but not the least, nobody has been more important to me than my family members. I would like to thank my Mom and Dad whose love and guidance are with me in whatever I pursue, you are my life-coach and the ultimate role models. My four troublemaking brothers Ali, Mustafa, Osama, and Zaid for supporting me spiritually throughout my study abroad and my life in general. I would not be able to survive and to be who I am today without your love and supports. Many thanks! I am also grateful to my other family members and friends who have supported me along the way.

Finally, and most importantly, I wish to thank my loving and supportive wife, with gratitude for her never-ending patience during the seemingly interminable working and writing of this dissertation and my three wonderful children, Zakariya, Elias and Joan, who provide unending inspiration. I owe you my whole life, for all the great sacrifices that you made to get my Ph.D. degree done.

Thank you very much, everyone!

Kutaiba Al-Marzoki, New Jersey, 02nd of March 2018

Dedication

To my precious wife *Nawras*

and my two musketeers, *Zakariya, Elías* and little princess *Joan*

Without whom this work would have been completed two years earlier

Table of Contents

LIST OF FIGURES

LIST OF TABLES

LIST OF ABBREVIATIONS

TEOS	Tetraethylorthosilicate
TMOS	Tetramethylorthosilicate
PhTES	Phenyltriethoxysilane
PhTMS	Phenyltrimethoxysilane
DPhDES	Diphenyldiethoxysilane
DPhDMS	Dimethyldiethoxysilane
MTES	Methyltriethoxysilane Phenyltriethoxysilane
DMDES	Dimethyldiethoxysilane
DCCAs	Drying Control Chemical Additives
EAcAc	Ethylacetoacetate
ORMOCERs	Organically Modified Ceramics
ORMOSIL	Organically Modified Silicon
CERAMERS	CERamic polyMERs
POLYCERAM	POLYmeric CERAmics
POSS	Polyhedral Oligomeric Silsesquioxanes
R'	Organic Group
OLED	Organic Light Emitting Diodes
SEM	Scanning Electron Microscopy
SAXS	Small-angle X-ray scattering
DTA	Differential Thermal Analysis
DSC	Differential Scanning Calorimetry
FT-IR	Fourier Transform Infrared Spectroscopy
NMR	Nuclear Magnetic Resonance

EtOH	Ethanol
MeOH	Methanol
OI	Organic/Inorganic
MNPs	Metal Nanoparticles
COPs	Conducting Organic Polymers
ABC	Amphiphilic Block Copolymers

I love fools' experiments. I am always making them.

Charles R. Darwin in Francis Darwins "*The Life of Charles Darwin"*, 1902

Kohn's Second Law: An experiment is reproducible until another laboratory tries to repeat it.

Alexander Kohb in N Sreedharans "*Quotations of Wit and Wisdom*", 2007

You make experiments and I make theories. Do you know the difference? A theory is something nobody believes, except the person who made it. An experiment is something everybody believes, except the person who made it.

Albert Einstein in Gerald Holtons, "*The Advancement of Science, and Its Burdens"*, (1986),

The most exciting phrase to hear in science, the one that heralds new discoveries, is not 'Eureka!' (I found it!) but 'That's funny ...'

Isaac Asimov (1920 - 1992)

Chapter One
Introduction

1.1 Introduction

The field of materials is immense and diverse. Historically, materials utilization began with the emergence of man himself. The ages of civilization are classified according to materials, such as Stone Age, Bronze Age, and Iron Age. Since materials are an essential part of our daily life, the necessity of exploring new materials to make our lives better increases as the civilizations grow.

There is an enormous demand for novel materials to meet the recent technological challenges related to health, sustainability, and environmental protection that cannot be satisfied using the well- established materials, such as metals, ceramics, or plastics. Naturally, the necessity of formulates and developing new functional materials that could improve the quality of life, and that can contribute to advanced technologies is of supreme importance. The ultimate realization of these technological advancements will be based on our ability to synthesize and organize matter into controlled geometries on the nanoscale.

Mixing of different classes of materials can show superior properties compared with their pure counterparts. With the surge occurring in the area of chemistry and physics, material scientists and chemists have managed to manipulate existing resources and design new-engineered materials where one can add or eliminate specific properties by choosing the suitable processing routes. Thus, many new materials came into existence, which were either a replica of natural materials with desired changes or completely new materials.

These new-engineered materials were categorized into two major groups: Composites (engineered combination of at least two different materials) and advanced materials (used in new technology applications) including semiconductors, biomaterials, smart materials, and nanoengineered materials. [1]

In general, a composite is considered to be any multiphase material that exhibits a substantial proportion of the properties of both constituent phases such that a better combination of properties is realized. In addition, the constituent phases must be chemically dissimilar and separated by a distinct interface. Composite materials can occur in nature, such as wood, which consists of strong and flexible cellulose fibers surrounded and held together by a stiffer material called lignin. Also, bone is a composite of the strong yet soft protein collagen and the hard, brittle mineral apatite. Composites also can be artificially made such as fiberglass-reinforced polymers and concrete. Recognition of this novel concept of combining dissimilar materials during manufacture led to the identification of composites as a new class of materials. [2]

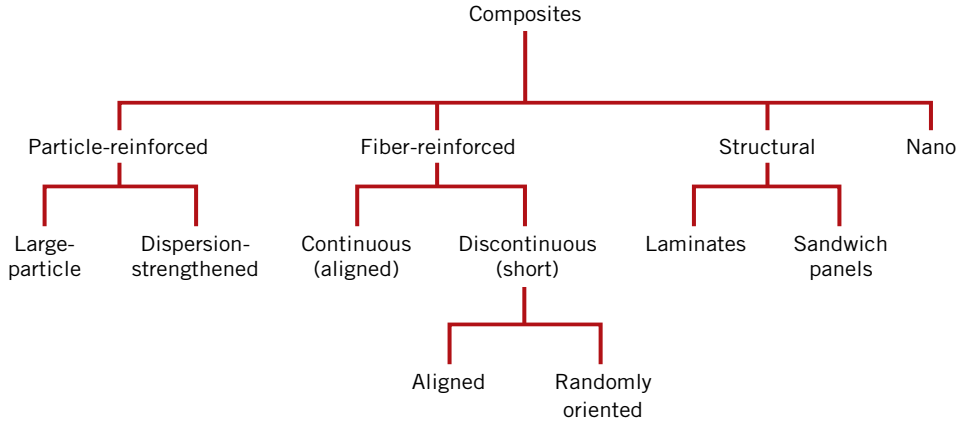

Figure 1.1: A classification scheme for the various composite types. [1]

Composite materials can be simply classified into four main divisions as shown in Figure 1.1, which consists of: particle-reinforced, fiber-reinforced, structural, and nanocomposites. [1]

Macroscopic composites, especially fiber-glass-reinforced epoxy, are well-known composite materials. Despite the fact that they are essential to many industries, such as electronics, aerospace, and automotive, recently macroscopic composites have lost some of their fascination with the emerging of nano-science field. Now the excitement in advanced materials is nanocomposites. A rapidly growing field of materials under this category is Inorganic/Organic Hybrid Materials. Hybrid is the generic term used for an inorganic–organic material and nanocomposites refer to the family of materials where the inorganic and organic components are mixed on the nanometer scale. [3]

The present chapter aims to provide a general overview about hybrid nanocomposites and the different synthetic methods developed for the preparation of organic–inorganic polymer based nanohybrids/nanocomposites with emphasis on sol-gel technique and of their applications in various fields including biomedicine, sensing, energy, catalysis, optoelectronics, environmental remediation, and finally in construction, automotive, and coating technologies.

The objective of this dissertation is to formulate and characterize different types of organic/inorganic hybrid nanocomposites. The precursors used in the manufacturing process are monosubstituted, disubstituted alkoxysilanes and tetralkoxysilane. A suitable application for these hybrids is as coating metals to protect them from corrosion.

1.2 Polymer Hybrid Nanocomposites

An astonishing archaeological discovery was made on 1964 in Mexico known as Bonampak (Maya painted walls). This ancient Mayan mural was built in the 8th century characterized by bright blue and ochre colors that had been miraculously preserved. A special feature of these wall paintings was precisely their bright blue hues. Maya blue was known for its remarkable durability. Despite the harsh environment and biodegradation, Maya blue withstood more than twelve centuries. Also showing unique stability when exposed to acids, alkalis and organic solvents. At the end of the 20th century with the availability of advance analytical techniques, the Mayan blue secret was uncovered. These pigments are the first manmade hybrid organic-inorganic material with molecules of the natural blue dye known as indigo encapsulated within the channels of a clay mineral known as palygorskite. [4]

The pursuit to combine properties of organic and inorganic components in a single composite material starts with the beginning of the industrial era. The real development of hybrid organic-inorganic materials exploded only very recently with the birth of soft inorganic chemistry processes ("Chimie Douce"), where mild processing conditions, particularly the low reaction temperatures, open the opportunity to assemble chemically designed hybrid organic-inorganic materials. Where organic materials are characterized by ease of processing, lightweight, and flexibility, inorganic materials exhibit superior thermal and mechanical behavior as well as unique optical, electrical, catalytic, and magnetic properties, especially when they are in nanoscale dimensions. Recently the field of organic-inorganic materials has become more sophisticated, including structural hybrid materials

based on carbon-silicon networks. Classical macroscopic composite materials include adobe, a mixture of clay and straw that used to make bricks in dry climate regions throughout history, and reinforced concrete that built the infrastructure. When it comes to the microscopic field, and particle sizes are reduced to the nano scale level, components interact at a molecular level, increasing the importance of the interphase and causing a tremendous boost to the physical and chemical properties in composite mixtures. [5]

The hypothesis behind using building blocks having nanosize dimensions is to make it possible to create new polymeric materials exhibiting new or improved physical properties, such as unrivaled flexibility with complementary strengths. [6]

This approach has been used successfully in recent years for producing hybrid polymers, particularly structural hybrid materials, based on mixed silicon-carbon networks prepared by sol-gel methods. In this field, scientists aim to produce structural materials with properties between those of inorganic glasses and organic polymers. The expectations go beyond mechanical strength, thermal and chemical stability. These new materials can exhibit unusual behavior, relative to optical transparency, dielectric and electrical properties, luminescence, ionic conductivity, biological compatibility and biological activity, as well as chemical or biochemical activity. [7]

1.3 Classification of hybrids nanocomposites

Hybrid nanocomposites can be classified according to several criteria. The first and simplest way is according to the properties and the type of application for which they are designed and used, in particular, into the broad groups of structural and functional materials with the emphasis on functionality and on functional hybrid materials. The applications of this kind of materials are enormous. A large number of hybrids are based on electro-active

inorganic compounds and conducting organic polymers (COPs), which are also electro-active. Such materials improve applications like electrocatalysis [8] or energy storage [9] where the electrochemical activity is paramount property.

In a review article Romero [5], proposed a new scheme for classification of functional hybrid composites into three categories according to the nature of host and guest molecule. The first one is organic-inorganic (OI) materials or compounds where the matrix is the organic phase surrounding an inorganic guest. The second one is the inorganic-organic (IO) material where the inorganic is the host and organic phase is the guest (Fig. 1.2). The third category, which falls in between these two major classes, can be called "nanocomposite hybrids", where neither the inorganic nor organic components acts as the host or guest molecules as the predominant matrix, but each part of the hybrid maintains its own structure with increased interfacial interaction due to the nanometric particle size. It is noteworthy that inorganic species, which will form hybrid materials, can be either molecular or extended in nature. In OI hybrids, the organic phase is responsible for structural support while the inorganic molecules in general contribute their chemical activity to become part of a useful solid material. On the other hand, in IO hybrids, it is the inorganic phase fulfilling the structural task, although the inserted organic polymer can also imprint its polymeric nature onto the material. Some of the properties of organic and inorganic materials and their relation to structure are summarized in Table (1.1). [10]

A classification widely used for all sorts of hybrid materials relies on the nature of interaction between organic and inorganic components. The properties of these materials are not just the sum of the individual contributions from each phase. The role of the interfaces is predominant. According to the nature of the interface, these materials are

divided into two distinct classes [10,11]. Class I is organic/inorganic materials mixed with each other and held via weak bonds (hydrogen, van der Waals or sometimes ionic bonds), which are amorphous or ordered. In Class II, the two phases are bonded to each other through primary chemical bonds (covalent or partially-covalent bonds). Some hybrids materials from class II may contain weak bonds likewise in class I hybrids.

Table 1.1: General properties of the organic and inorganic materials. [10]

Property	*Organics (polymers)*	*Inorganics (SiO_2 and TMO)*
Nature of bonds	Covalent [C-C] + (weaker van der Waals or H bonding)	Ionic or iono-covalent [M-O]
Tg	Low (- 100 to 200 ^{O}C)	High (> 200 ^{O}C)
Temperature stability	Low (< 350 ^{O}C except polyimides, 450 ^{O}C)	High (>> 100°C)
Density	0.9-1.2	2-4
Refractive index	1.2-1.5	1.15-2.7
Mechanical properties	Elasticity, plasticity, rubbery-like (depending on T,)	Hardness, strength fragility
Hydrophobicity permeability	Hydrophilic, hydrophobic, permeable to gases	Hydrophilic, low permeability to gases
Electronic properties	Insulating to conducting, redox properties	Insulating to semiconducting (SiO_2, /TMO), redox properties (TMO)
Processability	High molding, casting, machining, thin films from solution, viscosity control	Low for powders needs to be mixed with polymers or dispersed in solutions, high for sol-gel materials (similar to polymers)

Another name for this classification, proposed by Klein and Wojcik, is physical nanocomposites and chemical nanocomposites depending on the nature of the bond. The former one can be subdivided into interpenetrating networks and soluble polymers, while the latter one can be classified into monomer systems, monomer–polymer systems, and copolymers. [3]

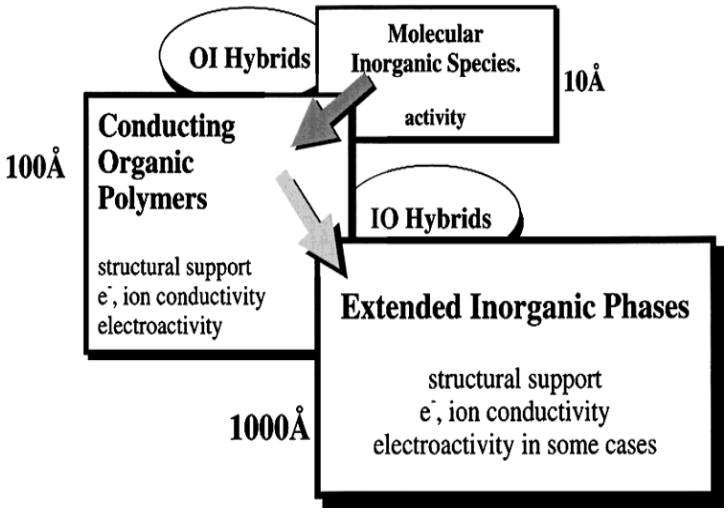

Figure 1.2: Schematic representation of the three major groups of hybrids materials and their combinations to form OI and IO hybrids. [5]

The term organic-inorganic hybrid is most commonly used in a general way due to the indistinct use of both terms organic-inorganic and inorganic-organic hybrids in the literature.

1.4 Synthetic Techniques of Organic–Inorganic Polymer Hybrids

In the following section, the different synthetic approaches used for synthesizing organic–inorganic hybrids are described. These different processing methods were reviewed in different articles and books. [12-14]

1.4.1 Blending

Blending includes two methods. The first one is solution and melts blending which is the simplest way to produce organic-inorganic nanocomposites. In this method, a polymer solution is formed first by dissolving the polymeric material in an appropriate solvent followed by the addition of the inorganic nanoparticulates. Mixing of the two phases occurs though mechanical stirring or ultra-sonication. Upon solvent removal, the intercalated structure remains, resulting in an OI nanocomposite. Despite the fact that this process is simple and cheap it has drawbacks such as when nanoparticles agglomerate in order to reduce their surface energy. Inorganic nanoparticles are usually functionalized with either organic molecules or macromolecules to ensure good solubility and mixing at a molecular level with the polymer matrix as schematically depicted in Figure1.3. [15]

Blending of polymer melts does not require the use of organic solvents to prevent aggregation and inhomogeneity, which makes it an environmentally benign process compared to the solution blending method. The process is carried out under similar processing conditions of the parent polymers and it is compatible with current industrial processes, such as extrusion and injection. The inorganic nanoparticles could be, but are not limited to, nanoclays [16], silica [17], and metal nanoparticles (MNP) [18].

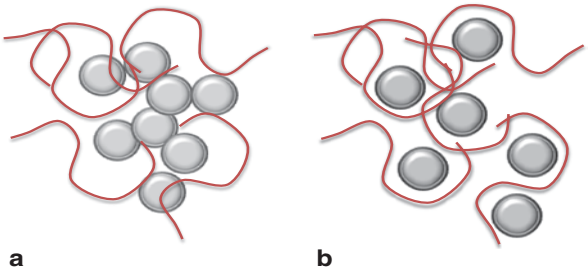

Figure 1.3: Organic–inorganic nanocomposite material **a)** nanoparticle agglomeration takes place and **b)** nanoparticles are well dispersed within the polymer matrix. [14]

The second blending method is powder-blending. This method does not require any solvent or polymer heat treatment. Moreover, it overcomes the problems associated with the high nanoparticle loading which tends to increase the viscosity especially in the melt method making the process difficult. Usually, high-energy ball milling is used in this method ensuring homogeneous dispersion between the constituents on a Nanoscale level.

1.4.2 Emulsion Polymerization

Emulsion polymerization is a common synthetic method for polymer nanocomposites, where polymer is dispersed in an aqueous solution containing a surfactant. With the help of emulsifier and the action of the mechanical stirring, the monomers are dispersed in water emulsion and polymerized by the initiator and precursor. Emulsion polymerization can be divided into two methods. In the inverse emulsion polymerization, a non-polar solvent is used, and the monomers are dispersed in the oil phase with the help of emulsifier. This technique has many advantages such as higher polymerization rate at low temperature, high molecular weight and small molecular weight distribution of the product. Second method is seeded emulsion polymerization that is used often for preparation of inorganic-organic nanocomposites. In this method the inorganic compounds are pretreated with a coupling agent in order to achieve good compatibility between the hydrophilic inorganic particles and the hydrophobic organic monomers. Meanwhile polymer latex particles that are generated in the emulsion system serve as seeds for the monomer agglomeration. [12]

1.4.3 Photopolymerization

Photopolymerization is a common method used to synthesis polymer-based nanocomposites materials. This process uses of an intense ultraviolet (UV) irradiation in the presence of photoinitiators within monomers or oligomers to induce photo-crosslinking polymerization process [19]. In the presence of inorganic nanofillers, polymer–inorganic nanocomposites are generated. Organic–inorganic polymer nanocomposites prepared by photopolymerization processes have many applications particularly in the coating industry for the protection of all types of materials. Advances in this field enabled the fabrication of polymer-based nanocomposite coatings with improved physical, chemical, and biological properties. Other applications include printing inks, adhesives, microelectronics, printing plates, and three-dimensional imaging and microfabrication processes [20]. Some of the polymers used in this process include, acrylates, methacrylates, epoxy and, vinyl ether-based systems combined with metal oxide nanoparticles including silica, titania and alumina, clays, and MNPs [14]. Figure 1.4 shows a simple sketch for metal/polymer nanocomposites by photochemical processes. [20]

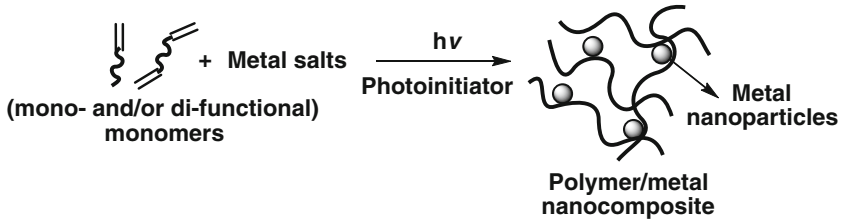

Figure 1.4: General schematic of photopolymerization synthesis of polymer metal nanocomposites. [20]

1.4.4. Intercalation

Generally, this process is easier than the sol-gel synthesis method. Fundamentally intercalation consists of polymerization of dispersed monomers inside inorganic compounds that have layered structures such as silicate clay, phosphate, graphite, metal oxide, disulfide, and tri-phosphorus sulfide complex. Three approaches of intercalation synthesis are possible depending on raw materials, which are intercalation polymerization, solution intercalation and melt intercalation. The monomers intercalate within the inorganic layered structure, then polymerize and expand. As a result, the weak forces that stack the layered structure of the inorganic material together are exfoliated in an appropriate solvent. Consequently, the layers are nanometer in scale and dispersed within the polymer matrix. In solution and melt intercalation, similar process occurs to embed the polymer into the channels of the inorganic compound, resulting in polymer nanocomposites [12,21].

1.4.5. Microwave Irradiation

Recently, microwave irradiation has been used as an effective alternative energy source for polymer synthesis and processing. High-purity nanocomposites products can be obtained using microwave irradiation synthesis method in a few minutes. The principle of this process is based on applying an electromagnetic field on molecules having permanent dipole moments. The molecules couple with the applied field and generate heat. One of the most important advantages of this process is the fast polymer formation, which is crucial to encapsulate inorganic nanoparticles before agglomeration. Microwave-assisted

preparation of polymer nanocomposites has application in different fields like biomedicine, environmental materials, electronic materials, photoconductive materials, fuel cells, magnetic materials, and photonic crystals [12,22].

1.4.6. Electrochemical Synthesis

Electrochemical synthesis is a convenient way to prepare polymer-based nanocomposites films. The film is directly deposited on an electrode surface through the electrochemical polymerization of electroactive monomers, such as aniline, thiophenes, and pyrrole in the presence of inorganic nanoparticles. The process is usually done in an electrochemical workstation [12]. For instance, polythiophene-magnetite composite layers have been prepared through the electropolymerization of 3-thiophene-acetic-acid in the presence of Fe_3O_4 nanoparticles in nitrobenzene and as a consequence modified electrodes with magnetic properties can be prepared for magnetic electrocatalysis. [23]

1.4.7. Surface Grafting

Surface grafting is the process of tethering of polymeric chains to the surface of nanoparticles to construct what are called polymer brushes [24]. Polymer brushes are ultrathin polymer coatings consisting of polymer chains, which are tethered by one chain end to a surface or an interface, generally a solid substrate. Improving the interface interactions between the polymeric and the inorganic species is the main requirement to develop organic-inorganic nanocomposites. For this purpose; two grafting techniques are known. The “grafting to” strategy involves the attachment of presynthesized polymers via either physisorption or chemisorption (covalent bond) to the particle surface, typically by

using reactive chain ends to achieve the coupling process. In the "grafting from" approach, the polymerization is directly initiated from initiator-functionalized surfaces using controlled polymerization techniques such as anionic polymerization, cationic polymerization, ring-opening polymerization, ring-opening metathesis polymerization, and free radical polymerization. The "grafting from" method is favorable in controlling brush thickness, composition, and architecture [25]. Polymer brushes are used in many applications such as new adhesive materials, protein-resistant biosurfaces, chromotographic devices, lubricants, polymer surfactants and polymer compatibilizers. [26]

1.4.8. Self-Assembly

This process is based on electrostatic attractive forces (hydrophobic interactions hydrogen and coordination bonding) developed between oppositely charged organic and inorganic species. Self-assembly is a useful chemical strategy, which is able to form polymer nanocomposites by direct assemble of the various structurally well-defined nanomaterials into the complex architectures with hierarchical structures. The mild conditions allow easy design of chemically hybrid organic–inorganic materials. The possible synthetic methods include *in-situ* self-assembly, template-induced self-assembly, evaporation-induced self-assembly, and layer-by-layer assembly [27]. Figure 1.5 shows a simple sketch for layer-by-layer self-assembly method. [14]

1.4.9. Amphiphilic Block Copolymer-Mediated Synthetic Approaches

Amphiphilic block copolymers (ABC) represent a class of polymers known as soft materials, a new class of functional polymers. They are formed by two or more chemically

homogeneous polymer fragments (blocks) joined together by covalent bonds with different chemical natures, making them amphiphilic.

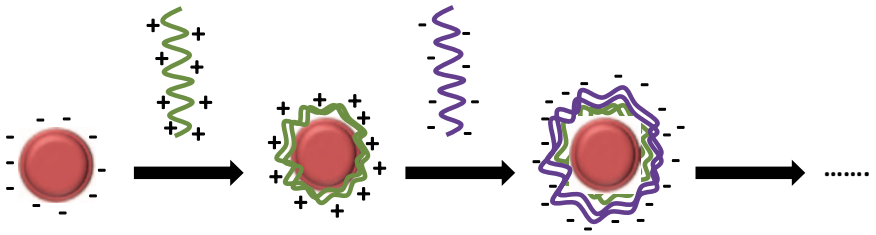

Figure 1.5: The layer-by-layer self-assembly approach used for the synthesis of polymer-based nanocomposites. [14]

ABCs architectures can be prepared in different structure such as di-block, tri-block, multiblock, graft, or star copolymers. Amphiphilic block copolymers are important in technology for different kinds of problems related to interface and particle stabilization. In order to prepare stable organic-inorganic hybrid materials using ABCs approach, the interface between polymer/inorganic has to be sufficiently stabilized. That can be obtained by employing functional blocks that bind to the inorganic material providing sufficient adhesion between the two phases. Block copolymers provide a large variety of microstructures for use in the synthesis of nanocomposites hybrid materials. An overview of these structures is given in Figure 1.6. Amphiphilic copolymers find the way to numerous applications like emulsifiers, dispersants, foamers, thickeners, rinse aids, and compatibilizers. [28]

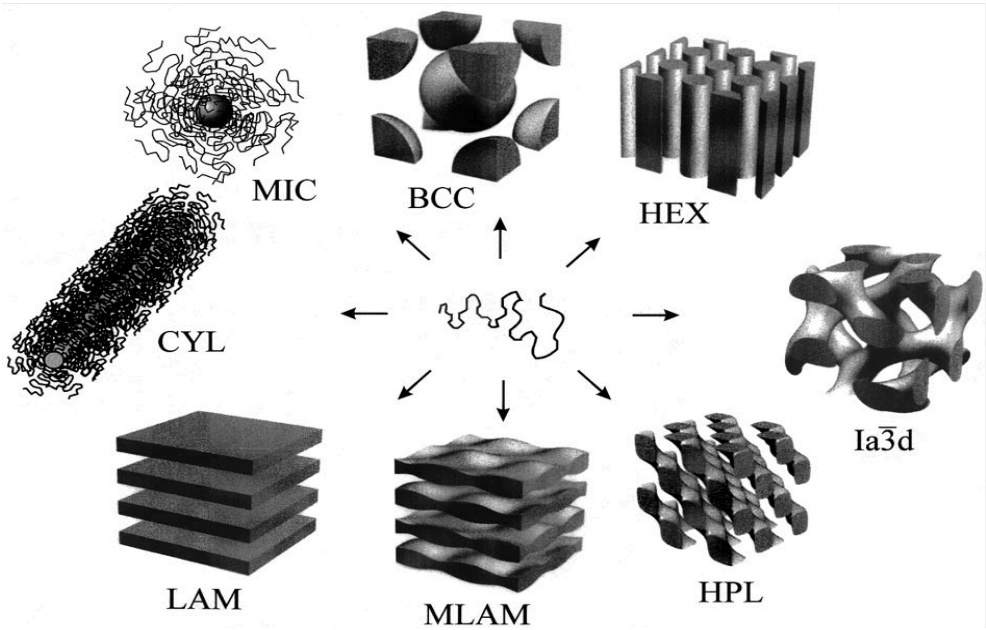

Figure 1.6: Common morphologies created by *ABCs*: body centered cubic (bcc) packed spheres (BCC), hexagonally ordered cylinders (HEX), gyroid (Ia3d), hexagonally perforated layers (HPL), modulated lamellae (MLAM), lamellae (LAM), cylindrical micelles (CYL), and spherical micelles (MIC). [28]

1.4.10. Sol–Gel Synthesis

Organic/inorganic hybrid nanocomposite materials prepared by the sol-gel method have drawn much interest in the field of materials science research. This is related to their diphasic structures, homogeneous, and high-purity products, which are mostly inorganic oxide, can be made at ambient temperatures rather than at the very high temperatures leading to multifunctional materials. In the past few decades the explosion of activity in this area- the increase in the volume and the quality of published work- has made tremendous progress in both the fundamental understanding of the sol-gel process and the development and applications of new organic/inorganic hybrid materials. Sol-gel synthesis

offers a degree of control over composition and structure at the molecular level unachievable with traditional sintering or precipitation methods. A great deal of research has focused on silica-based gels where the physics and chemistry involved in the synthesis were detailed in books that also explain the process to some extend for nonsilicate-based gel [29, 30].

Glasses and ceramics can be synthesized through powderless processing via the sol–gel route. Moreover, the easy control of the rheology of the colloid states (sol) and gels allows the formation of product in a variety of forms like monoliths, fibers and thin films. Films are produced with controlled thickness directly from the solution by techniques like dip-coating, spin-coating and spin-drawing. Powders can result from a sol-gel process with particles of controlled size and shape. [31]

Organic-inorganic composite materials synthesized using the sol-gel route can be divided into five major classes based on their macromolecular structures and phase connectivities: [7]

Type I: Soluble, preformed organic polymers embedded in a xerogel.

Type II: Embedded, preformed organic polymer connected covalently to the inorganic network.

Type III: Mutually interpenetrating organic-inorganic networks.

Type IV: Interpenetrating networks with covalent links between the organic and inorganic phases.

Type V: "Non-shrinking" sol-gel composite materials.

1.4.10.1. Background and Basics of the Sol–Gel Method

As early as the mid-1800s, Ebelman and Thomas Graham had prepared gels of silica through hydrolysis of tetraethylorthosilicate (TEOS), Si(OC_2H_5), under acidic conditions. Therefore sol-gel process is by no means a new method for the preparation of materials. [32,33]. A solution is a single-phase liquid while a sol is defined as a colloidal dispersion of stable solid particles in a liquid. Colloids are in turn described as solid particles with dimensions in the range of 1nm to 1μm (10-10^4 A^o), each containing 10^3 to 10^9 atoms per particle. A gel is a three-dimensional interconnected network that contains a continuous solid skeleton enclosing a continuous liquid phase: the liquid prevents the solid from collapsing; the solid prevents the liquid from escaping. The term "gel" includes a diversity of combinations that can be classified into four categories as discussed by Flory:(1) well-ordered lamellar structures; (2) covalent polymeric networks, completely disordered; (3) polymer networks formed through physical aggregation, predominantly disordered, and (4) particular disordered structures [34]. Presently a more acceptable classification of gel used by ceramists is polymeric and colloidal gels [30]. Thus, the formal definition of sol – gel processing is the growth of colloidal particles and their linking together to form a gel, even though gelation may not occur (particle formation). [35]

Organic/inorganic hybrid materials prepared by the sol-gel process can be generated using different synthetic techniques by incorporating various starting inorganic and organic components with varied molecular structure. The organic component can be

introduced as (i) a precursor, which can be a monomer or an oligomer, (ii) a preformed linear polymer (in molten, solution, or emulsion states), and finally (iii) a preformed polymer network, physically (e.g., semicrystalline linear polymer), or chemically (e.g., thermosets, elastomers) crosslinked. The mineral part can be introduced as (i) a monomer (e.g., a metal alkoxide), (ii) preformed nanoparticles, whiskers, or platelets, and finally (iii) an existed nanoporous structure (e.g., aerogel). [36] Additives of different kinds can be added to the liquid mixture before it gels as a composite. [37]

When using alkoxides, the first step in sol-gel synthesis is the hydroxylation of the precursors, which occurs upon hydrolysis of the hydrolyzable alkoxy groups as follows: [29]

$$\boldsymbol{M - OR + H_2O \Leftrightarrow M - OH + ROH} \qquad \textit{Eq. (1.1)}$$

During hydrolysis, the alkoxide groups (-OR) are replaced via the nucleophilic attack of the oxygen atom of a water molecule and release of alcohol and the formation of a metal hydroxide. Then they undergo polycondensation reactions ***via*** two competing mechanisms:

(a) Oxolation is the formation of an oxygen bridge between two hydroxylated metal species liberating water (oxolation) or between a hydroxide and an alkoxide releasing an alcohol (alcoxolation) leading to M-O-M bonds.

$$\boldsymbol{M - OH + HO - M \Leftrightarrow M - O - M + H_2O} \qquad \textit{Eq. (1.2)}$$

$$\boldsymbol{M - OR + HO - M \Leftrightarrow M - O - M + R - OH} \qquad \textit{Eq. (1.3)}$$

(b) Olation is the formation of a hydroxo bridge, when the coordination number of the metal is higher than the valence state {(N-z) > 0}. [29]

$$\boldsymbol{M - OH + HO - M \Leftrightarrow M(OH)_2M} \qquad \textit{Eq. (1.4)}$$

These reactions can be described as S_N2 nucleophilic substitutions. The chemical reactivity of metal alkoxides toward hydrolysis and condensation depends mainly on the electronegativity of the metal ion. Electronegativity is defined as the power of attraction for the electrons in a covalent bond. The partial charge δ_M, and the ability of the atom to exhibit several coordination numbers N. As a general rule, the electronegativity of metal atoms decreases as their size increases, and the chemical reactivity of the corresponding alkoxides increase as shown in Table (1.2). Therefore, silicon alkoxides are less reactive than transition metals. [38, 39]

Table 1.2: Electronegativity (E_N), partial charge (δ_M), ionic radius (r), maximum coordination number (*N*), and degree of unsaturation (N-z) of some tetravalent metals (z = 4). [39]

Alkoxide	E_N	δ_M	r (A°)	*N*	*N-z*
$Si(OPr^i)_4$	1.74	+0.32	0.40	4	0
$Ti(OPr^i)_4$	1.32	+0.60	0.64	6	2
$Zr\,(OPr^i)_4$	1.29	+0.64	0.87	7	3
$Ce(OPr^i)_4$	1.17	+0.75	1.02	8	4

The resulting morphology and structure of the metal-oxo macromolecular network depends on many parameters. It is very sensitive to slight changes in any of the synthesis conditions. The simultaneous occurrence of hydrolysis and condensation affects the chemical reaction rates, which are dependent on many factors such as reaction temperature, pH, and amount of water, solvent, and precursor used, and the use of complexing agents. In general, increasing the temperature will increase the reaction rate. The pH of the solution

is controlled by adding catalyst (acid or base) to control the rates of these reactions. Under acid-catalyzed conditions, hydrolysis proceeds rapidly, and the initial sol contains many small oligomers and particles. Therefore acid-catalyzed gels are aggregates of very small ultimate particles, which lead to formation of linear polymer chains. The very small sizes of the particles minimize light scattering effects and produce transparent gels that have numerous applications in optics. In contrast under basic catalysis, hydrolysis and particle nucleation steps are rate limiting (condensation is faster), so the sol will contain fewer, larger particles than in the acid-catalyzed case, which tend to result in lower surface area gels with high porosities (Figure 1.7) [40]. Solvent usually is added to prevent separation between liquid phases and solvent plays a major role during hydrolysis and condensation reactions. Typically, longer chain alcohols are used to solvate more complex compositions.

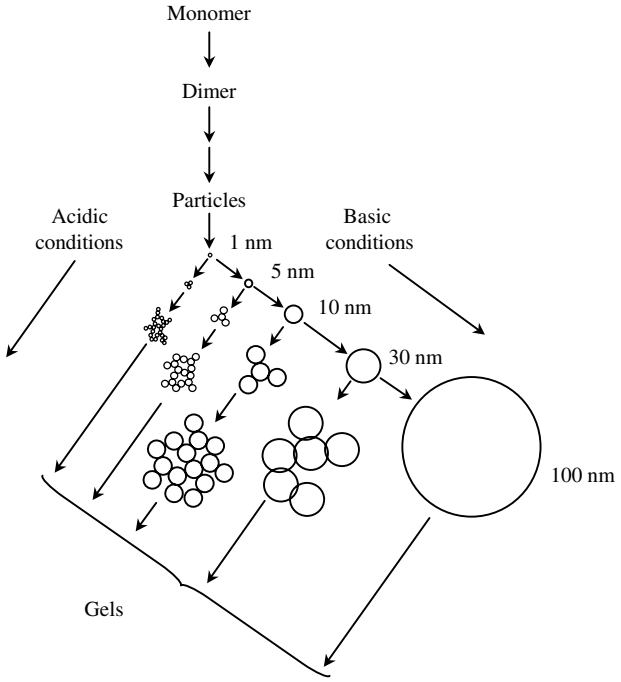

Figure 1.7: The pH dependence of growth and condensation of silica particles during gel formation. [40]

Addition of solvents may promote esterification or depolymerization the reverse of Eq. (1.1 and 1.3). The overall effect of solvent on rate of reaction can be summarized as follow: [41]

- Fastest rates for, non–polar, aprotic solvents (i.e. dioxane),
- Intermediate rates for, polar, aprotic solvents (i.e. DMF, acetonitrile),
- Slowest rates for, polar, protic solvents (i.e. methanol, formamide).

Choice of the precursors and control of their reactivity toward hydrolysis–condensation reactions largely determine the kinetics and the type of gel obtained and the structure of the resulting materials. The higher the molecular weight the slower the reaction rates so that methyl groups have the fastest rates [29,42]. The sol-gel transition occurs when the sol suddenly loses its fluidity and transform from viscous liquid to a solid phase by going through a gel-point. Hence the resulting "wet" gels are called aquagels, hydrogels, or alcogels depending on the predominant liquid exist inside the pores whether it is water or alcohol. At the sol-gel transition the chemical reactions do not stop since the pore liquid still contains condensable particles. The composition, structure, and properties of the gel continue to change with time in a process called aging. Continued polymerization increases the cross linking of the gel network. Syneresis, which is spontaneous shrinkage of the gel by release of solvent, occurs during aging. Coarsening and ripening can occur, with an increase in pore size and reduction in surface area through dissolution and reprecipitation. Finally, segregation, phase separation or crystallization can take place during aging. Generally, the gels need to be aged for a certain period of time before drying. [43-44]

A gel is said to be dry when the physically adsorbed water is completely removed.

This occurs between 100 and 180 ºC. Capillary stresses arise whenever gas–liquid menisci appear at the pore boundaries, during evaporation of the pore liquid. When the pore liquid in the interconnected solid gel network is replaced by air without considerable shrinkage and collapse of the network, an is produced. This can be achieved using a variety of strategies such as synthesis of gels with large pores (>50nm), which would yield low capillary stress. Freeze-drying is accomplished by freezing the liquid and then removing it under vacuum sublimation. The drying process can be controlled by using drying control chemical additives DCCAs, such as formamide NH_2CHO, dimethylformamide DMF, and oxalic acid, that work to modify the pH during the course of the sol–gel reaction and produce larger and more uniform pore size. Supercritical drying, removal of the solvent at a temperature and pressure above the critical point of the liquid, eliminates the liquid–vapor interface and the surface tension effects. Aerogels can have pore volumes as large as 98% and densities as low as 80 kg/m^3. When the pore liquid is removed at ambient pressure by thermal evaporation, substantial shrinkage occurs, resulting in xerogels. Typical surface areas for xerogels are about (500-900) $m^2/g,$ while for aerogels they may exceed 1000 m^2/g. [29,45,46]

Heat treatment (densification) is necessary for the production of dense glasses and ceramics from dry gel. Dried gels still contain a considerable amount of chemisorbed hydroxyls on the surface of the pores and organic residue. The densification temperature depends mainly on the size of the pores, the connectivity of the pores, and surface area. The number of pores and their connectivity will reduce while the density increases as a consequence of heat treatment of a gel at elevated temperatures due to viscous flow sintering and/or atomic diffusion. Usually aerogels are densified at temperature around

1000 ºC whereas xerogels are treated at higher temperature. [30,46]

1.4.10.2. Types of Precursors

Sol-gel processes are a method of forming dispersed inorganic materials in solvents, through the growth of metal-oxo polymers [10]. There are two common types of precursors, metallic salts (chloride, nitrate, and sulfate) and alkoxides. Salts have the formula M_mX_n were M is the metal, X is an anionic group, m and n are stoichiometric coefficients, as in $AlCl_3$. Alkoxides have the general formula $M(OR)_n$ which points out that they are group of a cation M (M=Si, Al, Zr, Ti, Mo, etc.) with n of alkoxy groups (OR); for example, Aluminum ethoxide, $Al(OC_2H_5)_3$, and tetraethylorthosilicate TEOS, $Si(OC_2H_5)_4$ [30]. In metal salts, it is difficult to control their reactivity, but they are used when metal alkoxides are expensive or difficult to obtain. Many metal alkoxides are sensitive to moisture, heat, and light making long-term storage difficult. Besides titanium and zirconium, transition metal alkoxides are not readily available [47]. Metal salts normally dissolved in water and form oxide/hydroxide precipitates upon pH changes. Acid dissociation of hydrated metal ions increases, when the metal cation is more electropositive:

$$[\boldsymbol{M \ldots OH_2}]^{z+} \rightleftharpoons [\boldsymbol{M-OH}]^{(z-1)+} + \boldsymbol{H^+} \rightleftharpoons [\boldsymbol{M=O}]^{(Z-2)+} + \boldsymbol{2H^+} \qquad \textit{Eq. (1.5)}$$

The reaction above (Eq.1.5) proceeds to the right as long as the overall partial charge on OH is positive in the general species $[MO_NH_{2N-p}]^{(z-p)+}$. By applying the partial charge model, we can determine the equilibrium species formed in aqueous solution of metal salts. Another important factor is the ability of the metal to change their coordination number depending on the size and charge. Small size, high charge cations promote strong

electrostatic interaction with water [48,38]. During hydrolysis and condensation reaction of metal salts different ligands can be formed in solution (aquo, hydroxo, and oxo), which depends mainly on the valence of the metal and the pH as shown schematically in Figure 1.8. [30]

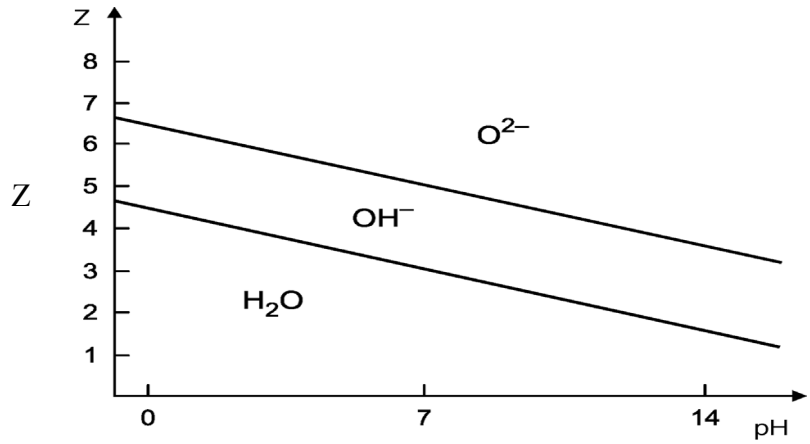

Figure 1.8: Charge (*Z*) versus pH diagram indicating the domains of aquo, hydroxo, and oxo species. [30]

For example, when aluminum salts are dissolved in water, the hydrated cation $[Al(H_2O)_6]^{3+}$ exists only below pH 3. As the pH is increased, the water ligands are deprotonated, and the ions $[Al(OH)_x(H_2O)_{6-x}]^{(3-x)+}$ are formed. Polymerization of metal salts complex usually occur if at least one hydroxo (OH) ligands is bonded to the metal cation, by adding catalyst to the solution. Condensation reaction proceeds to form one of two types of bridges between the two metal atoms as mentioned earlier in eq. (1.2 and 1.4). As for metal alkoxide the degree of unsaturation (N-z) beside electronegativity of the cation has been suggested as the main driving force for the reactivity of non-silicate metal alkoxides towards nucleophilic attack as show in table (1.2). Since silicon has a high electronegativity and a low degree of unsaturation, sol-gel reactions involving silicon

alkoxides are slow. Gelation occurs within several days after water has been added [49]. Thus, two important differences between silicon (as a semimetal) and typical main group or transition metals alkoxide are realized:

1. Metals are more electropositive (Lewis acidic) than silicon and therefore more susceptible to a nucleophilic attack.

2. The preferred coordination number of silicon is equal to its valence (+IV). For metals, especially transition metals, their oxidation state Z is often smaller than their usual coordination state N in an oxide network. The increase of the coordination number beyond the valence is reached by interaction with any nucleophilic (Lewis basic) entity in the system. This currently occurs via solvation or oligomerization (association via OR bridges).

Most metal alkoxides form precipitates spontaneously upon addition of water because their reactivity is so high. While the reaction of silicon alkoxide need a catalyst to boost the reaction. Therefore, the reaction rates of metal alkoxides must be modified to obtain gels instead of precipitates. In general, the same parameters discussed in previous section influence the rates of the hydrolysis and condensation reactions of metal alkoxides. A catalyst is not a necessity due to the higher propensity of metal atoms to interact with nucleophilic agents. An additional factor is the degree of oligomerization of the alkoxide precursors. The degree of association via OR bridges depend on the following: [39,49,50]

- Bulkiness of R groups: because of steric hindrance the larger the group R the smaller the units. For example, $\mathrm{Ti\ (OEt)_4}$ in ethanol has a trimeric structure, while

$Ti\ (OPr^{i})_4$ is monomeric in isopropanol solution.

- Size of the metal: the tendency to oligomerize increases with the size of the metal. For example, the average degree of oligomerization of $M(OEt)_4$ is 2.4 for M = Ti, 3.6 for Zr and Hf, 4.0 for Sn, and 6.0 for Th.

- Type of the solvent: the kinetics of the reaction and as a result the structure of oxide particles formed can be controlled via an appropriate choice of solvents. Oligomeric $[Zr(OPr^n)_4]_n$ species are formed in non-polar hydrophobic solvents such as cyclohexane, while solvates are formed in n-propanol. Precipitation occurs when $Zr(OPr^n)_4$ is dissolved in n-propanol while monolithic gels can be synthesized in cyclohexane [51].

One of the main drawbacks of metal alkoxides is their high reactivity that has to be moderated to control the reactions rate and to avoid fast precipitation. This can be accomplished by the addition of chemical additives (hydroxylated nucleophilic ligands) such as inorganic acids, carboxylic acids, polyols, β-diketones and allied derivatives. In most cases complexation by XOH species can be described as a S_N reaction as follows:

$$\boldsymbol{M(OR)_z + xXOH \rightarrow [\,M(OR)_{z-x}(OX)_x] + xROH} \qquad \textit{Eq. (1.6)}$$

For example, Ethylacetoacetate (EAcAc) complexes with metal alkoxides by forming metal-AcAc bonds, which are much less susceptible to hydrolysis than metal-OR bonds. This inhibition is likely related to steric factors and the strength of the metal-AcAc bond (i.e. the strength of the ligand). An important point that must be considered when using

complexing ligands is that they remain in the resulting material and hence may affect final properties [52]. Using of $[\mathrm{M(OR)_{z-x}(OX)_x}]$ compounds is very similar to that of organically modified silane ($R'Si(OR)_3$), but there is one important chemical difference. The $[\mathrm{M(OR)_{z-x}(OX)_x}]$ derivatives are coordination compounds, which means that they are prone to coordination/decoordination equilibria with other atoms while R' group stay at the silicon atom. [50]

Other precursors include organometallics, which differ from the metal alkoxide because they have a direct bond between metal and carbon atom (M-C). The simplest types of organometallics are those in which the organic part consists of an alkyl group with general formula MR_n. The most interesting and useful type of organometallics is the organoalkoxysilanes that containing organofunctional silicates based on $\mathrm{R_nSi(OH)_{(4-n)}}$, where n= 1, 2, or 3 with the designations of (monoalkyl), (dialkyl), and (trialkyl) substituted centers that behave differently from the other organometallics. [29,10] Organically modified silanes (ormosils) are a class of sol–gel precursors that are hybrid systems consisting of alkoxysilane ligands and at least one not an alkoxy group. Ormosils were developed in the eighties by Schmidt and co-workers at the Fraunhofer Institute, Wilkes and co-workers, and Philipp [53-55]. These hybrids materials belong to class II because they have organic groups directly bonded into the inorganic network. Hybrids made by this technique involving low molecular weight organics also are usually called ORMOCERs (organically modified ceramics), and CERAMERS (CERamic polyMERs) or POLYCERAM (POLYmeric CERAmics). These hybrids possess peculiar properties that are not available in others [56]. Examples of organically modifying and network

forming groups are shown in Table 1.3 and 1.4 [57]. Regarding precursors, such as transition metals, when M is more electropositive, the C–M bond is easily cleaved by hydrolysis. Therefore, the links generally used to build Class II hybrids are formed by strong complexing organic ligands, such as β-diketones, β-ketoesters, carboxylic acids, phosphates or phosphonates as explained earlier or by the formation of stable $\mathrm{M-O-Si-R}$. bonds. [58]

New precursors are being developed for the synthesis of silica-based hybrid materials. Polyhedral oligomeric silsesquioxanes (POSS) and polysilsesquioxanes bridges that form structurally well-defined cages represented by the generic formula $(RSiO_{1.5})_n$ (n=6, 8, 10, etc.). These materials are basically organic and inorganic groups that integrate at molecular length scales resulting in the formation of $\equiv \mathrm{Si-O-Si} \equiv$ bonds by sol gel techniques. [56]

The starting reagents of POSS are $\mathrm{R'-Si(X)_3}$, organotrialkoxy (X=OR), or trichloro (X=Cl) silanes or an acetoxy group which are able to polymerize and form silanol. On the other hand, the polysilsesquioxanes bridge precursors are also organotrialkoxy or (-chlore) silane containing two or more trialkoxysilyl groups separated by $\mathrm{R'}$ variable bridging organic groups $[\mathrm{(OR)_3-Si-R'-Si-(OR)_3}]$. Because Si-C bonds are hydrolytically stable the organic groups remain as an integral component of the final product. These precursors are usually processed together with unsubstituted alkoxide because of the difficulties in obtaining three-dimensional gel networks from organically substituted trialkoxysilane alone.

There are a vast selection of organic group R’ that can be chosen ranging from rigid

aromatic, alkyne, alkene, alkane, variety of functionalized groups such as amines, ethers, sulfides, phosphines, amides, ureas, carbamates, and carbonates or organometallics in which the metal is part of the bridge or pendant to the bridge. The structures of silsesquioxanes have been reported as random structure, ladder structure, cage structures, and partial cage structure, as illustrated in Figure 1.9. This type of materials has a plethora of applications since the control over physical and chemical properties of products can achieved. Applications include optical and electronic devices, catalysts, separations media, coatings, carcinostatic drugs, as well as ceramics precursors [59,60].

Table 1.3: Examples of alkoxysilanes for inorganic network modifying from Ref. [57] with permission..

Structure	Name	Comment
$H_2N—(CH_2)_3—Si(OMe)_3$	Aminopropyltrimethoxysilane /1/	Hydrophilic modification
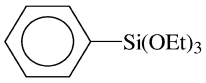	Phenyltriethoxysilane /2/	Hydrophobic modification
$CF_3—(CF_2)_5—(CH_2)_2—Si(OEt)_3$	Tridekafluoro-1,1,2,2-tetrahydrooctyl-triethoxysilane /3/	Hydrophobic and oleophobic modification
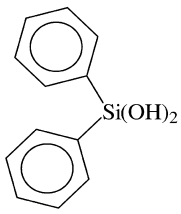	Diphenylsilandiol /4/	Bifunctional silane, linear Si-O-Si-chains, elasticity/hydrophobic
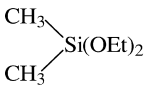	Dimethyldiethoxysilane /5/	Bifunctional silane, linear Si-O-Si chains

Table 1.4: Examples of alkoxysilanes for organic crosslinking/network forming from Ref. [57] with permission.

Structure	Name	Comment
H_2C—CH(O)—O—$(CH_2)_3$–$Si(OMe)_3$	Glycidyloxypropyl-trimethoxysilane /6/	Monofunctional organic crosslinking (polyether-type links)
O—$(CH_2)_3$—$Si(OMe)_3$	Methacryloxypropyl-trimethoxysilane /7/	Monofunctional organic crosslinking
HS—$(CH_2)_3$—$Si(OMe)_3$ H_2C=C(H)—$Si(OMe)_3$	Mercaptopropyl-trimethoxysilane /8/ Vinyltrimethoxysilane /9/	Thiol-ene-reactions - > thioether linkage
H_2C=C(CH_3)—CO_2—CH_2 CH—O_2C—NH—$(CH_2)_3$—$Si(OEt)_3$ H_2C=C(CH_3)—CO_2—CH_2	Dimethacrylate based silane /10/	Bifunctional organic crosslinking
CO_2—CH_2 CH—O_2C—NH—$(CH_2)_3$—$Si(OEt)_3$ CH_3 CO_2—CH_2 CH_3	Dinorbonene based silane /11/	Reduced shrinkage during curing
O —CH_2—O—$(CH_2)_3$—$Si(OMe)_3$ O O	Spiroorthoester based silane /12/	Reduced shrinkage during curing
	Carboxymodified dimethacrylate based silane /13/	Bifunctional organic crosslinking with carboxy modification for ionomer reactions
H_2C=C(CH_3)—CO_2—CH_2 CH—O_2C—C_2H_3—$(CH_2)_3$—$Si(OEt)_3$ H_2C=C(CH_3)—CO_2—CH_2 O=C—OH		

Beside these there are also metal acetates and metal acetylacetonates, in which the process is based on thermal decomposition rather than sol-gel, frequently referred to as non-aqueous sol-gel chemistry. [61]

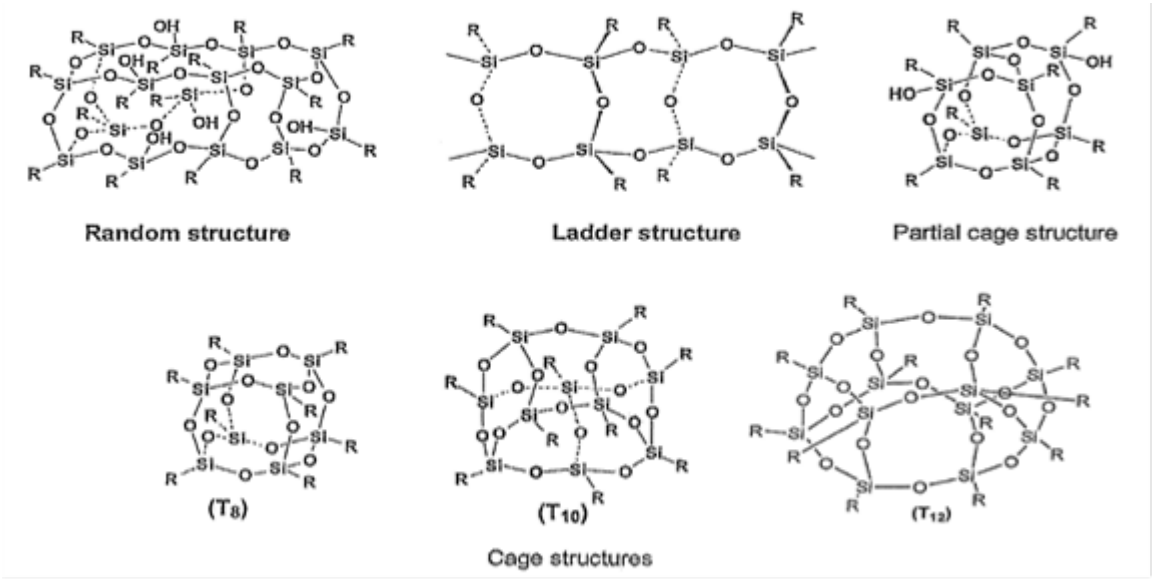

Figure 1.9 Structures of silsesquioxanes.

1.4.10.3 Melting Gel

Melting gels are a type of ORMOSIL that has the ability to soften upon heating to a temperature around (~110) °C and solidify again when cooled down to the room temperature. Once melting gels are heated to a temperature called the consolidation temperature, they do not soften again. The consolidation temperature varies with the composition. At the consolidation temperature, polymerization reactions (cross linking) between the precursors are completed. At the consolidation temperature, the melting gel is transformed into a hybrid glass. The process of softening and becoming rigid can be repeated many times, and the melting gels can be stored at room temperature for several years without losing their ability to soften. The low viscosity of melting gels at their

softening temperature makes it easy to pour and form shapes. [62]

Melting gels are prepared by mixing different organoalkoxysilanes (mostly mono-substituted organo-modified alkoxide $R'Si(OR)_3$ and di-substituted organo-modified alkoxide $R'_2Si(OR)_2$) precursors, in which the organic group R' is covalently bonded to the silicon atom via a Si-C bond. The sol-gel processing with mixtures of different alkoxides and organoalkoxides requires slow additions of one to another to maintain the miscibility. Some desirable properties of melting gels include hydrophobicity, corrosion protection, low dielectric constants, good scratch resistance, and hermeticity for food packaging, electronic and microelectronic devices. For example, mixtures of mono-substituted alkoxysilanes and di-substituted alkoxysilanes have been studied extensively to identify appropriate melting gel compositions. The mixtures and the resulting melting gels have been evaluated for their softening temperatures and consolidation temperatures, and their physical properties have been measured as well. [62-65]

1.4.10.4 Phase Separation: Phenomena and Kinetics

The degree of phase separation has to be controlled in order to obtain uniformly mixed hybrid materials. To control this, there should be a strong interface between organic and inorganic domains. The obtained gel morphologies depend on the competition between phase separation and gelation. If the gelation is faster than phase separation, then homogenous hybrids are obtained. If phase separation is faster, heterogeneous hybrids or sedimentation result. In general phase separation behavior in sol-gel systems depends on the nature of the precursors, the volume fraction, size, shape, and orientation of the organic

group, solvent composition, processing conditions and the state of adhesion between the two phases. This problem has been solved by adding a coupling agent, functionalizing the oligomer or polymer chain ends, selecting polymers with appropriate backbone structures, or by using copolymers possessing functional groups that can interact with the growing inorganic oxide network. [3]

To understand how the reactions influence the phase separation, arising from the formation of silanol (Si-OH) groups via hydrolysis and siloxane (Si-O-Si) bridges via the condensation reaction the ternary system TEOS- Ethanol- and water has been studied [66]. The polymerization process is chemically equivalent to the continuous physical cooling with respect to the chemical interaction (mutual solubility) and material transport (mobility of the solutes). That is, the polymerizing system resulting in a sol–gel transition is a likened to a continuously cooled system resulting in a glass transition.

A typical hydrolysis–polycondensation of alkoxysilanes under acidic conditions, gives a distribution of the molecular weight of the polymerizing oligomers. The molecular weight of the polymerizing species in a solution increases with reaction time by essentially irreversible polycondensation reactions among the monomers/oligomers. The thermodynamics of solutions requires that mutual solubility among the polymerizing species becomes lower as the average molecular weight increases. This is mainly due to the loss of entropy of mixing among the constituents.

The decrease in mutual solubility caused by polymerization increases the free energy of mixing. Making a single solution less stable as the $T\Delta S$ term value decreases. Changes in the polarity of oligomers with the generation and/or consumption of silanol

groups contribute to increasing the ΔH term, which also destabilizes the system. When the sign of the free energy of mixing of the system becomes positive, a thermodynamic driving force for phase separation is generated [67]. This has been demonstrated in various systems containing poly acrylic acid [68] and formamide [69].

1.5 Applications of OIH composites

The remarkable properties of organic–inorganic hybrid materials generated through a sol-gel process lead to innovative industrial applications. No doubt these new hybrid materials have applications in optics, electronics, energy, environment, membranes and separation devices, functional smart coatings, fuel and solar cells, catalysts, and sensors [10]. The interest in hybrid materials stems mainly from the fact that these materials have similar properties to inorganic glasses or ceramics but can be functionalized and processed like organic carbon-based polymers and without employing an expensive processing technology, such as vacuum methods. Transforming conventional gels into glasses, ceramics and inorganic–inorganic microcomposites that are nonporous requires temperatures ~1000-1400ºC. In comparison, heat treatment of organic–inorganic hybrids to form nonporous materials requires temperatures no higher than 200°C. [70]

Many books [50,70,71] and articles [72-74], are filled with current and potential applications for the sol gel process. One of the most interesting fields of applications is coatings based on their transparency, their good adhesion to various substrates, and chemical stability. Low temperature coating applications are important, where the coatings are able to provide corrosion- and abrasion-resistance [75]. Many advanced devices are entirely dependent on thin film coating, e.g. flat panel TV screens and solar cells, vision

lenses, smart phones, and other applications including: [72]

1- Protective and decorative coatings.
2- Barrier systems.
3- Dental applications.
4- Microelectronics.
5- Micro-optics.
6- Batteries.
7- Photovoltaic cell application.
8- Proton-exchange membrane fuel cell (PEMFC) applications.
9- Other applications such as adhesives, cosmetics, water-repellents and additives for paper release coatings, cable insulation.

Non-oxide ceramics such as silicon carbide (SiC), silicon nitride (Si_3N_4), and boron carbide (B_4C), processed through sol gel routes are also in demand because of their mechanical, electrical or even their optical properties, for space, defense, and aviation applications. [76]

1.6 Advantages and limitations of sol gel process

When interest in the sol-gel process was relatively new, Mackenzie pointed out potential advantages and disadvantages of sol-gel route early by comparing glasses produced via sol-gel route and conventional melting technique, Table 1.5 [77]. It was pointed out that sol-gel chemistry offered advantages for making multicomponent materials, or even completely new mixed organic-inorganic materials. Sol-gel materials

could be processed to form fibers, monolith, and coatings with chemical homogeneity at the molecular scale [49]. The liquid precursors could be purified to very high degree (e.g. by distillation or sublimation). The whole process aside from densification can be carried out at relatively low temperature (<200ºC), which allows the entrapment of organic groups such as biological species within an inorganic network via weak or strong bond without losing their functions. It is possible to incorporate ceramic oxides, metal ions, inorganic compounds, metallic particles, quantum dots, organic dyes, and biomolecules such as enzymes [50]. Since liquid precursors are used it is possible to form complex shapes such as SiC fibers from polycarbosilane [78], or thin films for optical component. [48]

The sol-gel process has some drawbacks that relate to the precursors, which are often expensive and sensitive to the light, and moisture, which limits their long-time storage. The process is time consuming and sensitive to slight changes in any of the process conditions. The large shrinkage of some of the products after drying and densification limit large scale production, when they are prone to cracking, so special care must be taken during aging drying and densification. Unwanted residues or contamination from reaction by-products such as carbon can be hard to get rid of, which may require post-treatments. Finally, some of the precursors present health hazards. These drawbacks have to be balanced with the need to use the sol-gel process when a product is not attainable by other methods. The challenge is to build hierarchically structured porous or nonporous, inorganic or hybrid materials under environment-friendly conditions by the sol-gel process.

Table 1.5: Some potential advantages of the sol-gel method over conventional glass preparation.

1	Better homogeneity - from raw materials	
2	Better purity - from raw materials	
3	Lower temperature of preparation:	
	a.	Save energy
	b.	Minimize evaporative losses
	c.	Minimize air pollution
	d.	No reactions with container, thus purity
	e.	By-pass phase separation
	f.	By-pass crystallization
4	New non-crystalline solids outside the range of normal glass formation	
5	New crystalline phases from new non-crystalline solids	
6	Better glass products from special properties of gel	
7	Special products such as films	

Chapter 2

Literature Review

2.1 History of sol-gel technology

Sol-gel technology is a nanotechnology since all gel products contain nanoparticles or are nanocomposites. According to Sakka [29] who is one of the pioneers, sol-gel processing plays a major role in the development of modern nanotechnology for the preparation of new materials, and it is now well known for the design of materials with mechanical, magnetic electrical and optical properties that are different from those on the microscale [79]. To sketch the history of this technology, first we have to understand what sol-gel encompasses. Despite the existence of an excellent text and review articles on sol-gel processing [29,30,50,70], a precise definition is still elusive.

There are several definitions for sol-gel processes. Dislich [80] considers that the sol-gel process involves only multicomponent oxides that are homogeneous at the nanoscale level. This does not include the colloidal coprecipitates of hydroxides and oxyhydrates, since they become homogeneous only by reaction at high temperature. Actually, here the term "sol-gel" is confined to the gels synthesized from alkoxides. For comparison, Segal [81] defines the "sol-gel" process as the production of oxide ceramics, either from metal alkoxide intermediates or from colloidal dispersion of hydrous oxides. The sol-gel process, however, no longer includes solely oxides but also some other components such as nitrides and sulfides that have been used recently in the synthesis of hybrid organic-inorganic materials [30]. Brinker and Scherer have defined sol-gel as the

preparation of ceramic materials by preparation of a sol, gelation of the sol, and removal of the solvent [29].

In 1845 Ebelmen [32] was the first to report the formation of a transparent material from slow hydrolysis of an ester of silicic acid (metal alkoxide). This product gelled on prolonged exposure to the atmosphere with normal humidity. Ebelmen hoped that his product could be used one day in the construction of optical instruments. On the other hand, Wohler described the preparation and properties of titania gels in 1850 while Cossa successfully synthesized the first alumina gels in 1870 [82, 83]. Since then, all kinds of inorganic gels have been synthesized using various techniques such as the supercritical drying that was invented by Kistler [84]. This method led to the production of the first aerogels by replacement of the water in a silica gel with alcohol followed by removal of the alcohol above the critical temperature [84].

The major developments for sol-gel processing in the 19th century even known as the "Golden Age of Colloids" [85] was the intensive study of physical and chemical properties of colloids by well-known scientists, including Becquerel, Graham and Faraday whose gold sols were so stable that they are still in existence at the Royal Institution in London. However, these developments were of interest only for chemists and had little impact in the development of sol-gel science field for the next 50 years. In 1919, Patrick of the Silica Gel Corporation began processing silica gel catalysts and absorbent materials by sol gel methods [86]. He showed that partially dried gel could be impregnated with metal salts to make supported catalysts [87]. By 1930 he had filed many patents in the sol gel field pertaining to supported catalysts in anticipation of the establishment of sol-gel technology [88]. Geffcken and Berger of the Schott Company succeeded in the 1930's to

prepare a thin oxide coating on a commercial glass surface using several metal-containing precursors and dip coating. These coating were found to densify at low temperature and could be processed to be antireflective or scratch resistant. By the early 1940's, a variety of industrial applications based on sol-gel science and technology emerged. In 1953 this novel treatment was employed in rear view mirrors for automobiles [89, 90]. Of all the areas, the most active ones were coatings and films [91].

D. Roy and R. Roy proposed a method for preparation of more homogeneous melts and glasses using a sol-gel process. This approach was used in phase equilibrium studies [92, 93]. In the early 1960's, a sol-gel approach was used in the nuclear fuel industry for dust-free preparation of thoria and urania microspheres. However, these results were classified for a long time [94]. In the early 1950's Schroeder followed up the pioneering work by Geffcken. Schroeder deposited transparent coatings on glass surfaces in order to change the refractive index using titanium butoxide [95]. Dislich [96] broadened the attention given to sol-gel processing. He made the scientific community aware that multicomponent oxide glasses, glass ceramics, and crystalline ceramics, which can be produced by traditional methods, can also be produced by hydrolysis and condensation of alkoxide complexes using the sol-gel process.

The ceramic industry began to show interest in sol-gel processing in the late 1960's and early 70's. Preparation of multicomponent glasses, ceramic fibers and monoliths using sol-gel routes and employing alkoxide and organometallic precursors was demonstrated [29]. One of the first applications of the sol-gel technology was the production of glass fibers by low temperature sol-gel synthesis. Amorphous fibers were drawn from viscous sols, followed by thermal treatment at temperatures substantially lower than the normal

melting temperature of SiO_2. These investigations lay out the basis for obtaining many types of optical fibers. [97]

A turning point was reached with the emergence of amorphous materials containing organic and inorganic components in their structure (organically modified silicates) and the development of organic-inorganic nanocomposites. It can be said that the pioneering studies of Schmidt [98,53,55] on the preparation of hybrid structures mark the start of an important era in the development of sol-gel science and technology. Schmidt successfully prepared what it is well known nowadays as ORMOSILs and ORMOCERs, new types of noncrystalline materials with strong chemical bonds between organic and inorganic components. At the same time, Avnir et al. [99] investigated another type of hybrid materials for incorporating organic dyes in oxide gels. The chemical bonds between the organic molecules and the inorganic matrix are not significant, making these structures nanocomposites. Many promising applications emerged upon the preparation of these hybrids related to the production of solar collectors, elements for nonlinear optics, sensors, biological markers, materials for fluorescence diagnostics and photodynamic therapy in medicine.

During the 90's many applications were based on the modern version of the method of Pechini [100]. A nanosized powder can be attained using this method, in which the particles are distributed within very narrow limits (monodispersity) and the reactivity of the powder is enhanced relative to the conventionally prepared powder. The progress in this area is summarized in a book of Ganguli [101]. Ceramic powders obtained by sol gel technology are characterized by lower sintering temperatures, improved stability with respect to grain growth (recrystallization) and, finally, formation of dense ceramics.

The possibilities of sol-gel processes for preparation of hybrid and nanostructured materials were reviewed in several excellent articles [11, 102-104]. A review by Sanchez [103] explained the possibilities of combining the sol gel process with templated growth of inorganic or hybrid networks, allowing design of nanostructured and/or microtextured inorganic and hybrid materials shaped as thick or thin films, microparticles and fibers.

The research field of the sol-gel reaction is increasing dramatically. The main interest for this process is to synthesize all kinds of new materials possessing controllable shape, unique microstructure, superior properties, and special application, through combining with other technologies, such as surface modification, hybridization, templating induction, self-assembly, and phase separation. [105]

2.2 Melting Gels

Generally, organic–inorganic materials are classified in two broad categories: materials where the organic and inorganic components are embedded together via weak bonds (Class I), and materials where there are strong covalent bonds between the inorganic and organic components (Class II) [11]. Ormosils belong to Class II hybrids, which are formed from $R'Si(OR)_3$-type organo-alkoxysilanes, where radical R has a network modifying effect and is used to introduce new functionalities into the inorganic network. As previously mentioned in section 1.4.10.3 melting gels are a class of ormosil that is rigid at room temperature, flows or softens at temperature $T_1 \sim 100°C$ and consolidates at temperature T_2 where ($T_2 > T_1$). The consolidation treatment increases the degree of cross-linking between polymer chains in the gel to a point where the network is permanently

rigid [63,106,107]. Generally, T_2 depends on the type of precursors and their molar ratio in the mixture.

Two common organo-alkoxysilanes, which act as network modifiers, are methyltriethoxysilane (MTES) [108] and phenyltriethoxysilane (PhTES) [109]. Hydrolysis and condensation of trialkoxysilanes alone results in the formation of silsesquioxanes $RSiO_{3/2}$ in which the organic groups R are covalently bonded to the polysiloxane network [60]. Bifunctional silanes of formula $R'R''Si\ (OR)_2$ can also be used to prepare Ormosils. Upon polymerization, these organoalkoxysilanes form cyclic species or linear chains and are therefore not able to crosslink and form networks themselves. Therefore, these materials are usually inorganically diluted by co-hydrolysis with tetrafunctional alkoxysilane $\mathrm{Si}\ (\mathrm{OR}')_4$ in any ratio to incorporate desirable functionality into the hybrid network. For example, hydrophobicity can be achieved by introducing a methyl, phenyl or fluoroalkyl chain as R [110,111].

There are also ormosils where radical R forms a bridge between two Si atoms. A good example of this is arylene or alkylene-bridged polysilsesquioxanes [59,112]. The functionality of these precursors decreases with the increasing number of the organic groups bonded directly to the silicon atom [62]. Consequently, the degree of cross-linking of the inorganic network decreases with the increasing in the number of organic groups. It has been shown that in some cases of ormosils containing hydrolytically stable organic groups, that these groups exhibit modifying effects on the inorganic network. These so-called ‘‘melting gels’’ were developed primarily to replace low melting temperature sealing glasses that melt around 600 °C. This temperature is too high for most electronic packaging, especially newer devices with organic light emitting diodes (OLED). [65]

The first report of softening gels is 1998, when Katagiri et al. [113] prepared continuous, transparent thick films on indium tin oxide (ITO) coated glass substrates by using electrophoretic sol–gel deposition of phenylsilsesquioxane ($PhSiO_{3/2}$) particles. The morphology of the thick films changed after heat treatment, from aggregates of particles with numerous open spaces among the particles to a monolith with no open spaces, accompanied by an increase in transparency and a decrease in the thickness of the thick films. Matsuda et al. [114] reported the softening behavior of melting gels, prepared with poly(benzylsilsesquioxane) particles. Gels obtained from poly(phenylsilsesquioxane) exhibited an irreversible glass transition temperature after repeated heating runs [115]. This method was applicable to the fabrication of microoptical devices. The development of the siloxane network during heat treatment was more significant in ($PhSiO_{3/2}$) than in ($BnSiO_{3/2}$).

Masai et al. [116] obtained organically modified polysilsesquioxanes with softening or melting behavior. They used hydrochloric acid first to hydrolyze the mixture, followed by ammonia for condensation. This study investigated the melting behavior of ($PhSiO_{3/2}$) and ($MeSiO_{3/2}$) synthesized using phenyltriethoxysilane (PhTES) or methyltriethoxysilane (MTES) alone. Next bifunctional siloxane, diphenyldiethoxysilane (DPhDES) or dimethyldiethoxysilane (DMDES) was added as a second component to the system. The glasses obtained showed softening temperatures except for ($MeSiO_{3/2}$) glass, which had a rubbery behavior above the softening point and could not be resoftened. All other gels showed a decrease in network connectivity by incorporation of bifunctional siloxane groups, making it possible to obtain melting gels. This can be explained by

considering that the formation of an infinite glass network is hindered by the incorporation of bifunctional units. Later ^{29}Si-NMR and gel permeation chromatography were used to study the viscoelastic properties of the complex structure of the gels in the (1-x)PhTES - xDPhDES and (1-y)(PhTES) - y(MTES) systems. ^{29}Si-NMR spectra showed that the molecular structures of the gels were three-dimensional siloxane networks with phenyl groups, which are distributed to maintain weak bonds with each other. The number of bridging oxygens between silicons and the intramolecular structure was shown to influence the viscosity, which follows a free volume model. [117,118]

Jitianu et al. [63] prepared melting gels consisting of mono-substituted alkoxide and a di-substituted alkoxide (MTES-DMDES). These gels were investigated for hermetic barriers for protection from humidity and atmospheric gasses for electronic devices. The BET surface area measurements showed that those gels were non-porous and suitable to seal metal envelopes for a long time. The consolidated gel had a helium transmission rate of ~ 8.6 x 10^{-5} cm^3/m^2 x day [119]. Another study focused on the preparation of melting gels from MTES–DMDES and MTMS–DMDMS systems to form hydrophobic coatings. Both groups showed the behavior of melting gels and formed coatings on mica substrates of ~ 1 mm thick with no visible cracks and contact angles greater than 90° [64].

Kamimura et al. [120] determined the activation energy for softening in phenyl polysiloxane glasses prepared using PhTES. The phenyl groups produced domains in the glass that allowed softening at low temperatures. A one-step acid catalysis method was used to synthesize melting gel using phenyl-substituted alkoxides. Phenyl-trimethoxysilane (PhTMS) with diphenyldimethoxysilane (DPhDMS) and PhTES with DPhDES were studied. The consolidation temperature increased with an increase in

disubstituted alkoxide for both systems. However, the glass transition temperature demonstrated an inverse trend. Continuous, hydrophobic thick coatings were obtained by pouring the softened gels onto different substrates [107].

The thermal behavior of melting gels in the MTES-DMDES system was studied. It was found that the consolidation temperature increases with an increase in the number of non-hydrolytic groups [121]. Also, these gels have glass-transition temperatures below 0°C, which makes them suitable for imprint lithography [122]. Some of these compositions are being investigated for low-k dielectric coatings and for multilevel interconnect structures. [62]

Hybrid glasses resulting from consolidation of melting gels have some advantages over epoxies in microelectronic packaging. The dielectric constant measured by impedance spectrometry was as low as 3.3 in the 50% MTES–50% DMDES composition at frequencies greater than 1 kHz. As direct Si–C bonds are less polarizable than Si–O–Si, the di-substituted alkoxysilane, DMDES, contributes to decreasing the dielectric constant [123]. Another study shows that varying the ratio of mono-substituted to di-substituted siloxanes or the substituted group from aromatic to aliphatic can be used to adjust the temperatures for softening and consolidation of melting gel [124]. The range between glass transition temperature (T_g) and consolidation temperature (T_{con}) is important within fields such as microfabrication, optoelectronics, chemical sensors that involving pattern transfer and imprinting. [125,126]

Recently, melting gels prepared from different precursors have been used as anticorrosive coatings for AISI 304 stainless steel [127,128] and titanium alloy [129]. Thick, hydrophobic, crack-free and nonporous coatings were formed. The coatings showed

some plasticity in scratch tests and good adhesion to the substrate through hydroxyl bonds. Electrochemical tests show excellent performance of the coatings against corrosion with no sign of degradation even after several months of immersion in alkali solution.

^{13}C and ^{29}Si NMR spectroscopy along with synchrotron-based SAXS and scanning electron microscopy (SEM) has been used to characterize the structure in detail. In particular, the SAXS results show that the glasses are homogeneous from the nm to micrometer length scales. The SEM images show surface that are uniform and free of defects. This study provides useful information that impacts the synthesis and design of a broader range of hybrid glass materials by consolidation of melting gels that are being developed for mechanical and electrochemical applications [130].

Chapter Three
Experimental Procedures

3.1 Introduction

The sol-gel synthesis of siloxane-based hybrid organic-inorganic compounds usually involves di- or trifunctional organosilanes co-condensed with metal alkoxides, mainly $Si(OR)_4$, $Ti(OR)_4$, $Zr(OR)_4$ or $Al(OR)_3$. Each of these components has specific roles that have been reviewed and discussed extensively [110]. Metal alkoxides and trifunctional alkoxysilanes are active crosslinkers that after condensation usually produce hybrid materials having high Young's modulus (E > 10 GPa) and either high glass transition temperature (T_g> RT) or no T_g. Difunctional alkoxysilanes co-condensed with metal alkoxides generate linear polymers and cyclic oligomers that behave as hybrid elastomers and exhibit low Young's modulus (E = 5 - 100 MPa) and low glass transition temperature (T_g< RT). Therefore, mixing these different molecular precursors (tri- and di-functional alkoxysilanes, metal alkoxides, functional macromonomers, etc.) leads to the ability for mechanical and functional properties of hybrid materials to be tuned between those of polymers and glasses [72].

The experimental procedures for preparing melting gels by mixing two components or three components, and the procedure to obtain the final condensed product are explained below, along with the characterization techniques used in this study.

Preparation of melting gels using two components (metal alkoxide and organoalkoxysilanes or two organoalkoxysilanes) has been reported in many studies [29,62,64,106]. One method is shown in Figure 3.1 from Klein et al., which is similar to our procedure in preparing melting gels with three components [107].

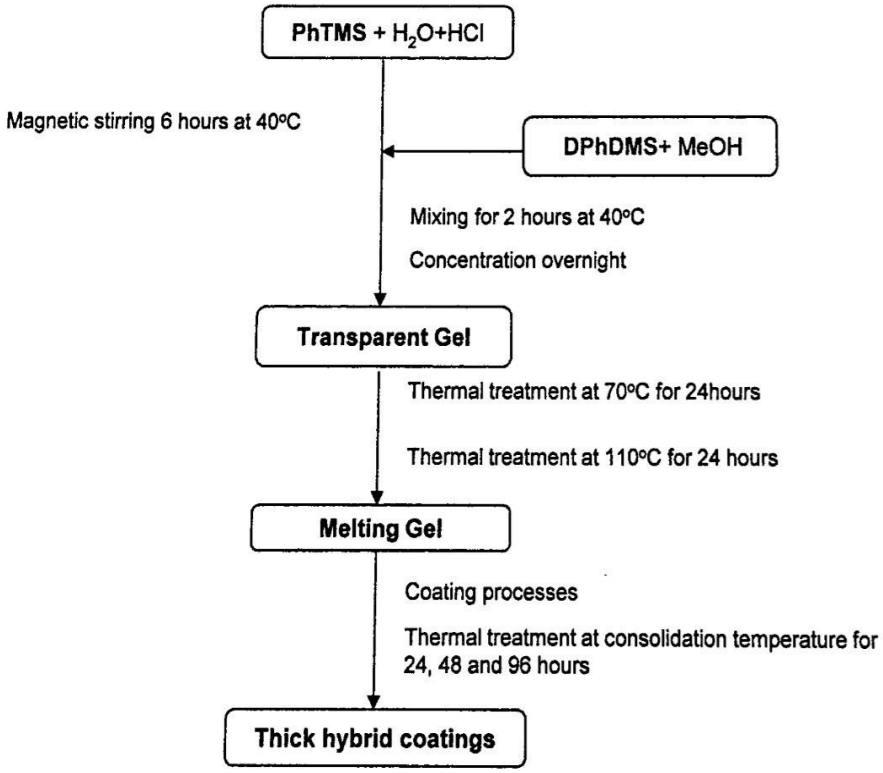

Fig 3.1: Flowchart of the synthesis of the melting gels in the phenyltrimethoxysilane (PhTMS)-diphenyldimethoxysilane (DPhDMS) system and the coating process. [107]

In this study, a one-step acid catalyst method was used to synthesize sol–gel hybrids (melting gels) using phenyl substituted alkoxides and tetra-alkoxysilane. Phenyltrimethoxysilane (PhTMS) with diphenyldimethoxysilane (DPhDMS) and phenyltriethoxysilane (PhTES) with diphenyldiethoxysilane (DPhDES), mixed either with tetraethylorthosilicate (TEOS) or with tetramethylorthosilicate (TMOS). In this study melting gels were prepared from mixing three components (di-substituted alkoxysilane, mono-substituted alkoxysilane, and tetraalkoxysilane) using the method illustrated in Figure 3.2. The purpose was (i) investigating the possibility of synthesizing melting gels

by mixing three precursors, (ii) comparing the effects of TEOS and TMOS on melting gels properties, and (iii) determining the limit of adding tetrafunctional alkoxide on producing melting gels. These gels were finally used to produce thick coatings on mica, and stainless-steel substrates.

The compositions under study are listed in table 3.1 along with the system names that are used throughout this dissertation. Hybrid gels were then investigated using different characterization techniques, including thermal characterization using (DSC, DTA, and TGA), hydrophobicity through contact angle measurements, density, micro hardness and FTIR for all samples according to the compositions listed in table 3.1. Scanning electron microscope (SEM) was done on some samples to investigate the morphology of the surface. The purpose was to compare the effects of TEOS and TMOS on melting gel properties. For that we prepared the systems listed in table 3.1 where the main difference between them is the tetraalkoxysilane component only. Hence, we can compare:

* Sys (1-1) compare with Sys (5-1).
* Sys (1-2) compare with Sys (5-2).
* Sys (3-1) compare with Sys (7-1).
* Sys (3-2) compare with Sys (7-2).

In all cases, the ratio of PhTMS to DPhDMS or PhTES to DPhDES was held constant at a mole ratio of 1 to 0.25.

Table 3.1: Compositions of the investigated melting gels systems.

System ID	*Composition*		
	TROS	*Mono. Sub.*	*Di.Sub.*
Sys (1-1)	TEOS (MeOH)	PhTMS	DPhDMS (MeOH)
Sys (1-2)	TEOS (EtOH)	PhTMS	DPhDMS (MeOH)
Sys (3-1)	TEOS (MeOH)	PhTES	DPhDES (EtOH)
Sys (3-2)	TEOS (EtOH)	PhTES	DPhDES (EtOH)
Sys (5-1)	TMOS (MeOH)	PhTMS	DPhDMS (MeOH)
Sys (5-2)	TMOS (EtOH)	PhTMS	DPhDMS (MeOH)
Sys (7-1)	TMOS (MeOH)	PhTES	DPhDES (EtOH)
Sys (7-2)	TMOS (EtOH)	PhTES	DPhDES (EtOH)
Sys 1 or Sys 5	-	PhTMS	DPhDMS (MeOH)
Sys 3 or Sys 7	-	PhTES	DPhDES (EtOH)

3.2 Gel Preparation:

The preparation of melting gels was carried out using the mono-substituted alkoxide which is either phenyltriethoxysilane (PhTES) or phenyltrimethoxysilane (PhTMS) both from (Gelest Inc., Morrisville, PA) mixed with water in which the pH=2.5 was adjusted using a 0.1M HCl (Fisher Scientific, Atlanta, GA) as a catalyst. Both mono-substituted alkoxide and water were continuously stirred using magnetic stirrer placed inside an oven at 40ºC for five hours in beaker sealed with Parafilm® (closed system) until clear solution was obtianed. The molar ratio between mono-substituted and water was (1:1.5). Clear solutions were achieved faster with PhTMS than the PhTES, due to the higher reactivity of the methoxy alkoxides, compared with ethoxy alkoxides [131].

Di-substituted alkoxide was either diphenyldiethoxysilane (DPhDES) or

diphenyldimethoxysilane (DPhDMS) both from (Gelest Inc., Morrisville, PA) diluted with parental anhydrous alcohol ethanol or methanol (Sigma-Aldrich) respectively. The molar ratio between di-substituted and alcohol was (1:4). Di-substituted alkoxide and alcohol were stirred separately for 30 minutes in closed system at room temperature before mixing with mono-substituted and water mixture. The tetra-alkoxysilane was either tetraethyl orthosilicate (TEOS) or tetramethyl orthosilicate (TMOS) (Sigma-Aldrich) diluted with anhydrous alcohol, ethanol or methanol (Sigma-Aldrich) with the molar ratio (1:1). The tetra-alkoxysilane and alcohol were also stirred separately at room temperature for 30 minutes in closed system before adding it to the other two components in the oven. These gels were prepared using the molar ratio of mono- to di-substituted alkoxides of (1:0.25). Then the clear sol was stirred in open system at room temperature until gelation occurred.

The synthesis route for all systems is shown in the flowchart Figure 3.2. Hence, all precursors were used without further purification. The percentage of tetra-alkoxysilane was increased gradually until we determined the limit of the systems that beyond we either get precipitation or the softening property of the melting gels is lost. Tetra-alkoxide was added in proportion to mono-substituted weight that was used in preparing the samples as shown in Tables 3.2, 3.3, 3.4 and 3.5 for all systems under study. After heat treatments at 70ºC to eliminate alcohol and 110ºC to remove the residual surface water from melting gels, the gels were clear and solid at room temperature, but they resoftened at ~110 ºC.

Noticing that, we tried another method to prepare the gel by adding the di-substituted alkoxide/alcohol and tetra-alkoxide/alcohol mixtures at the same time to the mono-substituted alkoxide/water mixture when a clear solution was obtained from it (after

5 hrs. of stirring). This procedure was not successful to prepare melting gels since the results often were not even a gel but rather a viscous liquid. These viscous liquids were stable and did not turn into gel even after a long time of stirring in open system (more than 170 hrs. of stirring) and more than three years of storage. We believe that the reason why we did not obtain gels through this procedure is that the reactions of hydrolysis and condensation among the three components are competitive ones. While the order of reactivity of the precursors increases from mono-substituted to non-substituted to di-substituted [62]. For this reason, the TEOS will react faster with available water than di-substituted alkoxide resulting in leaving the di-substituted alkoxide unhydrolyzed and only has the dilution effect on the sol. The properties and chemical formula of precursors investigated for melting gels are listed in Table 3.6.

Table 3.2: Mole ratio and mole percentage for system (1).
[PhTMS:DPhDMS:TEOS]

Mono-Sub. PhTMS		***Di-Sub. DPhDMS***		***TEOS***		
Mole ratio	***Mole %***	***Mole ratio***	***Mole %***	***Mole ratio***	***Mole %***	***Weight% TEOS/PhTMS %***
1	80	0.25	20	0	0	0
1	78.8	0.25	19.7	0.019	1.49	2
1	77.07	0.25	19.26	0.0475	3.66	5
1	74.35	0.25	18.58	0.095	7.06	10
1	69.45	0.25	17.36	0.19	13.19	20
1	65.14	0.25	16.28	0.285	18.56	30
1	61.35	0.25	15.33	0.38	23.31	40

Table 3.3: Mole ratio and mole percentage for system (3).
[PhTES:DPhDES:TEOS]

Mono-Sub. PhTES		***Di-Sub. DPhDES***		***TEOS***		
Mole ratio	***Mole %***	***Mole ratio***	***Mole %***	***Mole ratio***	***Mole %***	***Weight% TEOS/PhTES %***
1	80	0.25	20	0	0	0
1	78.55	0.25	19.63	0.023	1.8	2
1	76.48	0.25	19.12	0.0575	4.4	5
1	73.24	0.25	18.31	0.1153	8.44	10
1	67.54	0.25	16.88	0.2306	15.57	20
1	62.65	0.25	15.66	0.346	21.68	30
1	58.43	0.25	14.6	0.4614	26.96	40
1	56.56	0.25	14.14	0.0259	29.29	45
1	54.74	0.25	13.68	0.5768	31.57	50

Table 3.4: Mole ratio and mole percentage for system (5).
[PhTMS:DPhDMS:TMOS]

Mono-Sub. PhTMS		***Di-Sub. DPhDMS***		***TMOS***		
Mole ratio	***Mole %***	***Mole ratio***	***Mole %***	***Mole ratio***	***Mole %***	***Weight% TMOS/PhTMS %***
1	80	0.25	20	0	0	0
1	78.37	0.25	19.59	0.026	2.03	2
1	76.04	0.25	19.01	0.065	4.94	5
1	72.46	0.25	18.11	0.13	9.42	10
1	66.22	0.25	16.55	0.26	17.21	20
1	60.97	0.25	15.24	0.39	23.78	30
1	56.49	0.25	14.12	0.52	29.37	40

Table 3.5: Mole ratio and mole percentage for system (7).
[PhTES:DPhDES:TMOS]

Mono-Sub. PhTES		***Di-Sub. DPhDES***		***TMOS***		
Mole ratio	***Mole %***	***Mole ratio***	***Mole %***	***Mole ratio***	***Mole %***	***Weight% TMOS/PhTES %***
1	80	0.25	20	0	0	0
1	78.06	0.25	19.51	0.031	2.42	2
1	75.25	0.25	18.81	0.0788	5.93	5
1	71.03	0.25	17.75	0.157	11.2	10
1	68.728	0.25	17.182	0.205	14.09	13
1	63.89	0.25	15.97	0.315	20.12	20
1	58.03	0.25	14.5	0.473	27.45	30
1	53.19	0.25	13.29	0.631	33.51	40

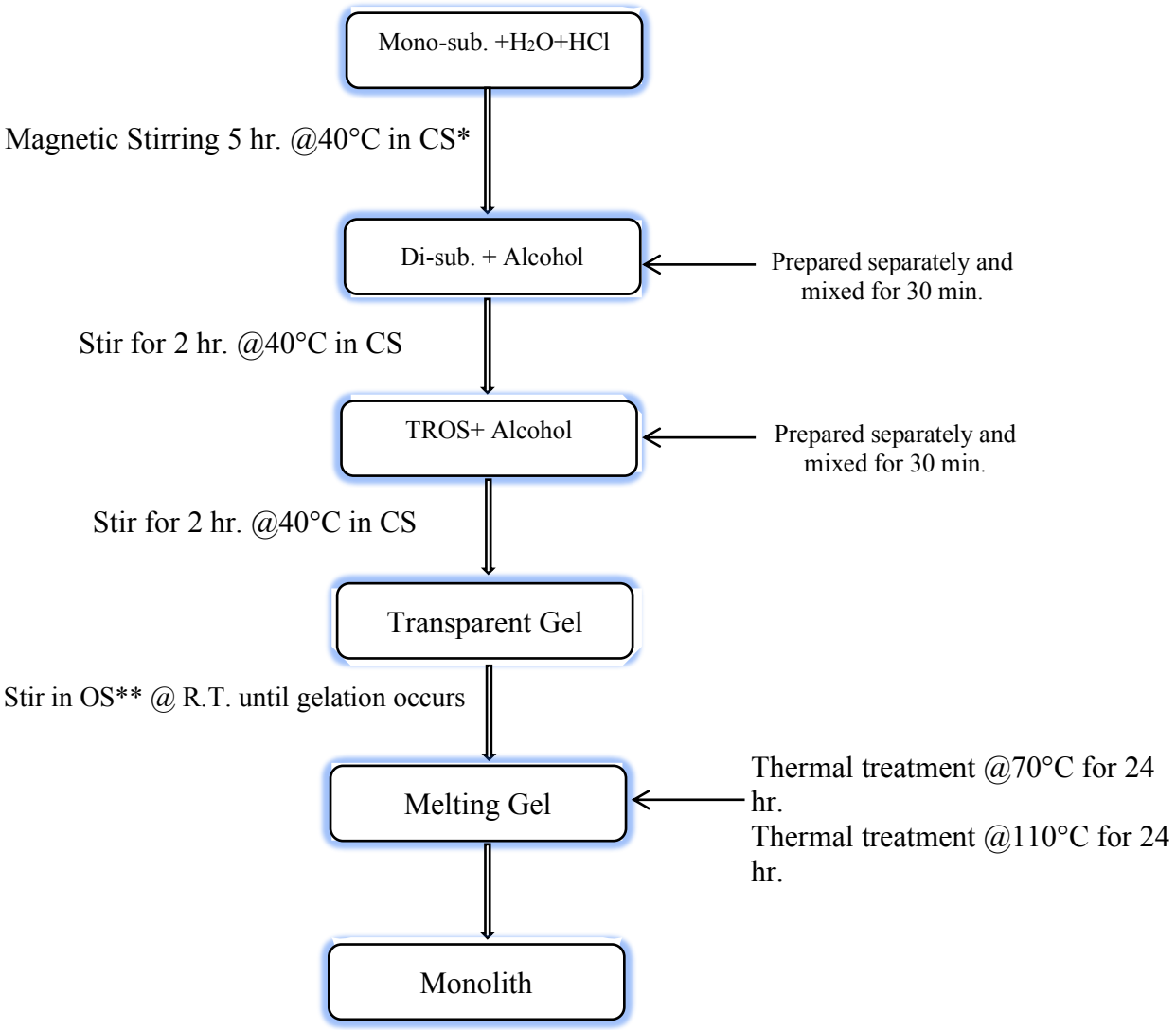

Fig. 3.2: Flow Chart of preparing melting gel from three components.

* Close System, ** Open System

Table 3.6: Molecular weight, formula, melting point, boiling point, specific gravity, solubility, functionality, silica content and structure of precursors investigated for Melting Gels.

Chemical Name	*Formula*	*Molecular Weight (g/mol)*	*Melting Point (°C)*	*Boiling Point (°C)*	*Specific Gravity*	*Solubility*	*Number of Reactive Groups*	*%SiO₂*	*Structure*
TEOS	$C_8H_{20}O_4Si$	208.33	-77	169	0.9335	Reacts with water. Solubility parameter: 7.87	4	28.8	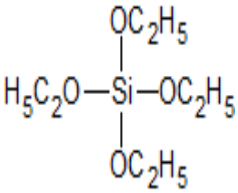
TMOS	$C_4H_{12}O_4Si$	152.22	-2	121	1.032	Reacts with water	4	39.5	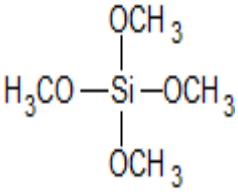
PhTES	$C_{12}H_{20}O_3Si$	240.37	10	113	0.996	Insoluble in water. Reacts with water	3	25.0	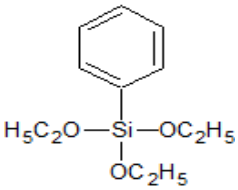
PhTMS	$C_9H_{14}O_3Si$	198.293	-25	211	1.064	Insoluble in water. Reacts with water	3	30.3	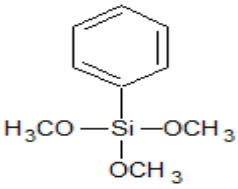
DPhDES	$C_{16}H_{20}O_2Si$	272.42	15	167	1.0329	Insoluble in water. Reacts with water	2	22.1	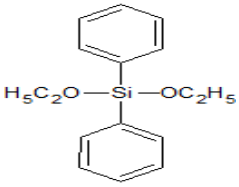

DPhDMS	$C_{14}H_{16}O_2Si$	244.36	15	161	1.0771	Insoluble in water. Reacts with water	2	24.6	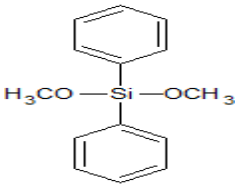

3.3 Materials characterization

To fully understand the melting gel behavior and properties, certain information is required such as: thermal properties, surface topography, chemical composition, hydrophobicity, mechanical properties, and corrosion protection behavior. There is no one technique that is able to provide all the necessary information; so it requires several techniques. In order to fully comprehend the behavior, properties, and to solve the particular problems is necessary to examine and analyze the different aspects of materials.

The Differential Thermal Analysis (DTA) and Differential Scanning Calorimetry (DSC) techniques were used to measure the thermal properties of the melting gel. Scanning electron microscope (SEM) was used to study the surface morphology of the melting gels film. The surface analysis and chemical structure of the hybrid coating materials were studied by using Attenuated Fourier Transform Infrared Spectroscopy (ATR-FTIR). Hydrophobicity was measured by recording the contact angle between a water droplet and the film. Micro hardness and apparent density were also examined using Vickers hardness and a helium pycnometer.

3.3.1 Thermal Analysis – DTA - DSC

The thermal behavior of the hybrid gels (glass transition temperature, energy liberated, reaction types exothermic or endothermic and weight loss of the melting gel) was studied using combined thermal analysis measurements (thermogravimetry TG and differential thermal analysis DTA) (Seiko EXTAR TGA/DTA 6200 thermal analyzer using platinum crucibles), and differential scanning calorimetry (DSC TA-Q-20, Thermal Analysis Instrument Specialists, Twin Lakes, WI). DTA and TGA were recorded at a 5°C/min-heating rate in the temperature range between 50 and 1000°C under flowing air (50 mL/min). The DSC analyses were recorded using a 5°C/min-heating rate between -90 and 500°C under nitrogen flow rate of 20 mL/min. Both of these techniques were used with melting gels that had not been consolidated.

3.3.2 Scanning electron microscope (SEM)

Microstructures of melting gels coating were visually examined, the surface and the cross-sections of the fractures of the hybrid glasses were evaluated using a HITACHI S-2700 SEM. The SEM was operated at 25 keV acceleration voltage. The SEM was equipped with an AMT digital camera system. Only two systems were topographically evaluated using this technique.

3.3.3 Fourier Transform Infrared Spectroscopy (ATR-FTIR)

Characterization of the hybrid glasses with infrared spectroscopy (FT-IR) was obtained by consolidation of the melting gels on mica substrates (Grade V-4 muscovite, SPI Co., West Chester, PA) (15 mm x 15 mm). The Fourier transform infrared

spectroscopy (FT-IR) spectra were recorded between 400 and 4000 cm^{-1} using Thermo Nicolet Avatar 360 FTIR spectrometer (Waltham, MA) equipped with a Smart Endurance Attenuated Total Reflectance (ATR) attachment (diamond crystal). The resolution for the FTIR was 2 cm^{-1} and 100 spectra were averaged. The spectra were acquired under a Leica (Buffalo Grove, IL) optical microscope at 50× magnification and were recorded at fourteen different points along a line of 100 μm.

3.3.4 Contact Angles

Hydrophobicity of the hybrid coatings was evaluated by measuring the contact angle between a water droplet and the coating film. Contact angles were measured on samples that had been fully consolidated for 24 h at their consolidation temperatures. The contact angle θ° was measured using a T-200 basic Theta Optical Tensiometer (Biolin Scientific, Stockholm, Sweden) equipped with LED blue light source and with a standard 60 fps camera with a special zoom lens. Five measurements were taken for each composition sample then the data were averaged. The contact angle data were analyzed using Pendant Drop Surface Tension Software 3.80 (Biolin Scientific). Measurement was made at room temperature.

3.3.5 Vickers Microindentation hardness

The microhardness of the hybrid glass was measured on consolidated samples at room temperature using LECO Corp. machine model (LM-248AT) equipped with a Vickers geometry diamond tip and 10X and 50X objective lenses. Vickers hardness for all samples was the mean average of five test results for each sample. Test load used was 50 gf and 10 sec dwell time for all samples. Hence increasing the load to 100, 200 gf gave

approximately the same result but could cause the shattering of the samples. The indentation measurements were performed at ambient temperature with relative humidity of 47±5%. Using the following formula, we calculate Vickers microhardness:

$$HV = 1.854\ (F/d^2)$$

where:

HV is Vickers hardness in (kgf/mm^2) to convert HV to GPa multiply by 0.009807.

F is the test load (kgf)

D is the average diagonal length of an indentation (mm)

3.3.6 True density

True density (ρ_t) of consolidated samples was measured using helium pycnometry (Accupyc-1430, Micromeritics Instrument Corp., Nocross, GA). Helium gas was used as the displacement medium in this technique. The coating was peeled off of the coating substrate by immersing the coated mica samples in liquid nitrogen, and then the coating was ground using ceramic mortar and pestle. Each test result was the average of five results for every sample.

3.3.7 Consolidation Temperatures

The consolidation temperatures, after which the gels no longer soften, were established experimentally by pouring the melting gels on mica substrate Mica (Grade V-4 muscovite, SPI Co., West Chester, PA) (15 mm x 15 mm) inside the furnace at 110°C, when the gels were fluid. Then perform a set of experiments on the coated substrate going through cycles of heating and cooling by increase the temperature gradually above 110°C and cool to room temperature until the gels no longer softened after reheating and the

behavior was no longer reversible. Following deposition, the coatings were treated at the consolidation temperatures for 24 h.

Chapter Four

Results and Discussions

4.1 Introduction

The objective of this chapter is to characterize organic-inorganic hybrid (OIH) melting gel systems and to study the effect of adding a tetrafunctional siloxane (TEOS/TMOS) on the overall properties and coating properties of the OIH systems. OIH melting gel systems without TEOS or TMOS were synthesized as control samples. The preparation of the control samples was identical to those with TEOS/TMOS except without the tetralkoxysilane component, as shown in Figure 4.1. During the formulation of OIH, the crosslinking structure of the hybrid nanocomposite is formed as is shown schematically

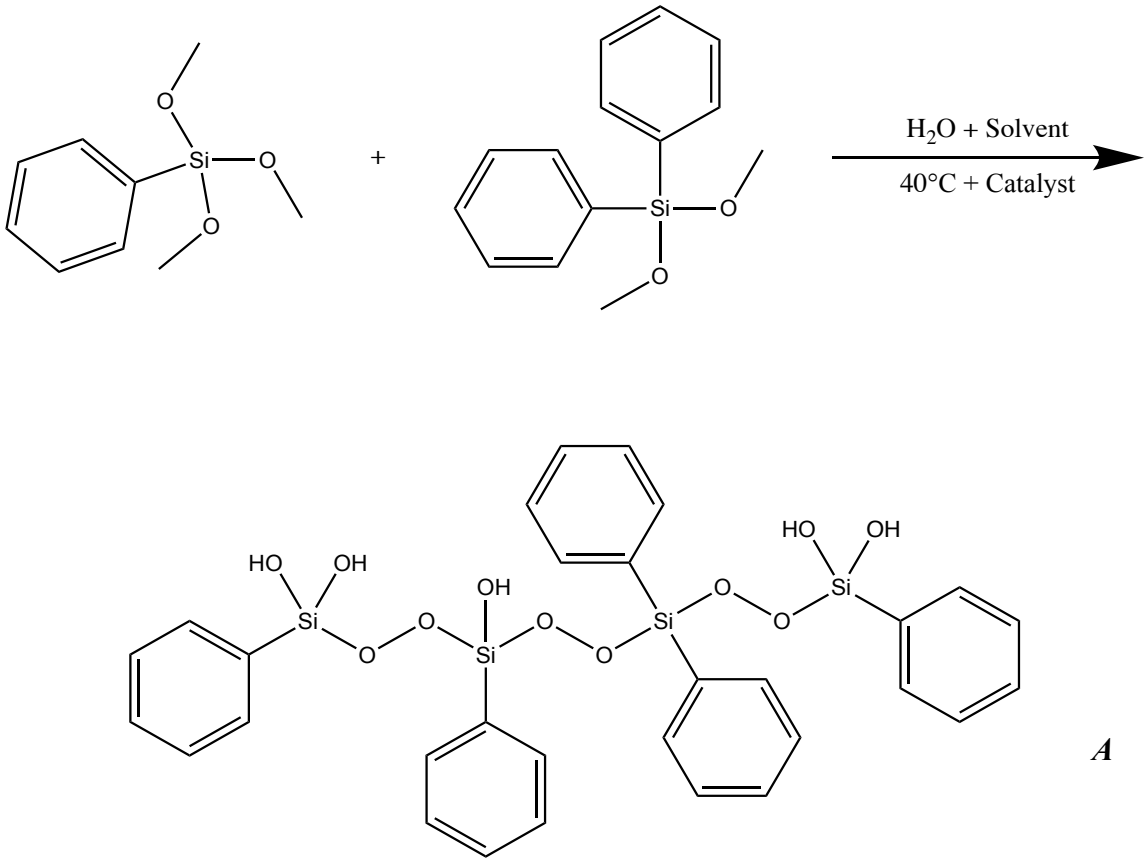

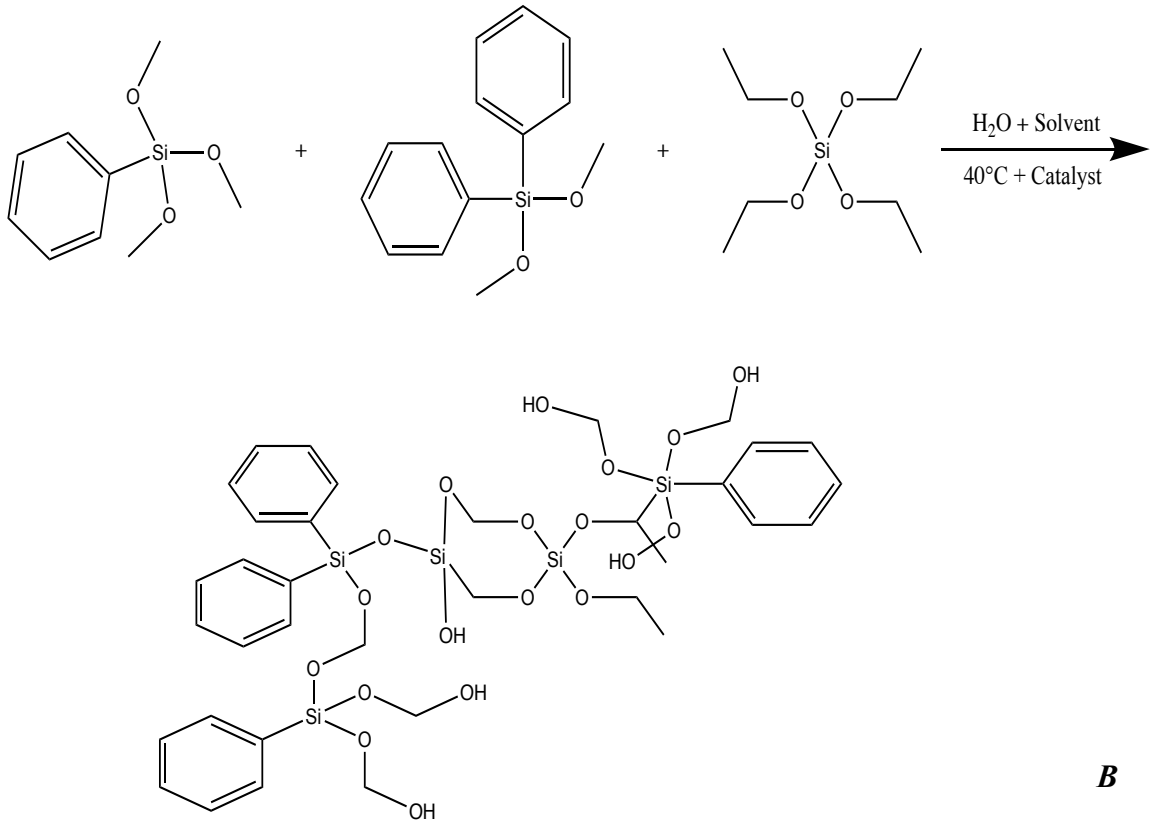

Fig. 4.1: Proposed formation of OIH melting gel from two components (A) and from three components (B).

in Figure 4.2. The organic phase is represented by the phenyl groups from the phenyl trialkoxysilane and diphenyldialkoxysilane. The inorganic phase is formed by the hydrolysis and condensation of the polysiloxane.

Nuclear magnetic resonance (NMR) spectroscopy can be used to get the most accurate structure of the gel. This technique has been widely used for many years to analyze the structure of small molecules such as proteins. Unlike x-ray crystallography, NMR does not depend on having a crystalline sample; it simply requires a small volume of concentrated solution that is placed in a strong magnetic field. [132]

^{29}Si and ^{13}C CP/MAS NMR spectroscopy were used to investigate the influence of substance specific parameters such as silane concentration, type of silane, pH, and moisture content of the filler on the silica/organosilane reaction mechanics. ^{29}Si spin lock CP NMR measurements were performed to characterize the solid structure of different polysilanes in the solid state [133]. Recent fundamental research on hydro-polymer gel systems by means of NMR techniques such as pulse NMR, pulsed field-gradient spin-echo NMR, solid state high resolution NMR and NMR imaging methods have been reviewed. [134]

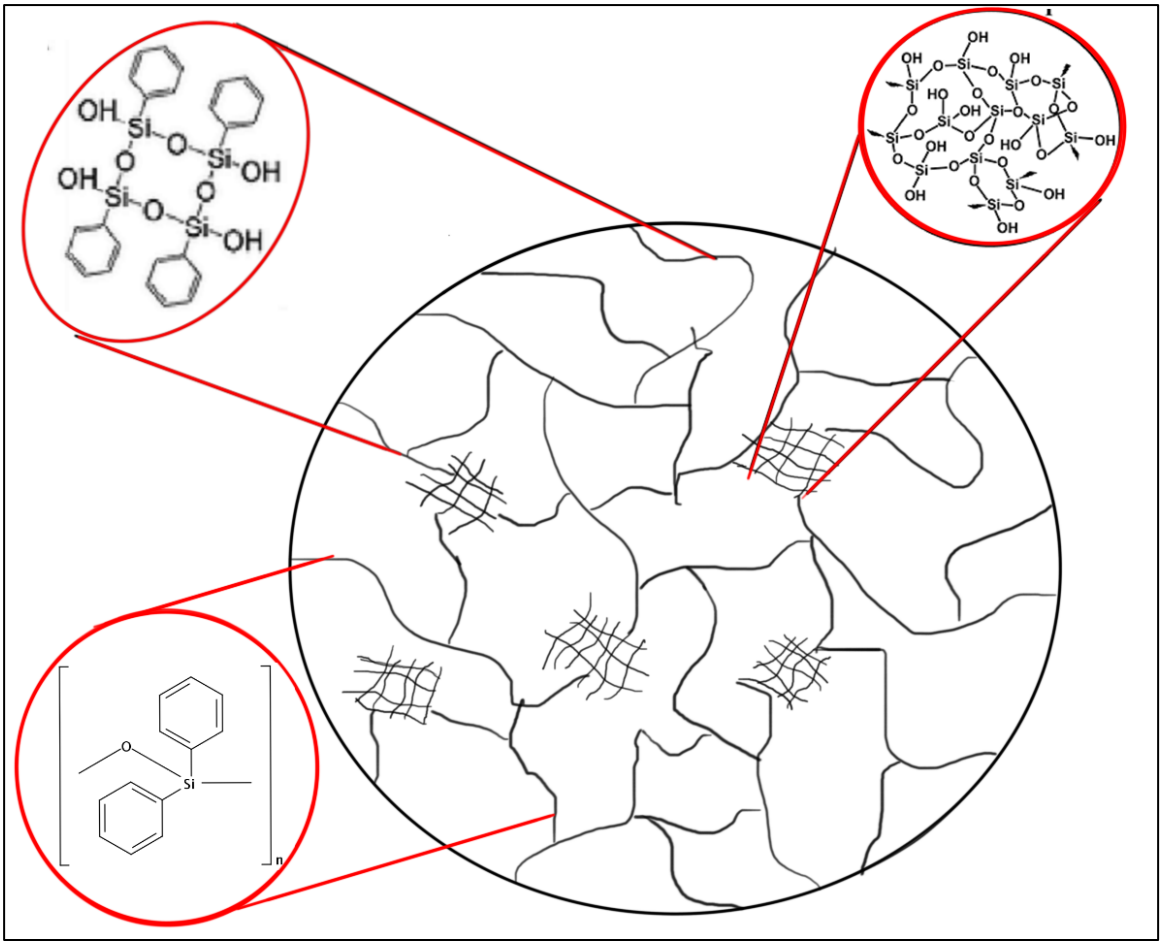

Fig. 4.2: Proposed crosslinking structure.

4.2 Thermal gravimetric analysis (TGA)

TGA was used to evaluate the thermal stability of the melting gels. TGA and DTA curves are shown in Figure 4.3 for the samples with TEOS as the inorganic phase which include systems (1-1), (1-2), (3-1), and (3-2), while Figure 4.4 is for the samples with TMOS precursor, which include systems (5-1), (5-2), (7-1), and (7-2). The degradation temperatures at maximum weight loss (T_{max}), which is obtained from the highest peak of first derivative of thermograms, were summarized in Table 4.1.

Incorporating the inorganic phase increased the maximum thermal degradation temperature. The enhanced thermal stability of hybrids is due to the higher dissociation energy of Si-O bond (798 kJ/mol) than C-C bond (335 kJ/mol) [6]. The TGA curves show that all samples have two steps of weight loss. For the methoxy-containing sample, the first weight loss is between 200°C and 400°C, which is likely due to the burning of methoxy groups and elimination of hydroxyl groups. For the ethoxy-containing samples, the first weight loss is between 200°C and 300°C. The second weight loss between 500°C and 660°C corresponds to combustion of the phenyl groups. The second weight loss is similar for both the methoxy-containing and the ethoxy- containing gels, supporting the assignment of this weight loss to the phenyl groups that the samples have in common. The DTA curves for the control samples show an exothermic peak at 330°C for the methoxy-containing sample and at 315°C for the ethoxy-containing sample. Combustion of the methoxy or the ethoxy groups gives rise to an exothermic peak. These peaks occur at lower temperatures when increasing the amount of TEOS or TMOS. However, the major exothermic peak for all samples occurs at ~ 600 °C, which is associated with the burning of the phenyl groups.

The maximum exothermic peaks and total weight loss were higher in systems with TEOS than with TMOS. The total weight loss decreases in most cases with the concentration of the tetralkoxysiloxane. The consolidation temperature trends in the same direction as the weight loss, as shown in Table 4.1 Increasing the amount of tetrafunctional alkoxide will increase the number of reactive sites and therefore, the number of bridges between the molecular species formed when the tetralkoxysiloxanes hydrolyze.

In sys (1-1) weight loss begins at lower temperature with higher amount of TEOS, and exothermic reactions shifts to higher temperature with increasing TEOS%. The opposite trend can be seen in sys (3-1) where the weight loss begins at higher temperature and exothermic reactions shifts to lower temperature with increasing TEOS%. This can be attributed to the methoxy and ethoxy group in the monosubstituent and disubstituent precursors and to the cosolvent that was used with TROS. While sys (1-2) and sys (3-2) show the opposite of the above trend for sys (1-1) and sys (3-1), the reason is that the transesterification reactions occurs faster in these two systems. All systems above used TEOS as inorganic component and tends to dilute the mixture especially when mixed with ethoxy containing components and decrease the mixture viscosity. This explains why systems with TEOS and ethoxy groups starts to decompose at higher temperature than systems with TEOS and methoxy groups. On the other hand, sys (5-1) starts to decompose at lower T with increasing TMOS%, and the exothermic reaction shifts to higher temperatures. In contrast, sys (7-1) starts to lose weight at a higher temperature and the exothermic reaction shifts to lower T with more TMOS%. Furthermore sys (5-2) and sys (7-2) behave exactly the opposed to sys (5-1) and (7-2) respectively. In all above systems

TMOS is used and it apparently increases the mixture viscosity especially when mixed with methoxy containing precursors and that promotes thermal decomposition at lower temperature.

Table 4.1: Composition and Thermal Characteristics of melting gel.

Sample ID	*Composition Monosub./Disub./TROS*	*TROS W% of (Mono)*	*Glass transition Tg (˚C)*	*Consolidation Temp. (˚C)*	*Thermal weight loss (%)*	*T (˚C) Max. Decomp.*
Sys (1-1)	*PhTMS/ DPhDMS/TEOS (MeOH)*	2	19.4	210	62.2	611
Sys (1-1)	=	3	24.09	185	63.28	622
Sys (1-1)	=	4	23.09	185	61.14	615
Sys (1-1)	=	5	2.89	180	62.97	606
Sys (1-2)	*PhTMS/ DPhDMS/TEOS (EtOH)*	2	13.02	215	57.7	600
Sys (1-2)	=	5	4.97	210	62	619
Sys (1-2)	=	10	24.48	195	58.84	605
Sys (1-2)	=	20	25.24	175	52.17	599
Sys (1-2)	=	30	30.94	160	57.02	612
Sys (5-1)	*PhTMS/ DPhDMS/TMOS (MeOH)*	2	19.91	210	62	598
Sys (5-1)	=	5	36.93	218	59.3	612
Sys (5-1)	=	10	41.3	190	58.35	615
Sys (5-1)	=	20	40.9	180	56	610
Sys (5-1)	=	30	26.63	165	55.84	600
Sys (5-2)	*PhTMS/ DPhDMS/TMOS (EtOH)*	2	38.13	205	58.13	607
Sys (5-2)	=	5	37.17	200	58.4	603
Sys (5-2)	=	10	26.51	195	58.66	604
Sys (5-2)	=	20	16.46	193	58.3	602
Sys (5-2)	=	30	-8.85	185	59.4	608
Sys (3-1)	*PhTES/ DPhDES/TEOS (MeOH)*	2	40.94	220	59.77	613
Sys (3-1)	=	5	28.12	195	61.53	610
Sys (3-1)	=	10	38.84	205	58.1	612
Sys (3-1)	=	20	10.82	175	59.3	605
Sys (3-1)	=	30	12.44	165	57.11	603
Sys (3-1)	=	40	-2.51	170	57.92	607
Sys (3-1)	=	45	22.1	155	56.27	607
Sys (3-1)	=	50	28.25	-	53.79	612
Sys (3-2)	*PhTES/ DPhDES/TEOS (EtOH)*	2	30.95	165	60.62	607
Sys (3-2)	=	5	25.23	180	60	607
Sys (3-2)	=	10	58.57	185	57.87	614
Sys (3-2)	=	20	49.00	175	56.43	613
Sys (7-1)	*PhTES/ DPhDES/TMOS (MeOH)*	2	37.9	200	57.42	607

Sys (7-1)	=	5	45.89	190	58.66	604
Sys (7-1)	=	10	47.92	180	57.62	622
Sys (7-1)	=	13	43.74	165	58.34	607
Sys (7-2)	*PhTES/ DPhDES/TMOS (EtOH)*	2	41.09	210	60.22	608
Sys (7-2)	=	5	32.58	200	58.53	605
Sys (7-2)	=	10	41.34	190	58.8	615
Sys (7-2)	=	20	42.55	185	57	611
Sys (7-2)	=	30	54.14	180	-	-
Sys1 or 5	*PhTMS/ DPhDMS*	0	25.97	175	62.16	604.7
Sys 3 or 7	*PhTES/ DPhDES*	0	1.24	185	63.3	611

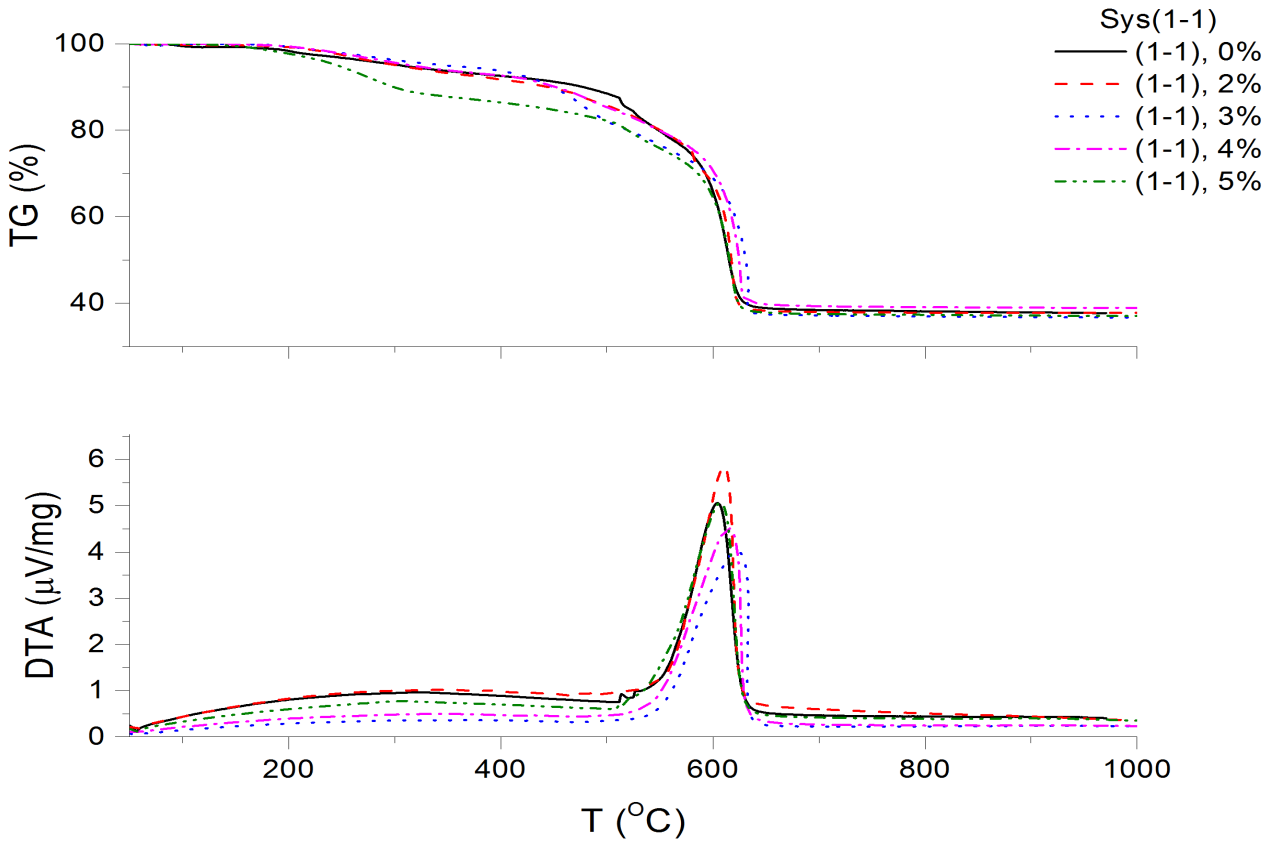
Sys(1-1)
(1-1), 0%
(1-1), 2%
(1-1), 3%
(1-1), 4%
(1-1), 5%
TG (%)
100
80
60
40
DTA (μV/mg)
6
5
4
3
2
1
0
200
400
600
800
1000
T (°C)

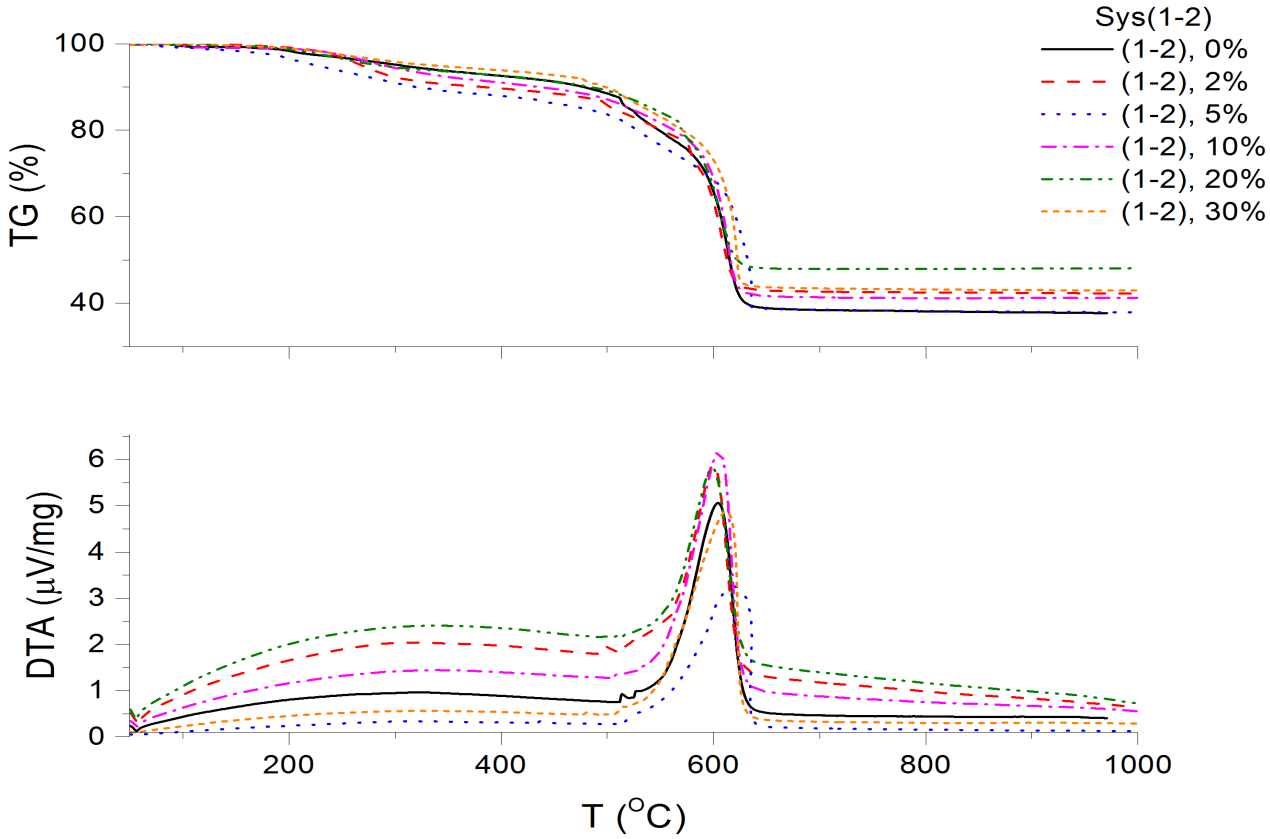
Sys(1-2)
(1-2), 0%
(1-2), 2%
(1-2), 5%
(1-2), 10%
(1-2), 20%
(1-2), 30%
TG (%)
100
80
60
40
DTA (μV/mg)
6
5
4
3
2
1
0
200
400
600
800
1000
T (°C)

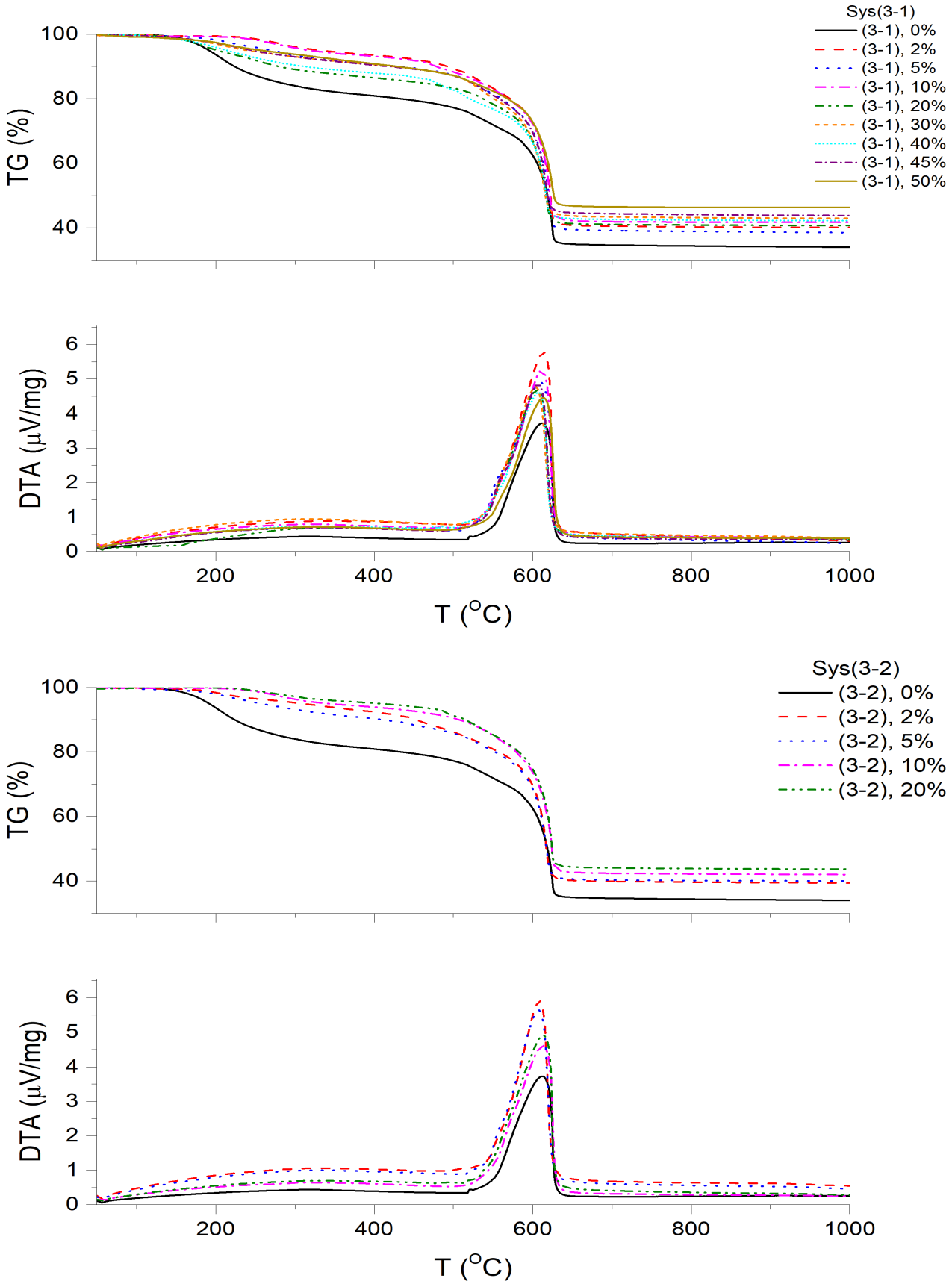

Fig. 4.3: Thermogravimetric analysis and differential thermal analysis curves of the systems with TEOS {(1-1), (1-2), (3-1), and (3-2)}.

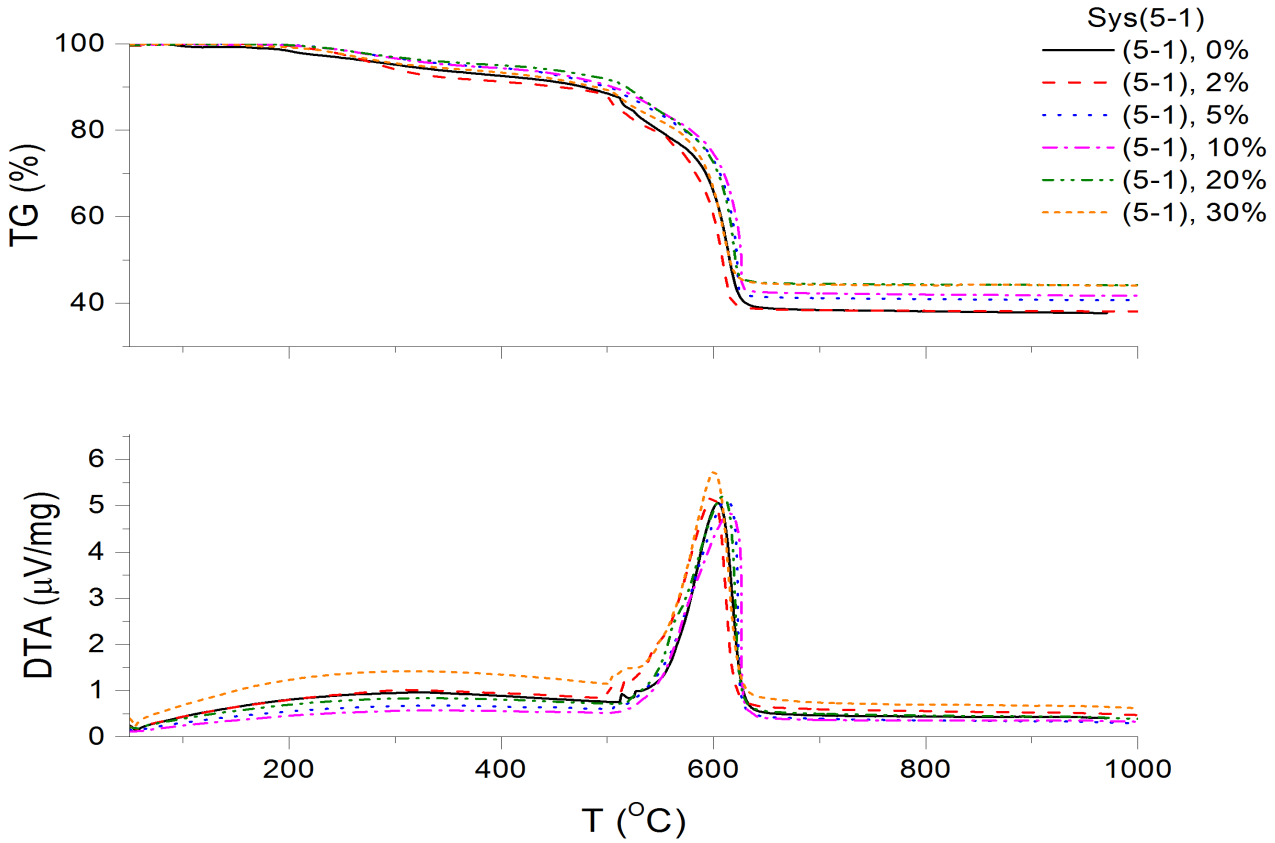
Sys(5-1)
(5-1), 0%
(5-1), 2%
(5-1), 5%
(5-1), 10%
(5-1), 20%
(5-1), 30%
TG (%)
100
80
60
40
DTA (μV/mg)
6
5
4
3
2
1
0
200
400
600
800
1000
T (°C)

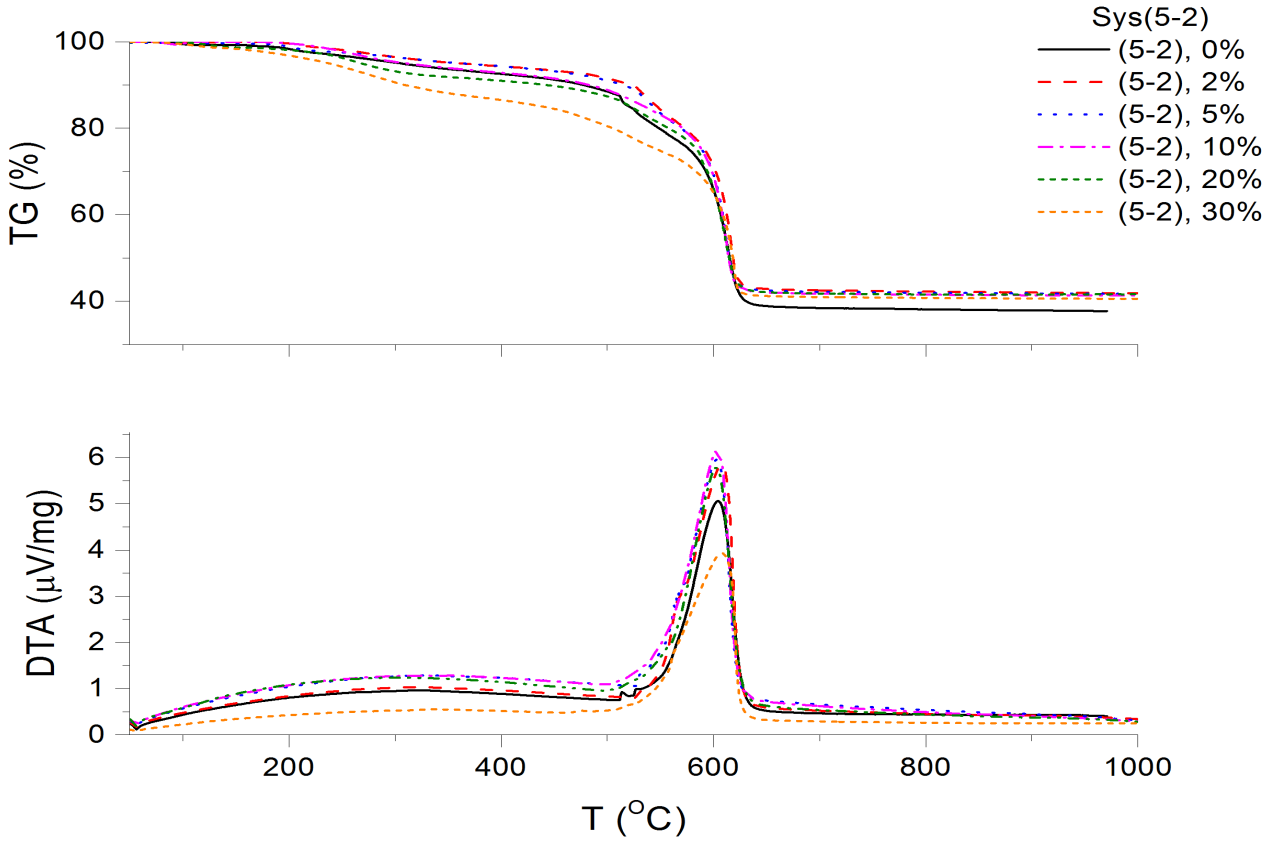
Sys(5-2)
(5-2), 0%
(5-2), 2%
(5-2), 5%
(5-2), 10%
(5-2), 20%
(5-2), 30%
TG (%)
100
80
60
40
DTA (μV/mg)
6
5
4
3
2
1
0
200
400
600
800
1000
T (°C)

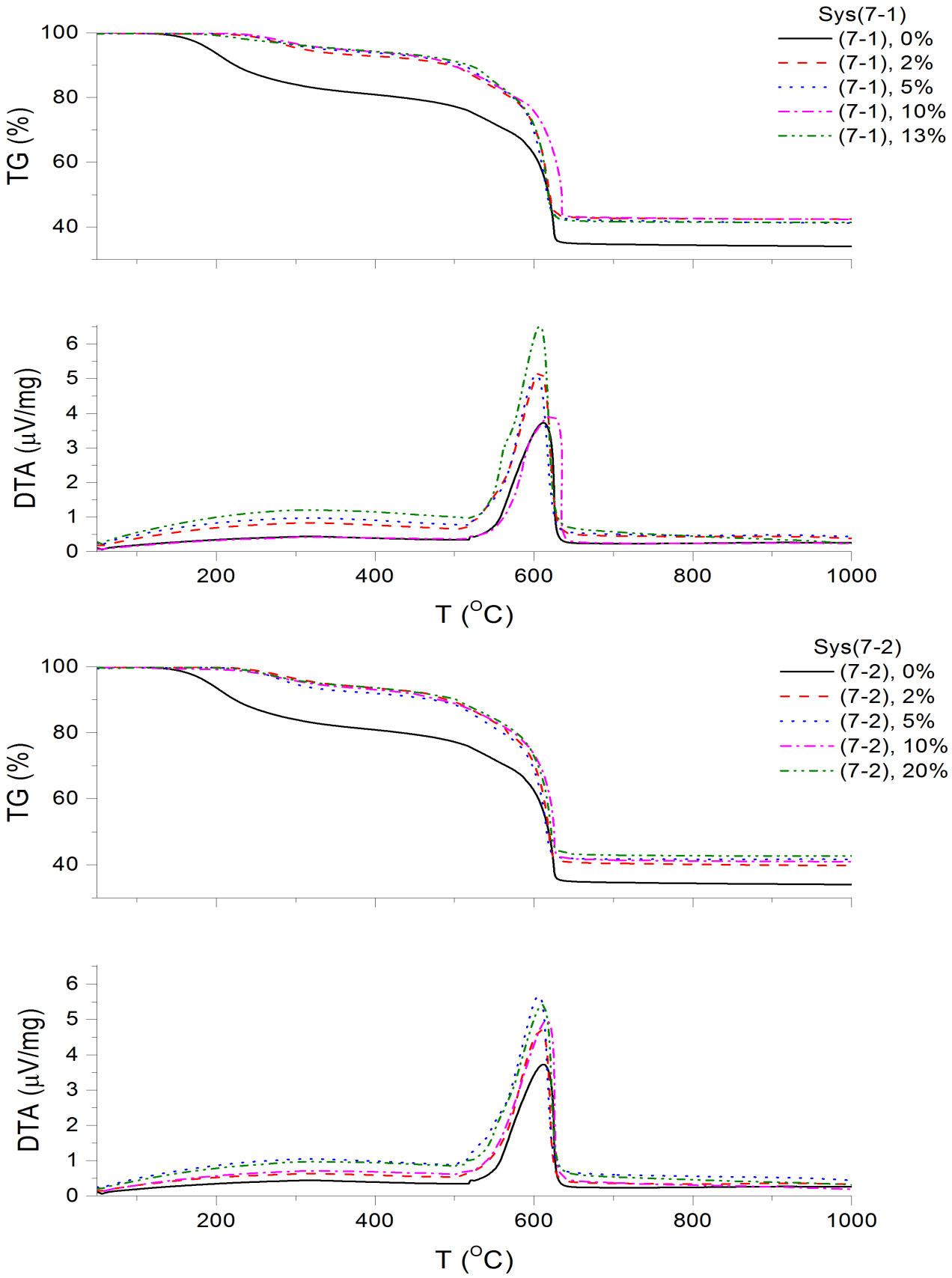

Fig. 4.4: Thermogravimetric analysis and differential thermal analysis curves of the systems with TMOS {(5-1), (5-2), (7-1), and (7-2)}.

4.3 Differential scanning calorimetry (DSC)

Figure 4.5 shows the DSC results for systems with TEOS which include systems {(1-1), (1-2), (3-1), and (3-2)}, while Figure 4.6 is for the samples with TMOS precursor, which include systems {(5-1), (5-2), (7-1), and (7-2)}. DSC was used to determine the glass transition temperatures for gels before consolidation listed in Table 4.1 and where exothermic and endothermic reactions take place on scale from -50 °C to 400 °C. It was obvious that for systems containing (TEOS/MeOH) the glass transition temperature (T_g) decreases with increasing its mole ratio, while the opposite is found in systems containing (TEOS/EtOH). The same trend is found in systems with (TMOS/EtOH), since the glass transition temperature decreases with increasing its mole ratio, while the opposite trend is observed in systems with (TMOS/MeOH) and both mono and di-substituted alkoxysilane.

In general, the glass transition temperature increases gradually with increasing tetra-alkoxide when it is diluted with the same alcohol group. The glass transition temperature decreases when it is diluted with a different alcohol group. This could be associated with transesterification reactions. Transesterification takes place between tetra-alkoxide and alcohol in the presence of acid catalyst. Transesterification reactions occur faster when the same organic groups exist in tetra-alkoxide, organoalkoxide and alcohols [29]. Overall, T_g values were higher for systems {(7-1), and (7-2)} phenyl-substituted ethoxysilanes with TEOS and lower for systems {(1-1), and (1-2)} phenyl-substituted methoxysilanes with TMOS, whether the solvent was methanol or ethanol.

The glass transition is generally thought of as the interval of transition between liquid states and glassy, amorphous states [135]. In another way, the glass transition reflects a number of macroscopic properties, such as viscosity, dielectric constant, and mechanical properties. Using the approach developed for traditional organic polymers and applied to inorganic silica-based polymers, the glass transition temperature is considered a measure of the degree of cross-linking in the silica network. In other words, the T_g increases with an increase in the number of oxygen bridges between silicon atoms. Hence the small additions of TROS in the three-component system increase the glass transition relative to the two-component system.

Despite the fact that methoxy groups are more reactive groups than ethoxy groups, and should achieve a higher degree of polycondensation, the T_g in three components systems is higher for samples with ethoxy groups than with methoxy groups. This could be attributed to the fact that samples with ethoxy groups have more time to hydrolyze and undergo polycondensation to form larger 3D networks, while methoxy groups that react faster have less time to undergo polycondensation. Another indication is that the gelling time for samples with TEOS and/or ethoxy groups are longer than for samples with TMOS and/or methoxy groups. In this sense, the addition of TEOS is a dilution, which extends the gelling time.

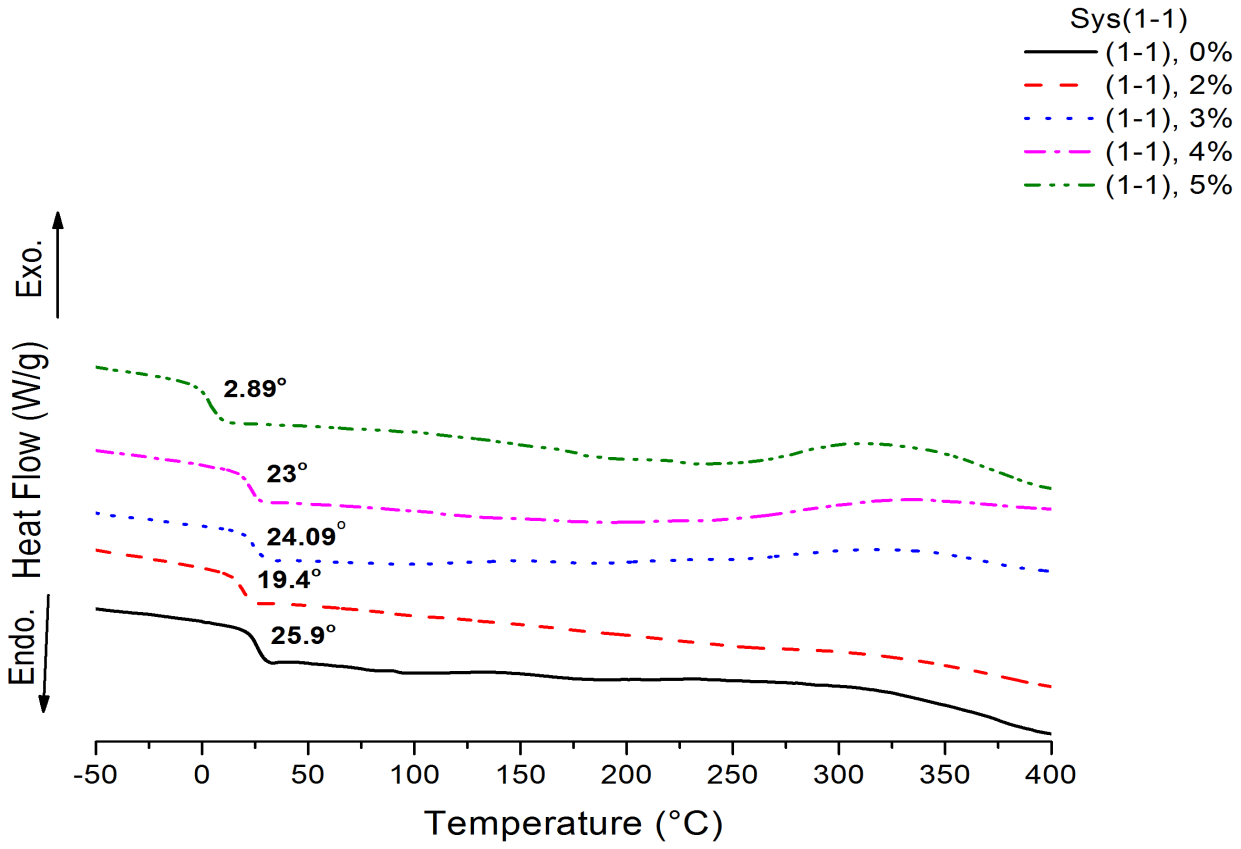
Sys(1-1)
(1-1), 0%
(1-1), 2%
(1-1), 3%
(1-1), 4%
(1-1), 5%
Exo.
Heat Flow (W/g)
Endo.
2.89°
23°
24.09°
19.4°
25.9°
-50
0
50
100
150
200
250
300
350
400
Temperature (°C)

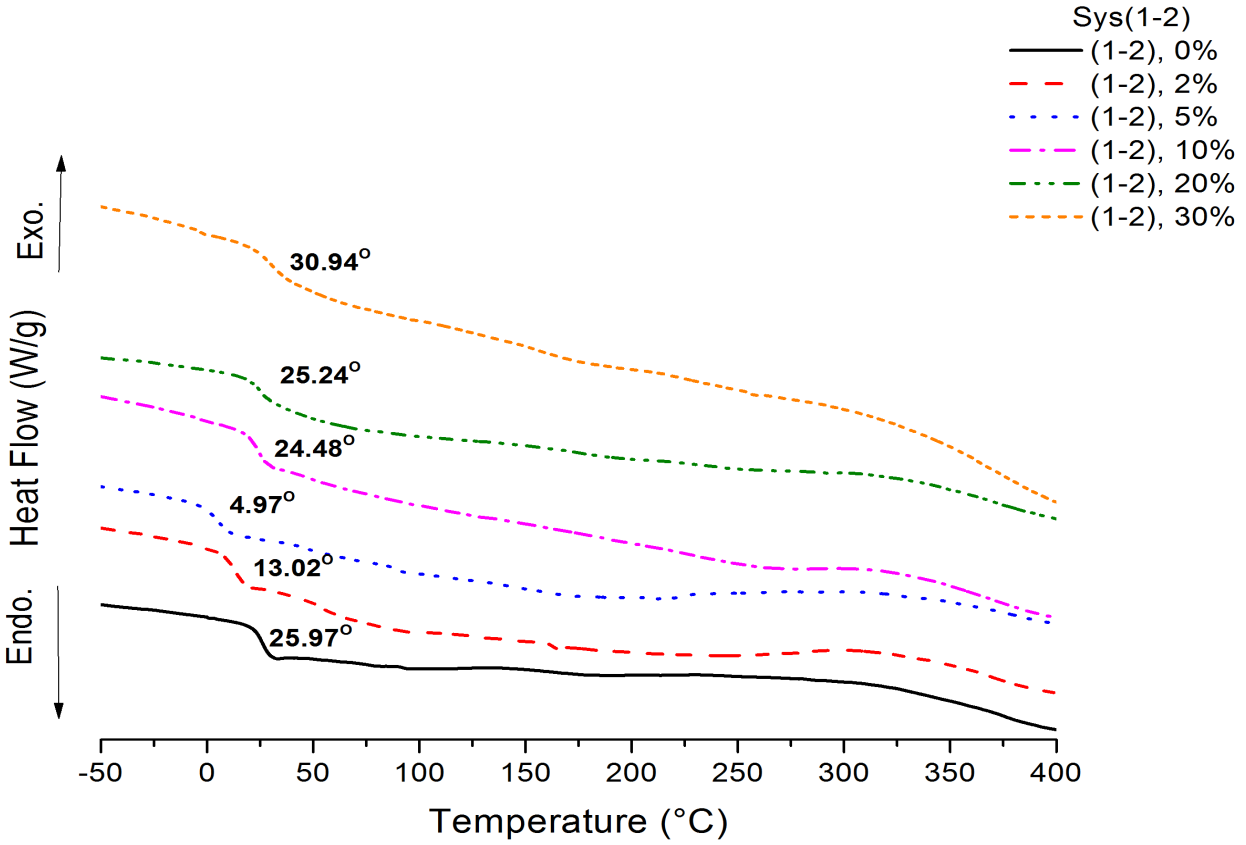
Sys(1-2)
(1-2), 0%
(1-2), 2%
(1-2), 5%
(1-2), 10%
(1-2), 20%
(1-2), 30%
Exo.
Heat Flow (W/g)
Endo.
30.94°
25.24°
24.48°
4.97°
13.02°
25.97°
-50
0
50
100
150
200
250
300
350
400
Temperature (°C)

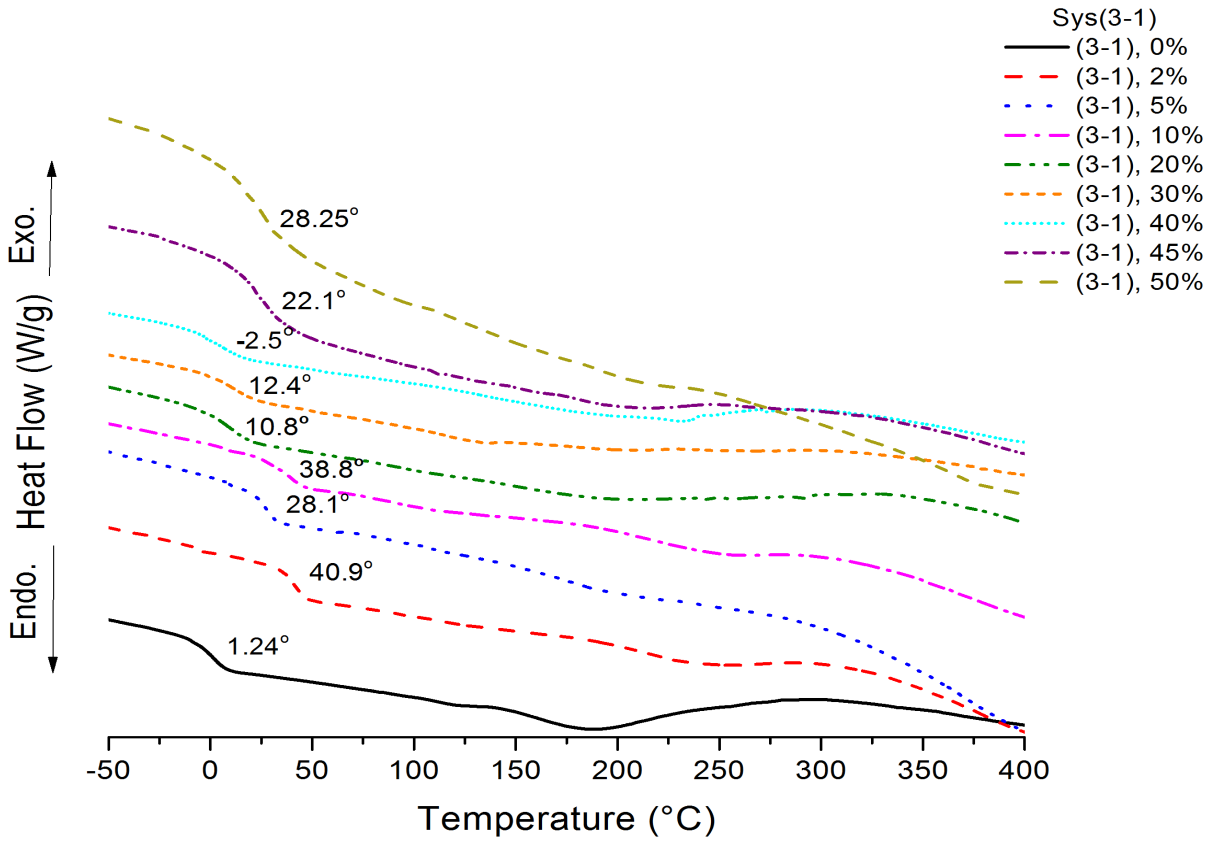

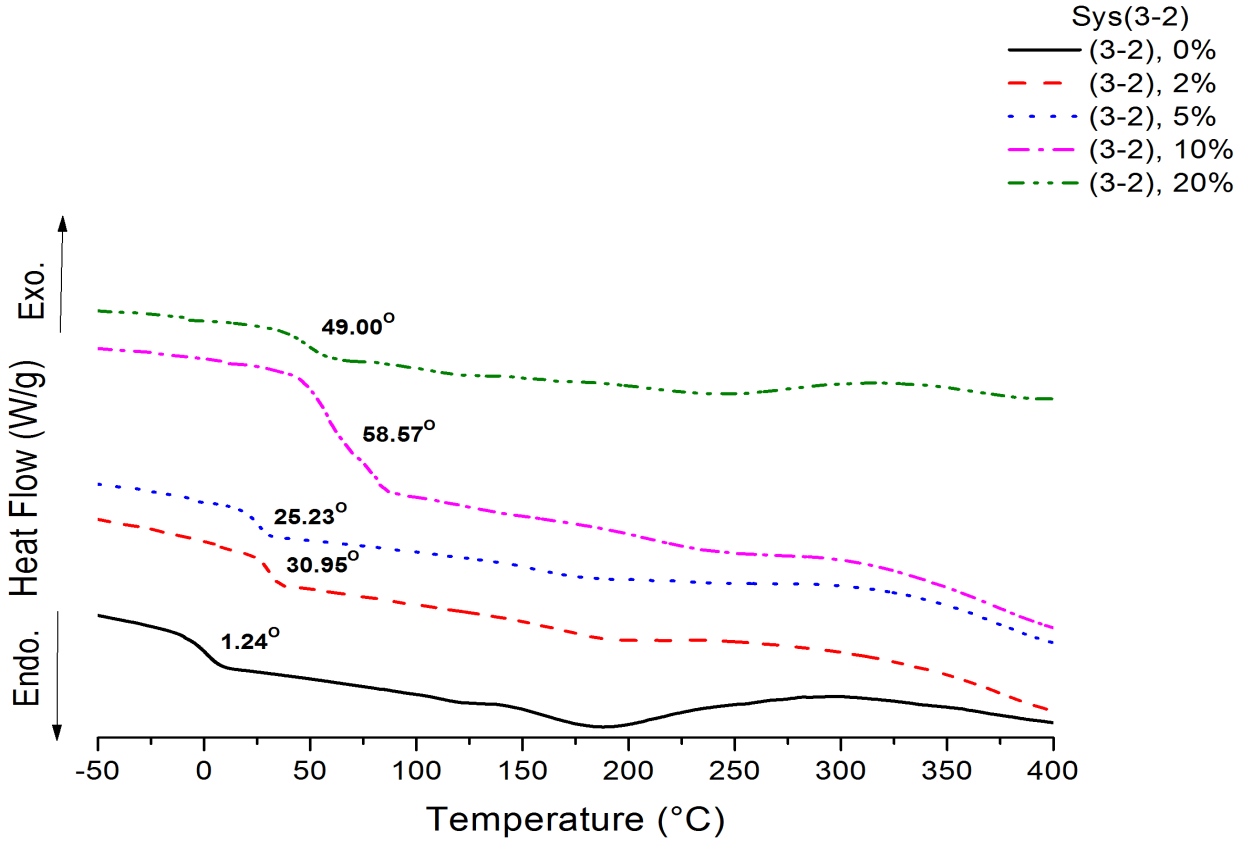

Fig. 4.5: Differential scanning calorimeter (DSC) curves of the systems with TEOS {(1-1), (1-2), (3-1), and (3-2)}.

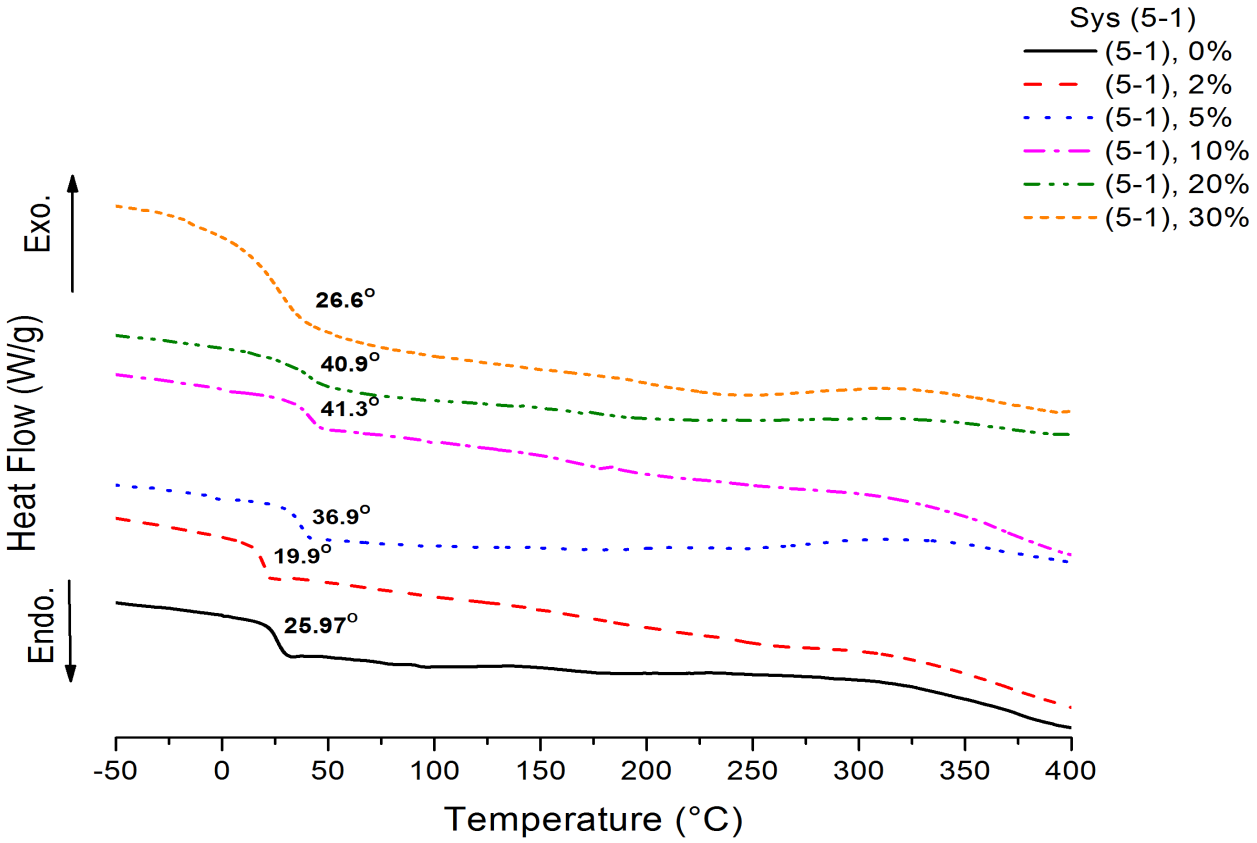
Sys (5-1)
(5-1), 0%
(5-1), 2%
(5-1), 5%
(5-1), 10%
(5-1), 20%
(5-1), 30%
Exo.
Endo.
Heat Flow (W/g)
26.6°
40.9°
41.3°
36.9°
19.9°
25.97°
-50
0
50
100
150
200
250
300
350
400
Temperature (°C)

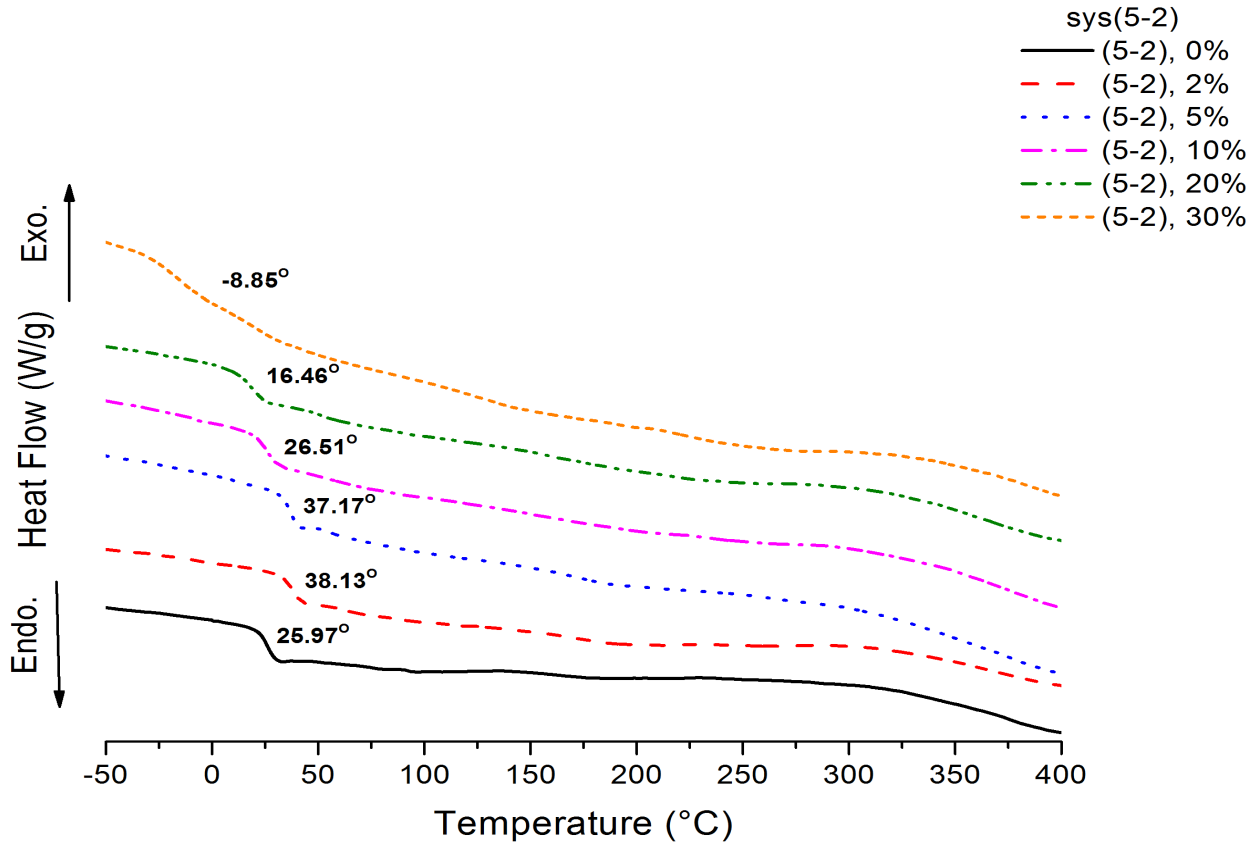
sys(5-2)
(5-2), 0%
(5-2), 2%
(5-2), 5%
(5-2), 10%
(5-2), 20%
(5-2), 30%
Exo.
Endo.
Heat Flow (W/g)
-8.85°
16.46°
26.51°
37.17°
38.13°
25.97°
-50
0
50
100
150
200
250
300
350
400
Temperature (°C)

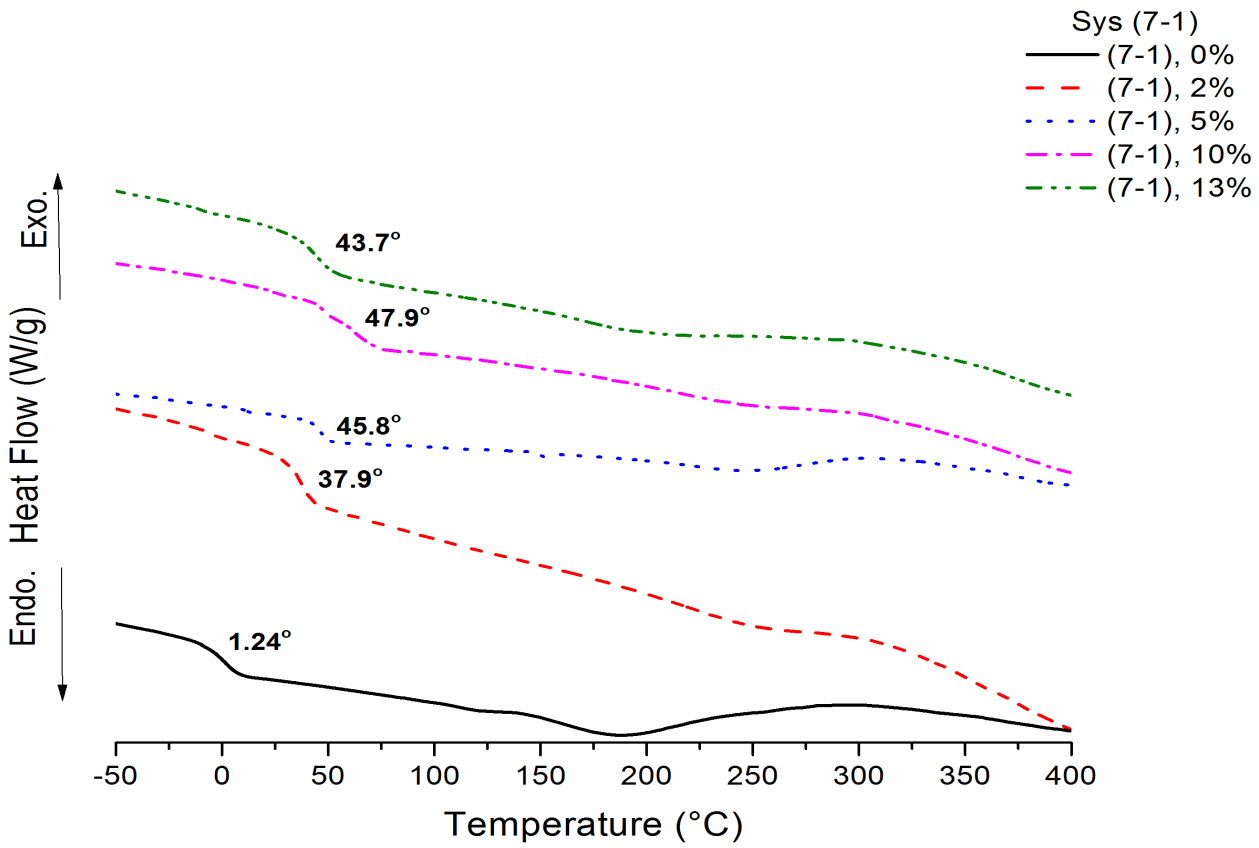

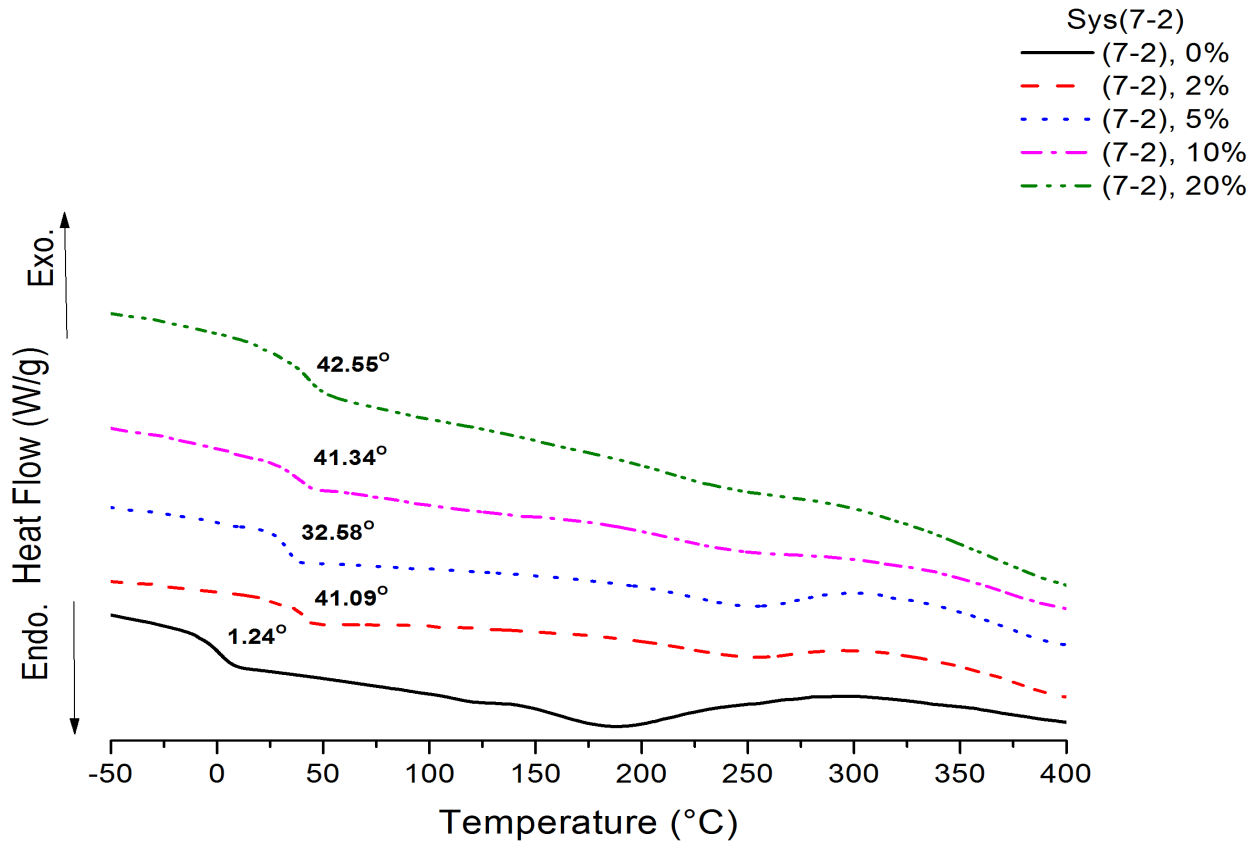

Fig. 4.6: Differential scanning calorimeter (DSC) curves of the systems with TMOS {(5-1), (5-2), (7-1), and (7-2)}.

4.4 Scanning electron microscope (SEM)

Scanning electron microscopy (SEM) was used to observe the morphology of the organic-inorganic hybrid gels and to evaluate the uniformity of consolidated gels on both surface and cross-sections of the coated mica substrates. Two representative systems were topographically evaluated using this technique. System (7-1) with [*PhTES/ DPhDES/TMOS (MeOH)]* and system (7-2) with [*PhTES/ DPhDES/TMOS (EtOH)]* were compared. Both have TMOS as the inorganic component diluted in one case with methanol and the other with ethanol. In both cases the coatings were transparent and uniform. Figure 4.7a-d presents the surface SEM micrographs for system (7-1) with 0, 5, 10, and 13% of TMOS, coated on mica substrates, while Figure 4.8a-d presents the cross-section SEM micrographs of the of the same system. All the images were obtained with the same magnification for purposes of comparison. System (7-1) has a methanol co-solvent.

Smooth and crack-free layers were observed for 0, and 5% TMOS except for one small blister, indicating no macrophase separation occurred. However, further increasing the TMOS concentration resulted in a surface that was rough with wavy lines, indicating possible liquid-in-liquid phase separation. Also, when more TMOS was added, some air bubbles were trapped in the coating. The bubbles may also be caused by evaporation of the co-solvent methanol, which occurred during thermal treatment. Nevertheless, all of the samples were nonporous, according to nitrogen sorption analysis.

Figure 4.9a-c and Figure 4.10a-c show the SEM images of the surface and cross section for system (7-2) with 2, 5, 20%TMOS respectively. System (7.2) has an ethanol co-solvent. This system shows rougher surfaces than those with methanol co-solvent. The

samples with ethanol co-solvent have more micro cracks and more bubbles with increasing TMOS wt%. As can be seen from the surface and cross section images more wavy lines or "fibrils" and sharp edges are clearly observed, which suggests that this system is more rigid than system (7-1). This observation is supported by the hardness measurements, which are higher for this system. As reported in the section on hardness measurements, increasing TMOS content increased the hardness. Similar to system (7-1), the coating is nonporous. There are indications of liquid-in-liquid phase separation specifically near system limit of 20% TMOS.

All of the samples on the mica substrates are shown in Figure 4.11. At this level, it is possible to read text through all of the samples. In addition, on visual inspection, the surfaces appear smooth and uniform, as shown in Figure 4.11.

Solvents can strongly control both the gelation time and the structure of the product. They behave as true chemical additives and are able to react with alkoxide precursors, changing their structure at a molecular level. Depending on the solvent and the metal, alkoxy bridging, solvation or alcohol interchange reactions may be favored leading to different morphologies. Oligomerization or solvate formation depends on the solvent. Therefore, different hydrolysis rates are expected leading to completely different oxide materials. As a result, the molecular structure of alkoxide precursors depends on the nature of the solvent [38, 39, 165]. In conclusion, it is observed that the morphology is smoother and appears more uniform when the co-solvent used in the mixture has the same parent alcohol group as the tetra alkoxide component as in sys (7-1). In sys (7-2), which has a different alcohol, the layer has a rough morphology.

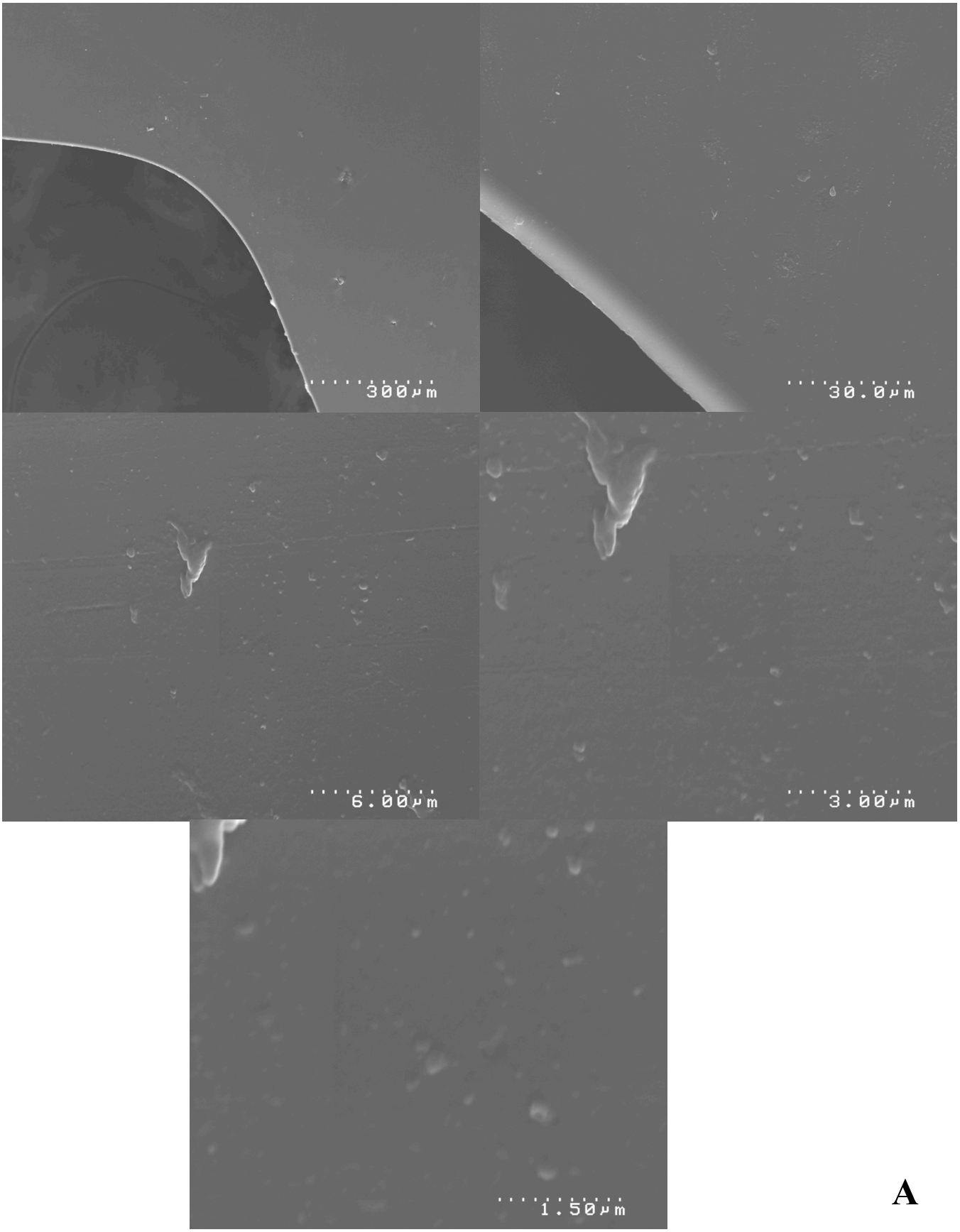

A

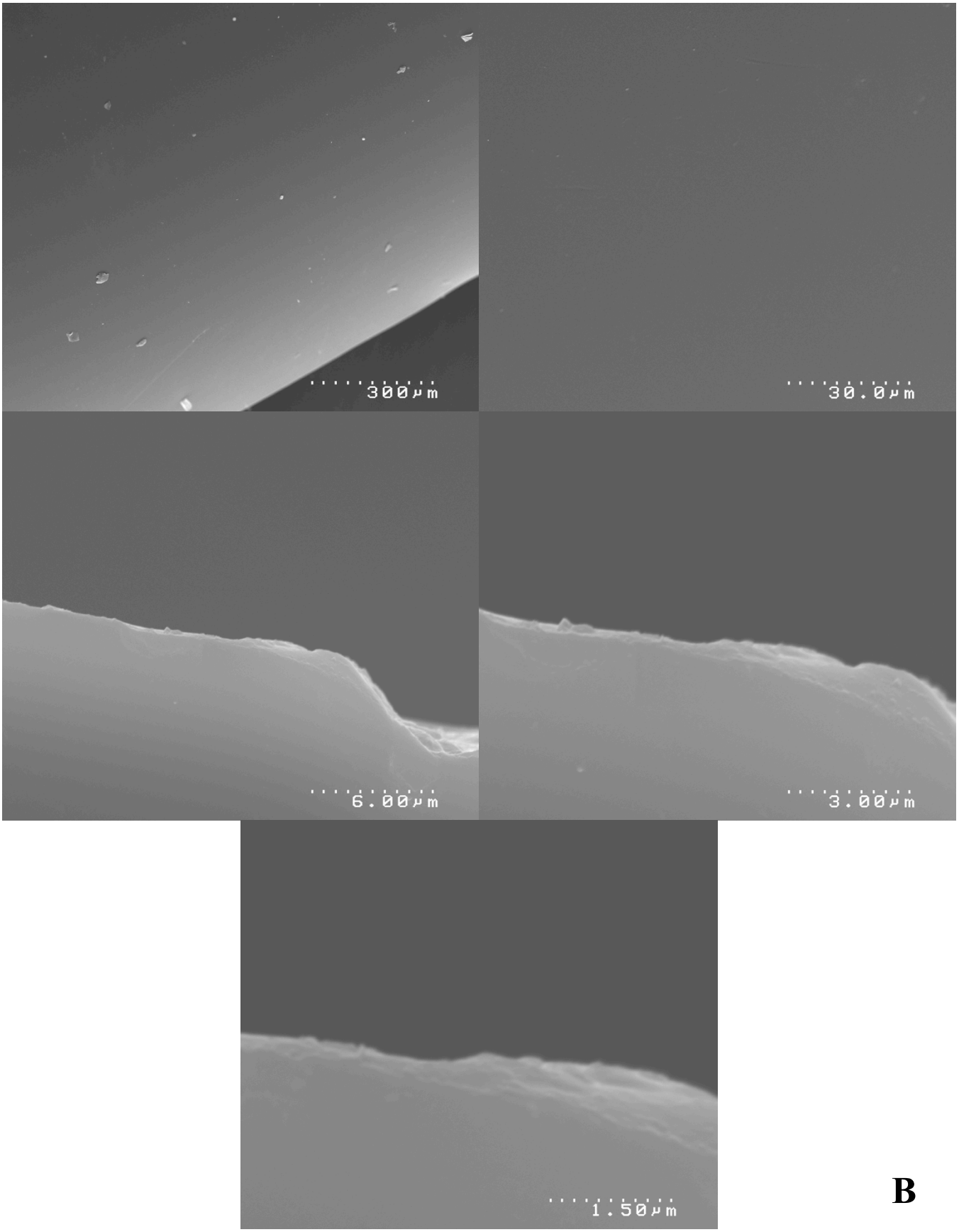

B

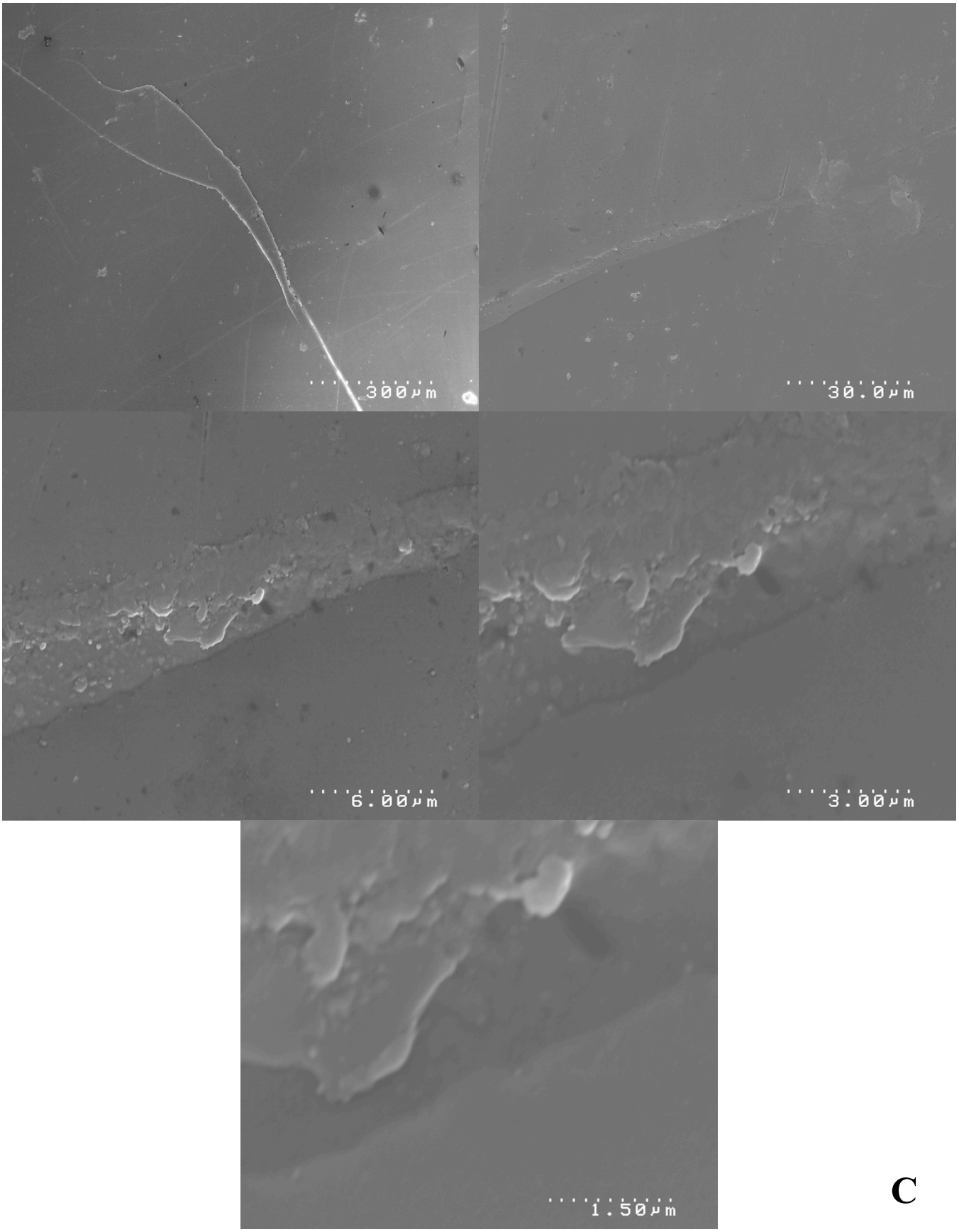

C

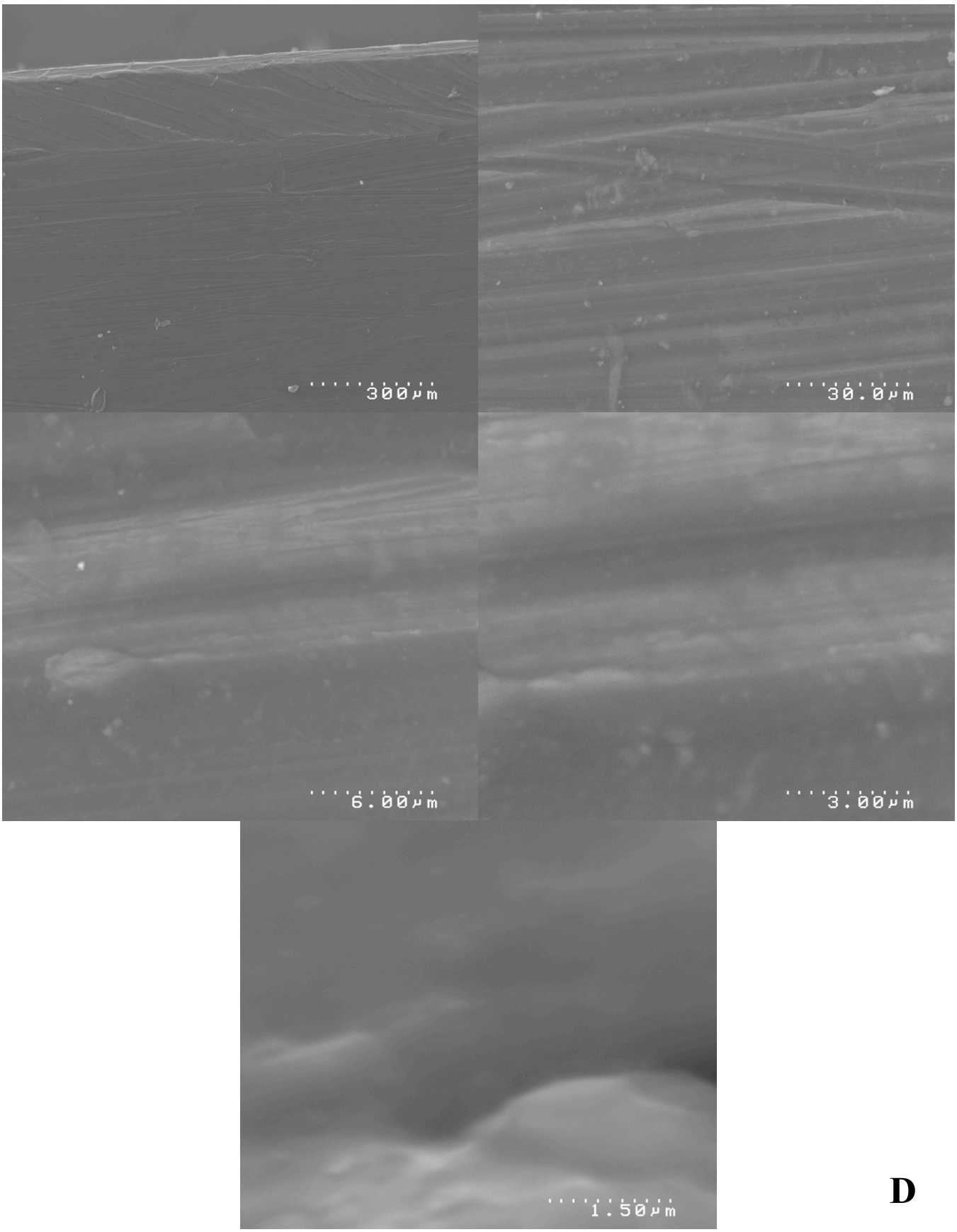

Fig. 4.7: Surface SEM images of system (7-1) [A: 0, B: 5, C: 10, D: 13] %TMOS.

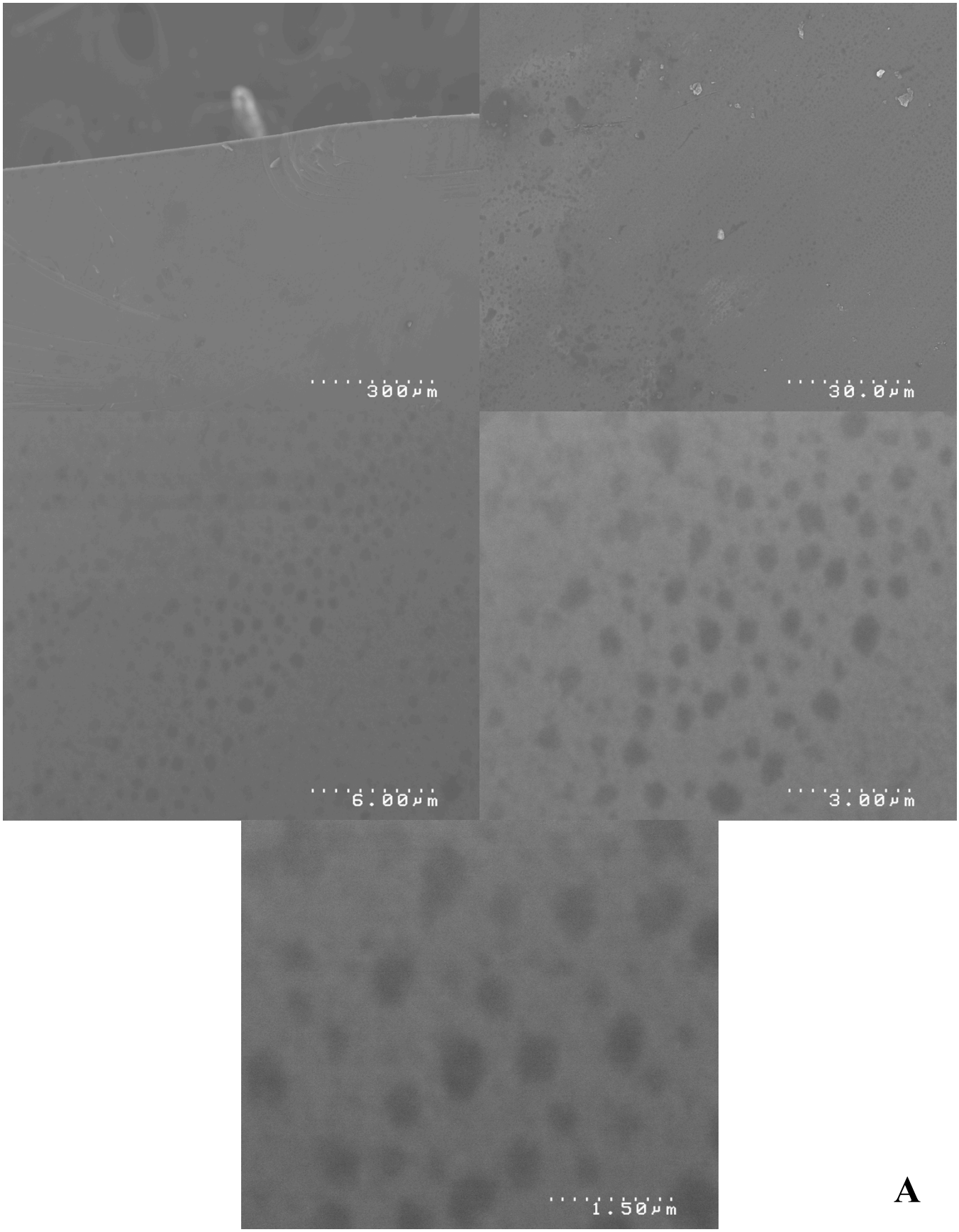

A

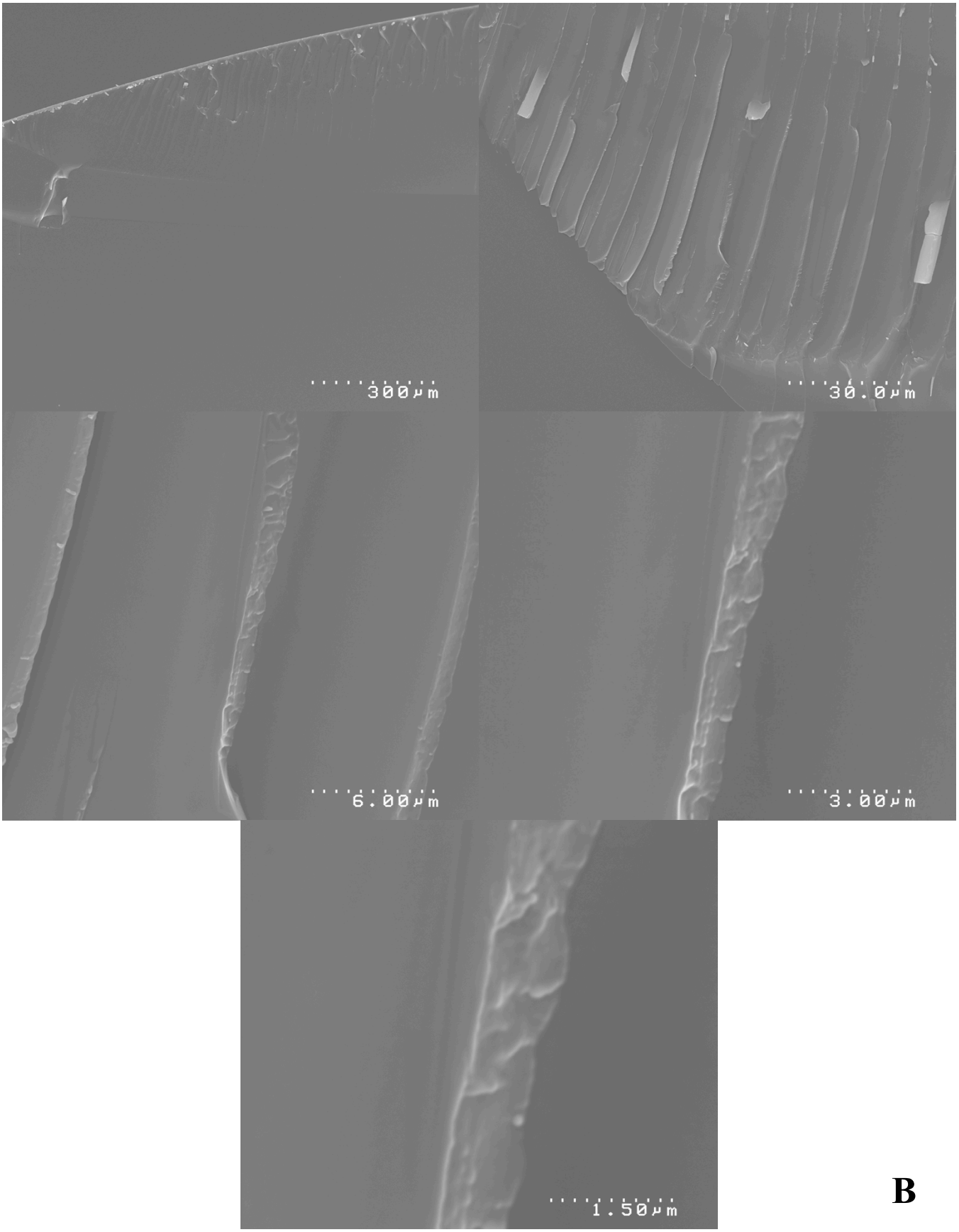

B

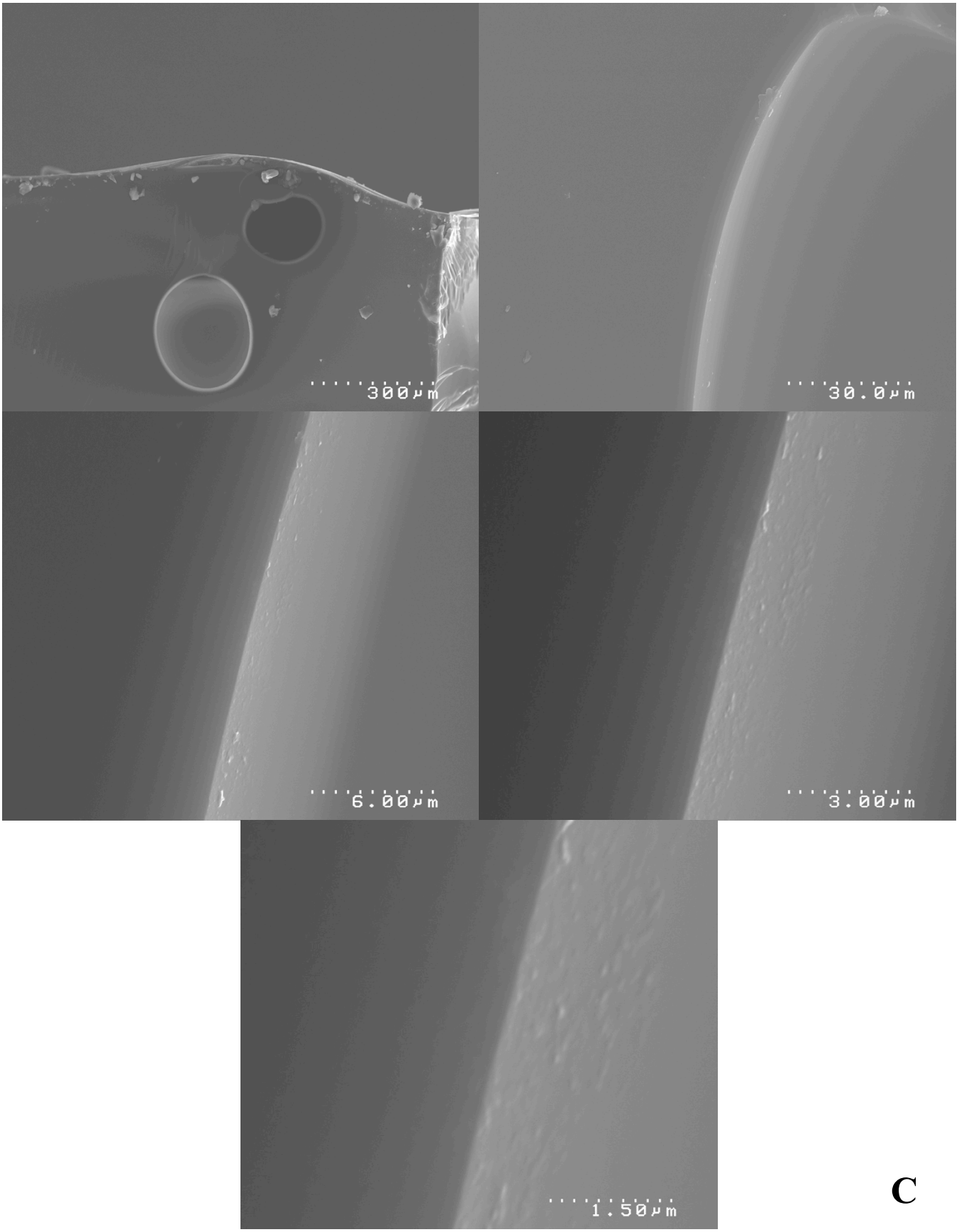

C

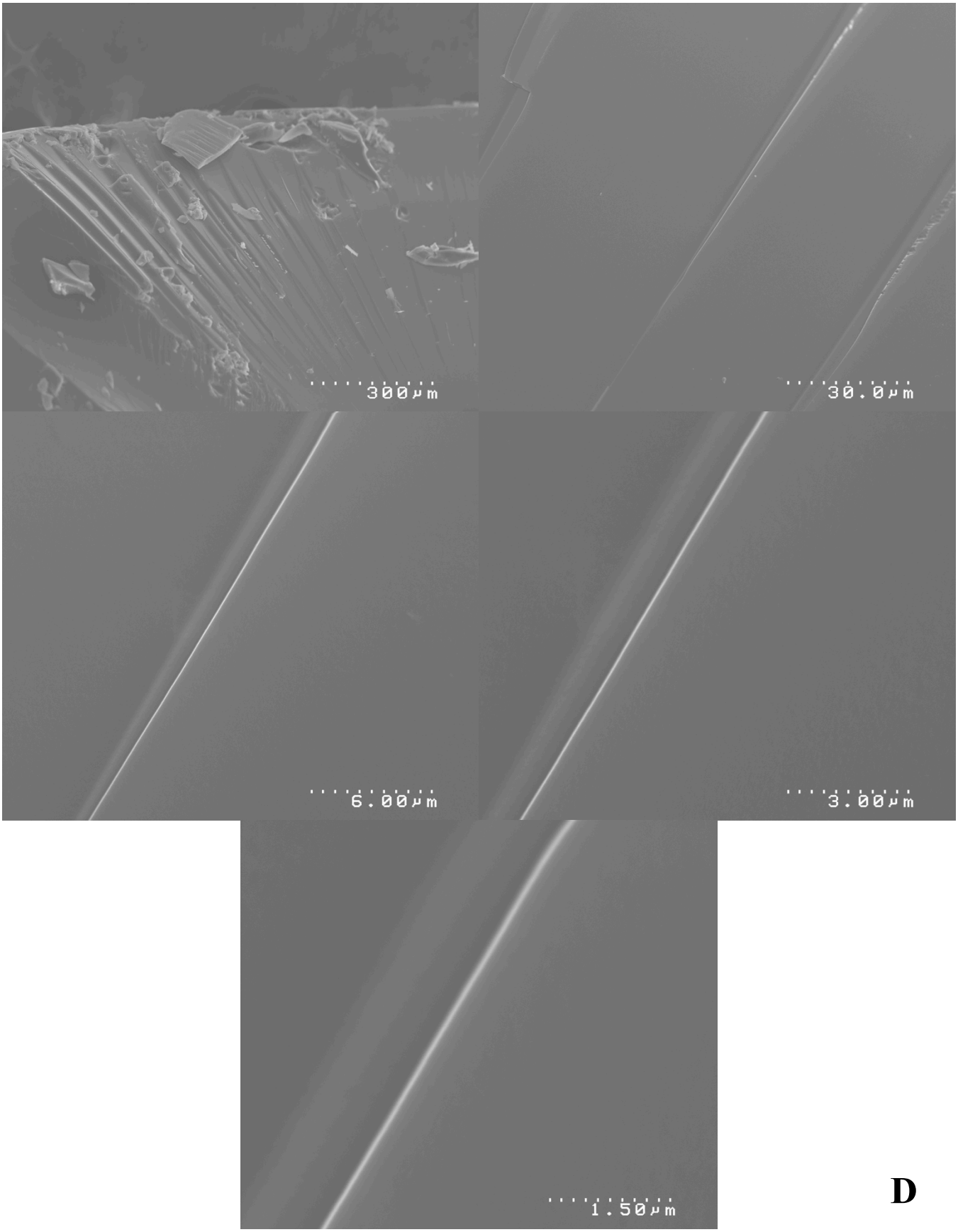

Fig. 4.8: Cross section SEM images of system (7-1) [A: 0, B: 5, C: 10, D: 13] %TMOS.

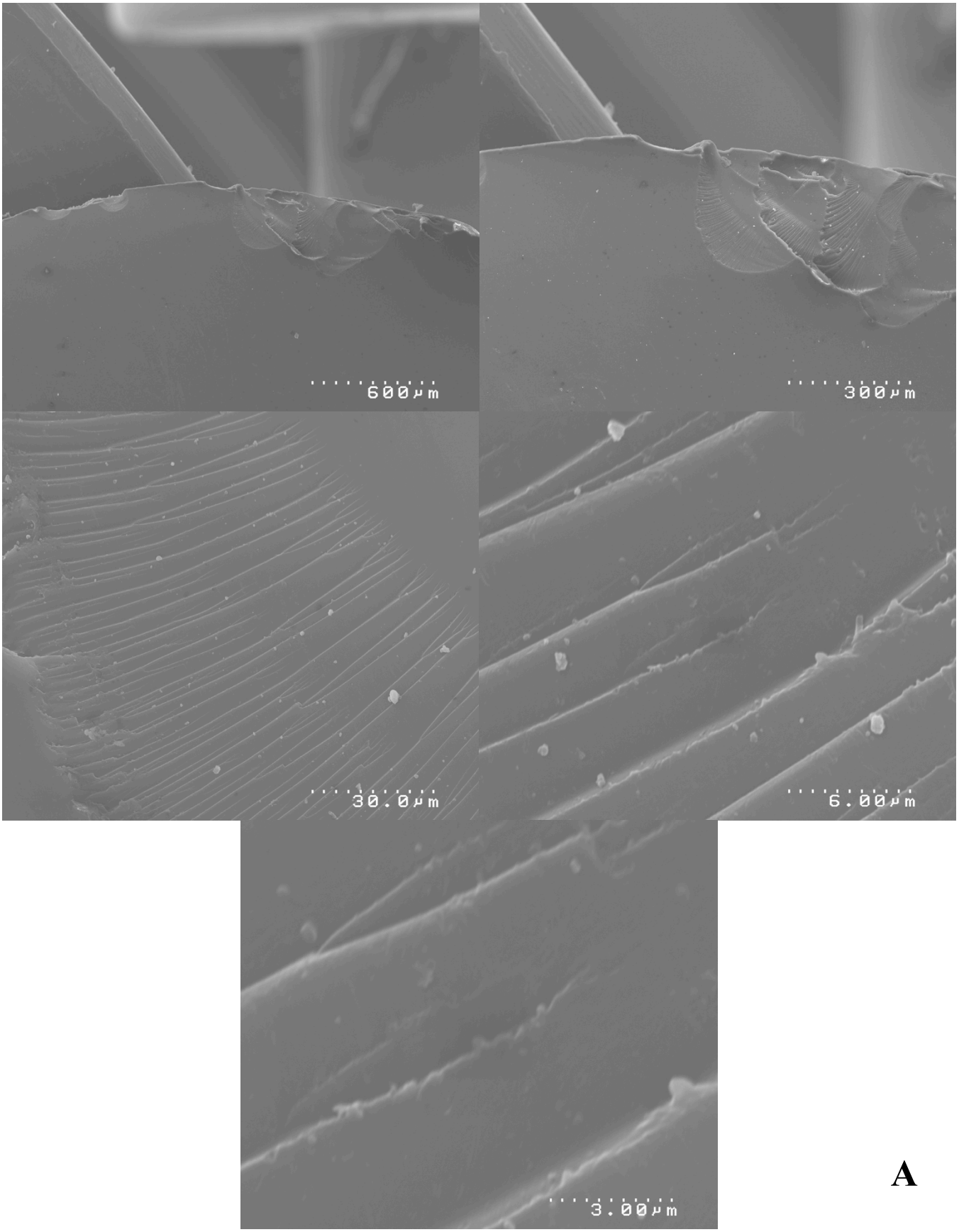

A

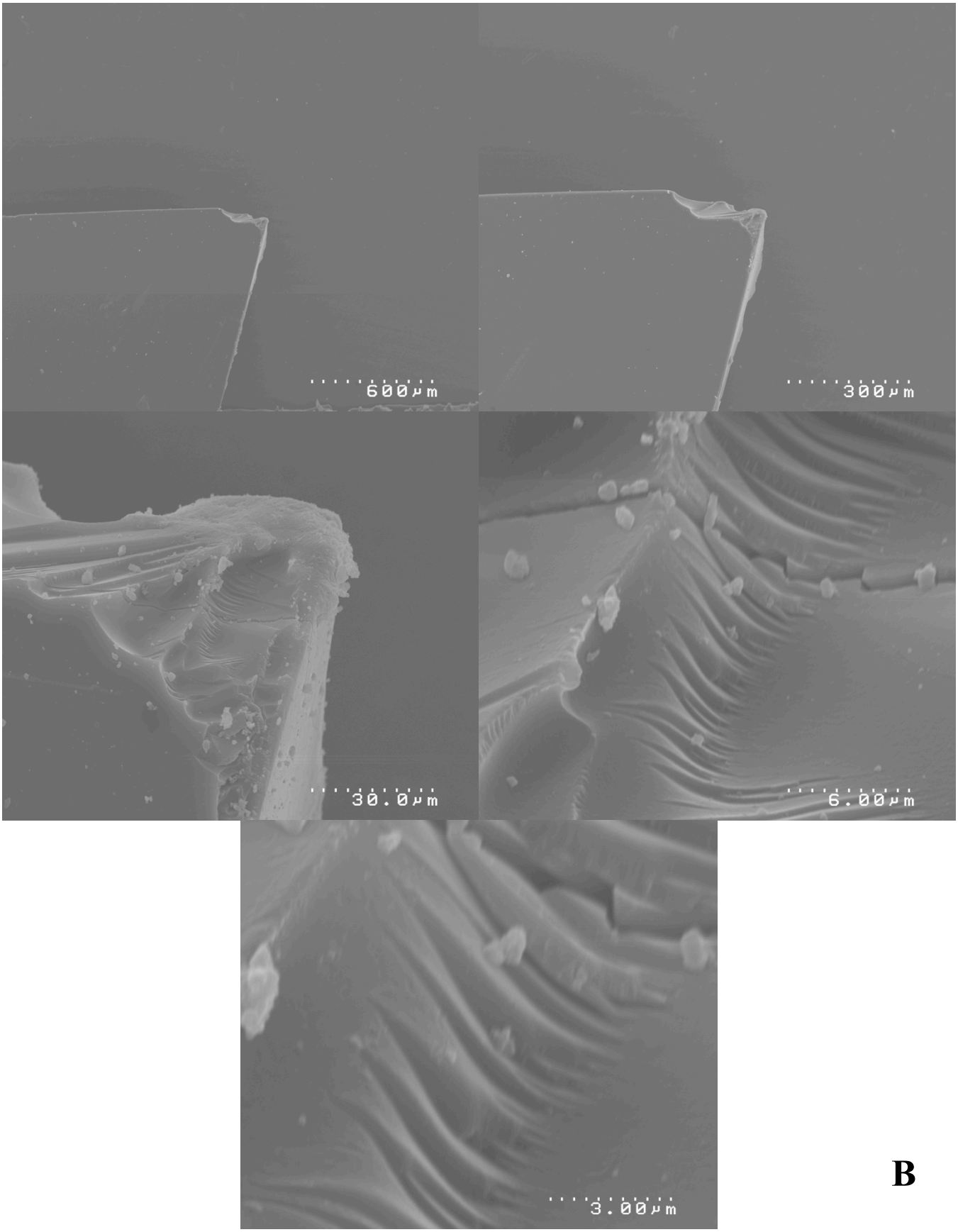

B

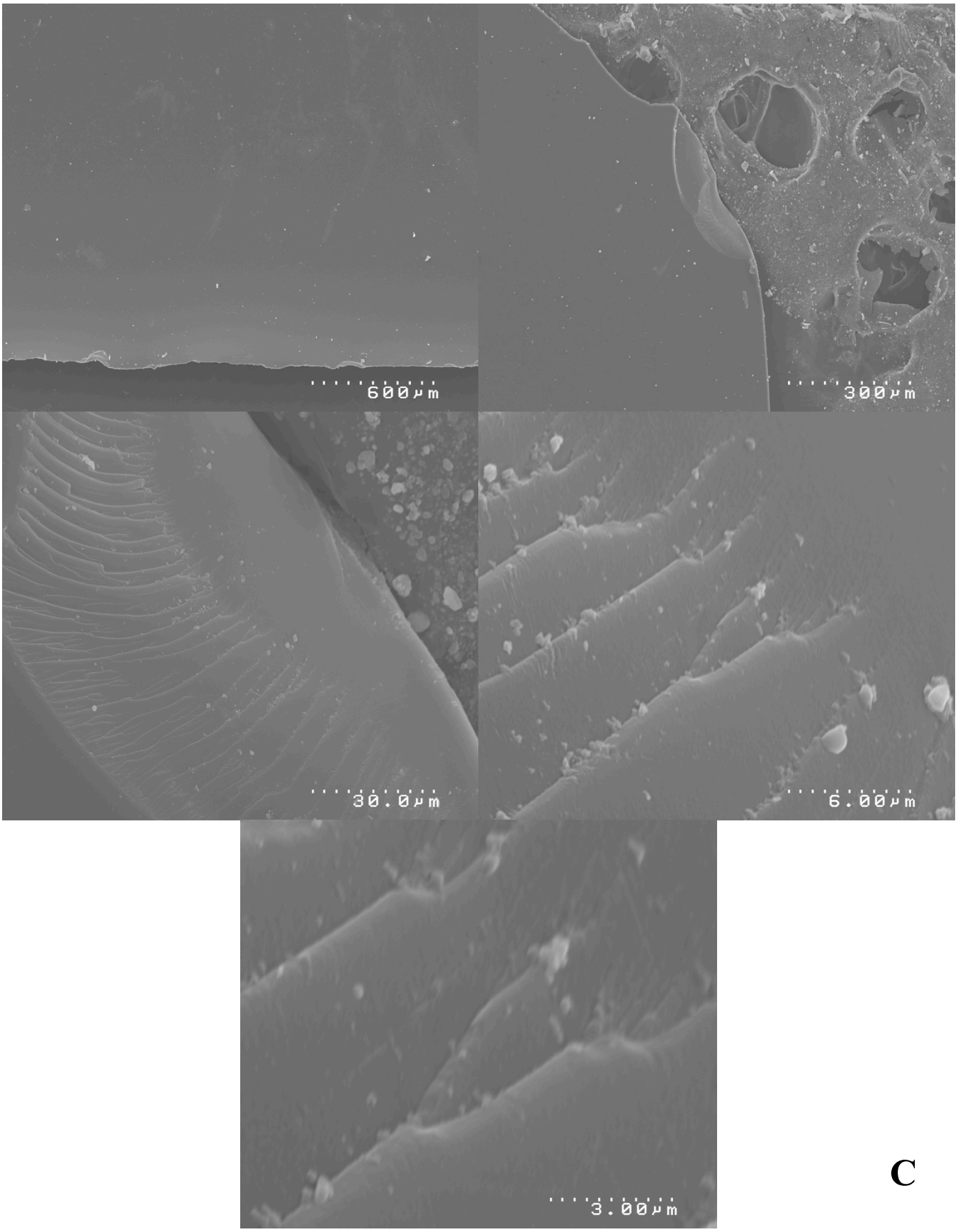

Fig. 4.9: Surface SEM images of system (7-2) [A: 2, B: 5, C: 20] %TMOS.

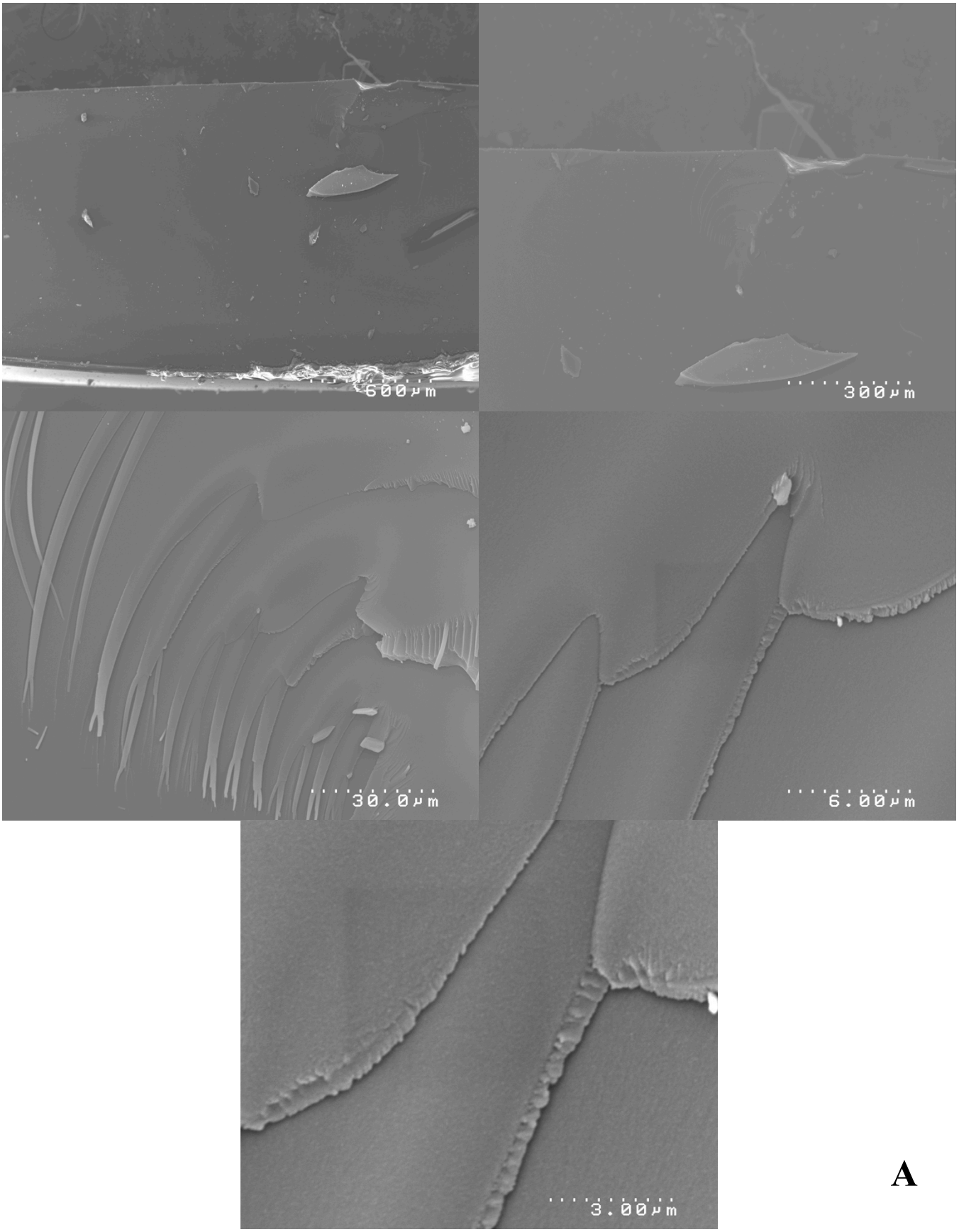

A

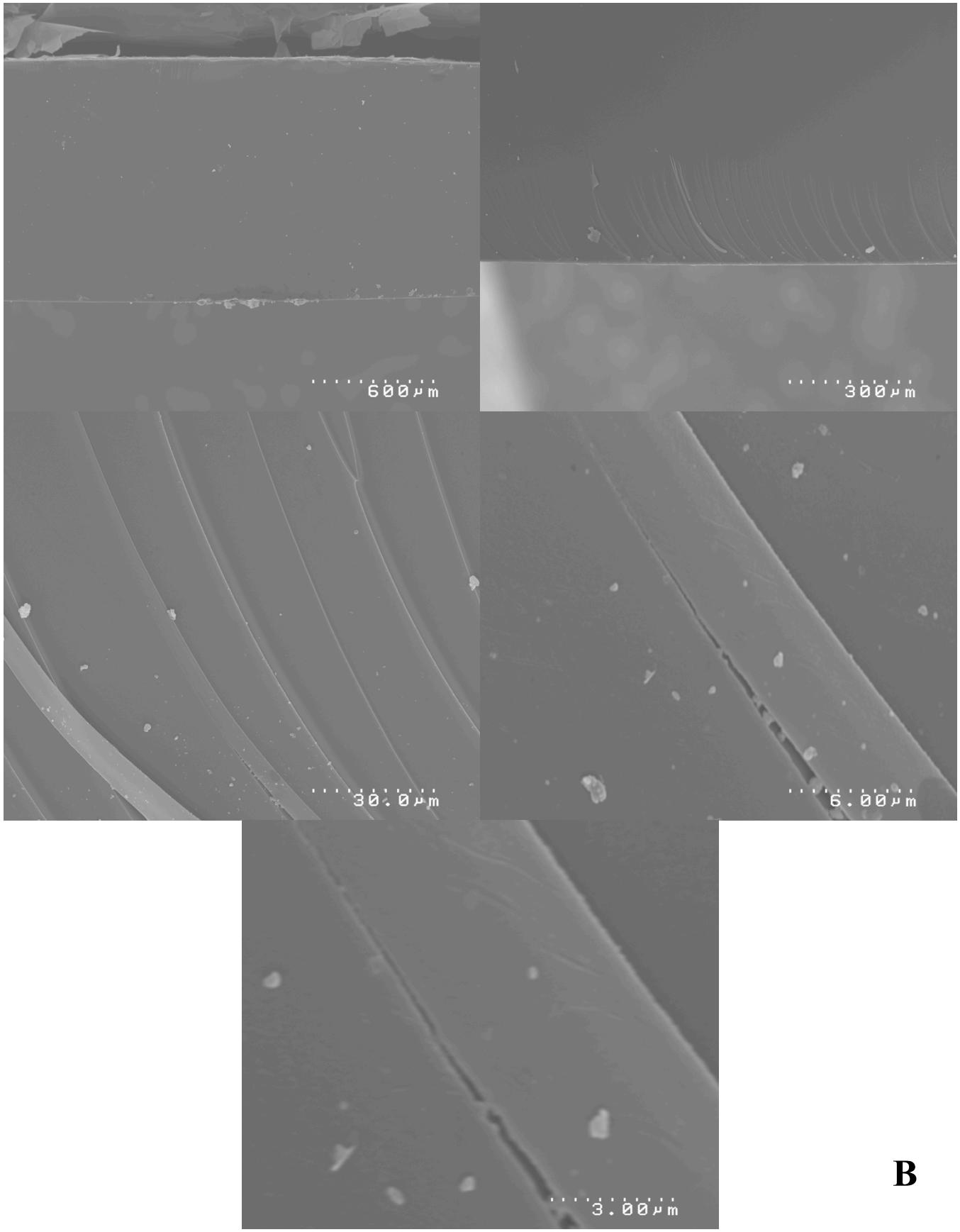

B

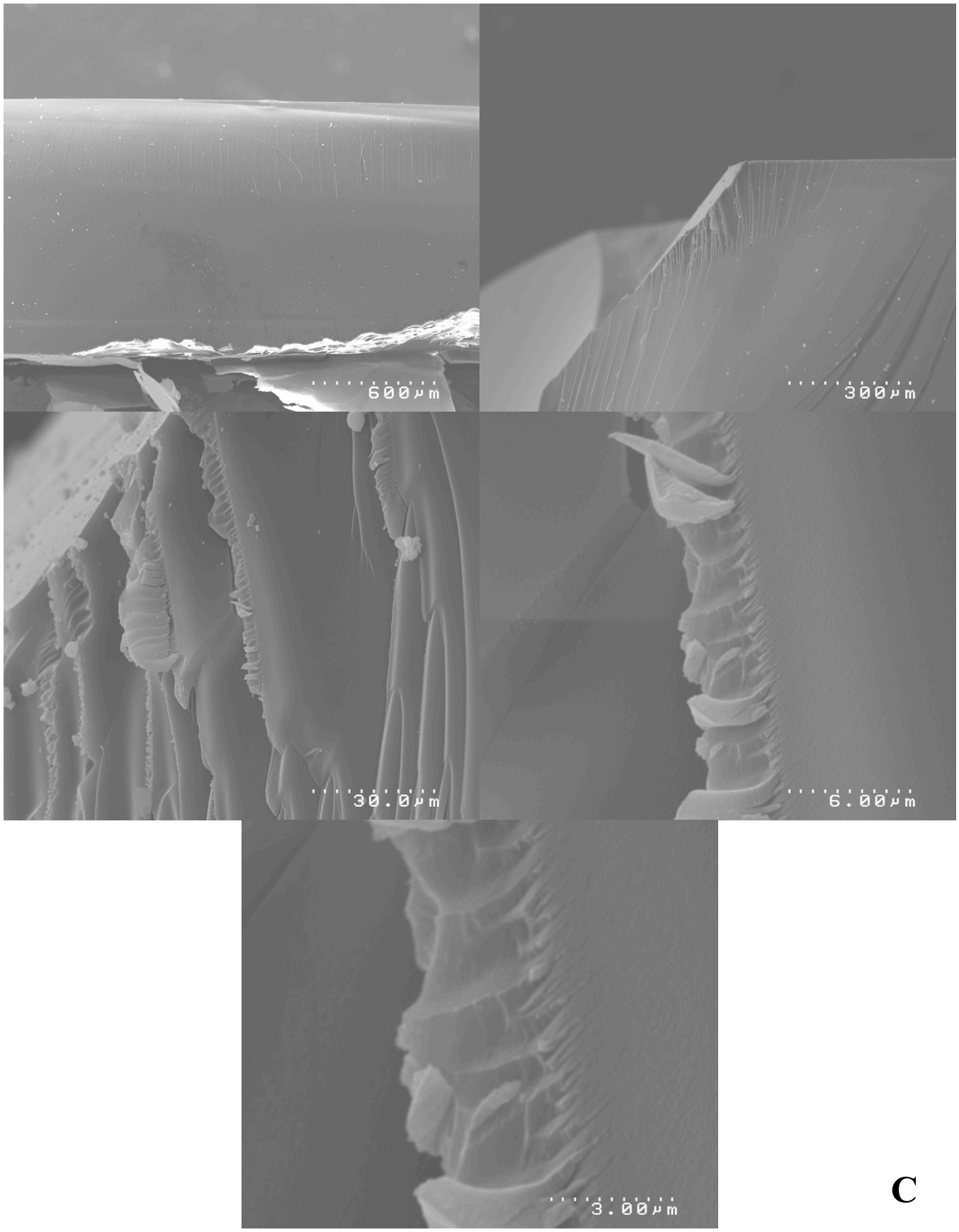

Fig. 4.10: Cross section SEM images of system (7-2) [A: 2, B: 5, C: 20] %TMOS.

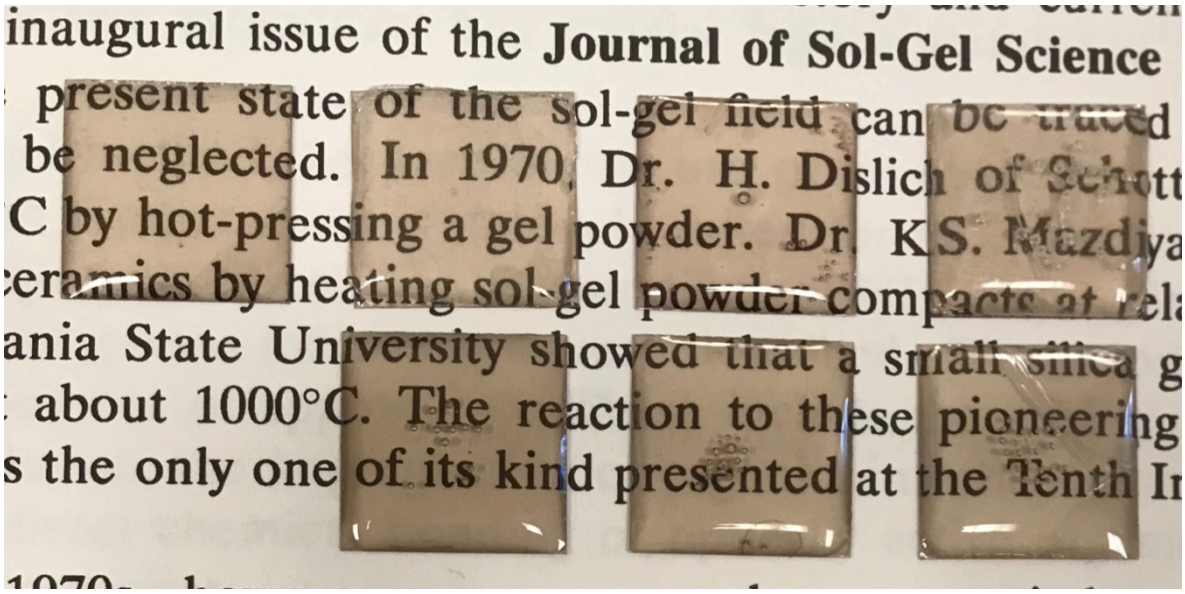

Fig. 4.11: images of coated mica samples **(top row left to right)** sys (7-1) (0, 5, 10, 13) %TMOS, **(down row left to right)** sys (7-2) (5, 10, 20) %TMOS.

4.5 Fourier Transform Infrared Spectroscopy (ATR-FTIR)

The melting gel materials were studied by FTIR spectroscopy, which revealed the presence of various chemical groups corresponding to the phenyl-substituted siloxanes, tetra-functional siloxanes and co-solvents, as well as groups formed after the reactions with water (hydrolysis) and between precursors and co-precursors (polycondensation). Vibration bands at around the same frequencies were found for similar systems, with some differences in their intensities. These changes in intensity and position are the basis for understanding the reactions and, consequently, the corresponding chemical groups within the solid network. Variations in the network structures result from differences in the hydrolysis rates and the nature of the precursors.

Figure 4.12 shows the FTIR-ATR spectra of the organic-inorganic hybrid coatings

after consolidation for the samples with TEOS as the tetra-functional addition. These include systems (1-1), (1-2), (3-1), and (3-2). The major IR band assignments are listed in Tables 4.2, 4.3, 4.4, and 4.5 for sys (1-1), (1-2), (3-1), and (3-2) respectively.

Figure 4.13 shows the spectra for the samples with TMOS precursor, which include systems (5-1), (5-2), (7-1), and (7-2). Tables 4.6, 4.7, 4.8, and 4.9 listed the major peaks for systems (5-1), (5-2), (7-1), and (7-2) respectively. In all cases, the spectra were normalized according to the maximum peak intensity.

The presence of phenyl groups is apparent in the hybrid glasses even after all the reactions of hydrolysis and polycondensation and also the thermal treatment. The presence of the organic groups was identified by the occurrence of the following absorption peaks in all systems: ν_{asym} CH from C_6H_5 at 3073 cm^{-1}, ν_{sym} CH from C_6H_5 at 3049 cm^{-1}, ν_{asym} CH_3 at 2977 cm^{-1}, ν_{sym} CH_3 at around 2924 cm^{-1} . All of these peaks increase in their intensity with increasing TROS% and then decrease near the solubility limit. The presence of the vibration of phenyl groups bonded to the silica matrix was indicated by the vibration ν C–C from C_6H_5 at 1429 cm^{-1}, δ_{sym} CH_3 from Si–CH_3 configuration at 1266 cm^{-1}, ρ CH_3 at 730 cm^{-1}, and τ C–C from the phenyl ring deformation at 692 cm^{-1}.

There is evidence for the existence of Si–C direct bonds in the FT- IR spectra by the presence of the absorbance peaks at ν Si–C from Si-C_6H_5 at 1129 cm^{-1}. This peak confirmed the presence of phenyl groups on the silica surface, and δ_s CH_3(Si-CH_3) from Si–CH_3 at 1265 cm^{-1}. The FTIR- spectra show that Si–C bonds remain intact during the hydrolysis-polycondensation reactions and gelation. The non-hydrolyzable Si–CH_3 and Si–

C_6H_5 bonds are retained as a part of the polymer network in the consolidated hybrid glasses.

The characteristic vibrations indicative of the Si–O–Si bonds in the organically modified glass network are found at around (778-795) cm^{-1} for ν_{sym} Si–O–Si, at (849-895) cm^{-1} for δ Si–O–C, at (1004-1014) cm^{-1} due to the ν_{asym} Si–O–Si (transverse) and at 1053 cm^{-1} due to ν_{asym} Si–O–Si (longitudinal). The band at 994 cm^{-1} corresponds to the Si-OH stretching of silanol groups, which increase with increasing tetra-alkoxysilane concentration. Furthermore, the broad band at around 3490 cm^{-1} corresponds to the stretching vibrations of O-H groups, which do not appear in two component melting gels. What is interesting about the three component gels is that the O-H group stretching vibration becomes stronger with increasing tetra-alkoxysilane addition as it will be discussed in more detail for each system later on. It appears that adding TEOS or TMOS increases the number of residual hydroxyls on the silica surface. This is supported by the contact angle measurements, which show that three component gels are less hydrophobic than two component gels. In addition, it appears that more water is released during hydrolysis and polycondensation reactions.

Obviously, the peak intensities increase dramatically when adding the tetra-alkoxide component to the melting gel and then decrease near the solubility limits. The peaks shift to higher wavenumbers in systems with TEOS due to the longer time of hydrolysis-polycondensation in the three-component based system. While in systems with TMOS the peaks shift to a lower wavenumber due to shorter time of gelation as mentioned in Table 4.10.

Another important observation to be made from FTIR is that most of the absorption bands of silicon-containing sol-gel derived materials are located in the region of 1265 to 778cm^{-1}. However, it is noticeable that the intensity ratio of the ν_{as}Si-O-Si (TO) absorption peak to the νC-C (C_6H_5) absorption peak is higher than that in two component systems. This ratio increases with increasing the amount of tetra-alkoxide in the three component systems, which is exclusively associated with the more intense absorption of the siloxane groups due to the on-going condensation reactions along with increasing the tetra-alkoxide weight percentage as shown in Figure 4.14 for all systems with tetra-alkoxide. These observations are in agreement with earlier studies on silica sol-gel process [66,166].

Significantly, as shown in Figure 4.14, the point when the ν_{as}Si-O-Si (TO)/ νC-C (C_6H_5) ratio reaches a maximum. In other words, at this amount of TROS, the hydrolysis reaction is being overtaken by condensation reactions, and thus more siloxane species are being generated at the expense of the silanol species, despite the fact that phenyl group is constant. After that point, the structure is incapable of continuing to extend the siloxane 3D network, because there are no more bridging oxygens present from the hydrolysis reaction of mono and di-substituent precursors. Any further increase in the ratio may be a sign of phase separation between the siloxane network and an insoluble phase. To understand what is happening requires other experimental techniques, for example, light or x-ray scattering.

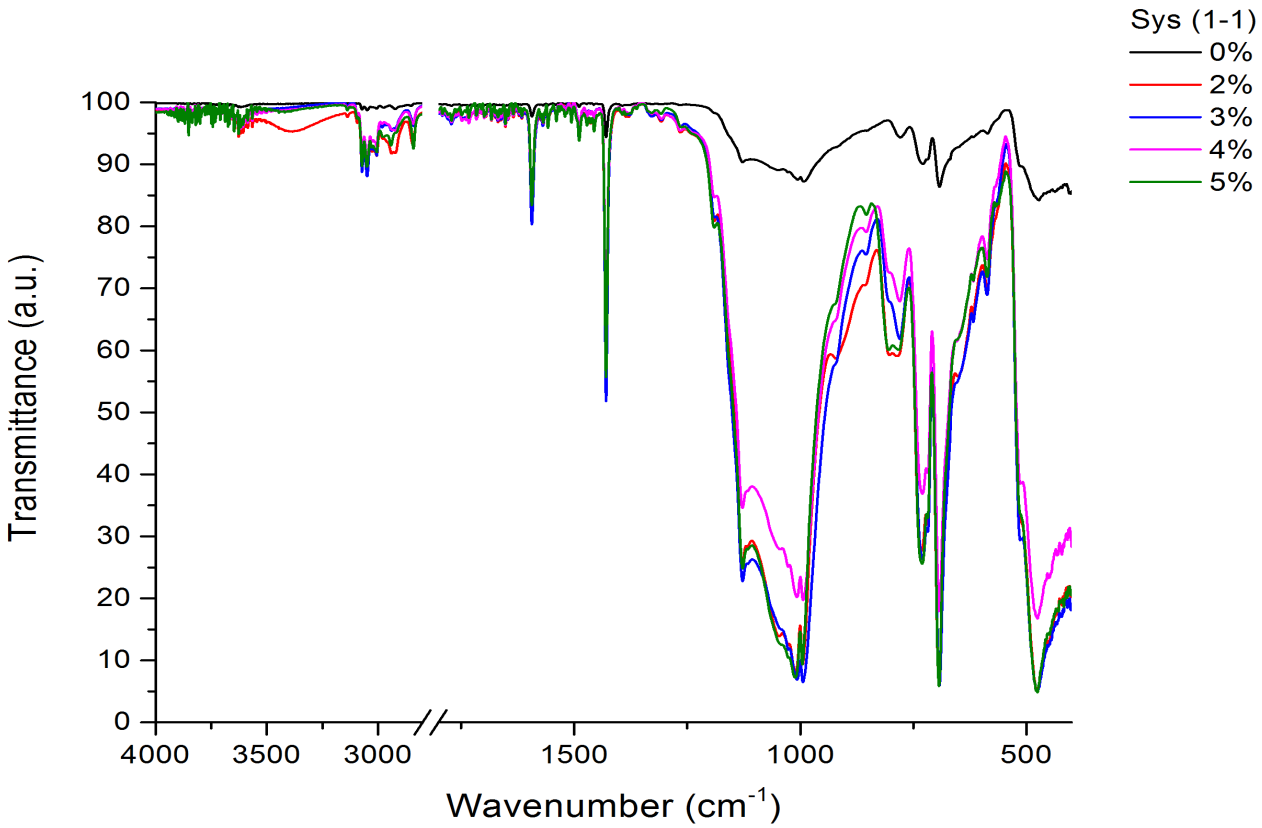
Sys (1-1)
0%
2%
3%
4%
5%
Transmittance (a.u.)
Wavenumber (cm-1)
100
90
80
70
60
50
40
30
20
10
0
4000
3500
3000
1500
1000
500

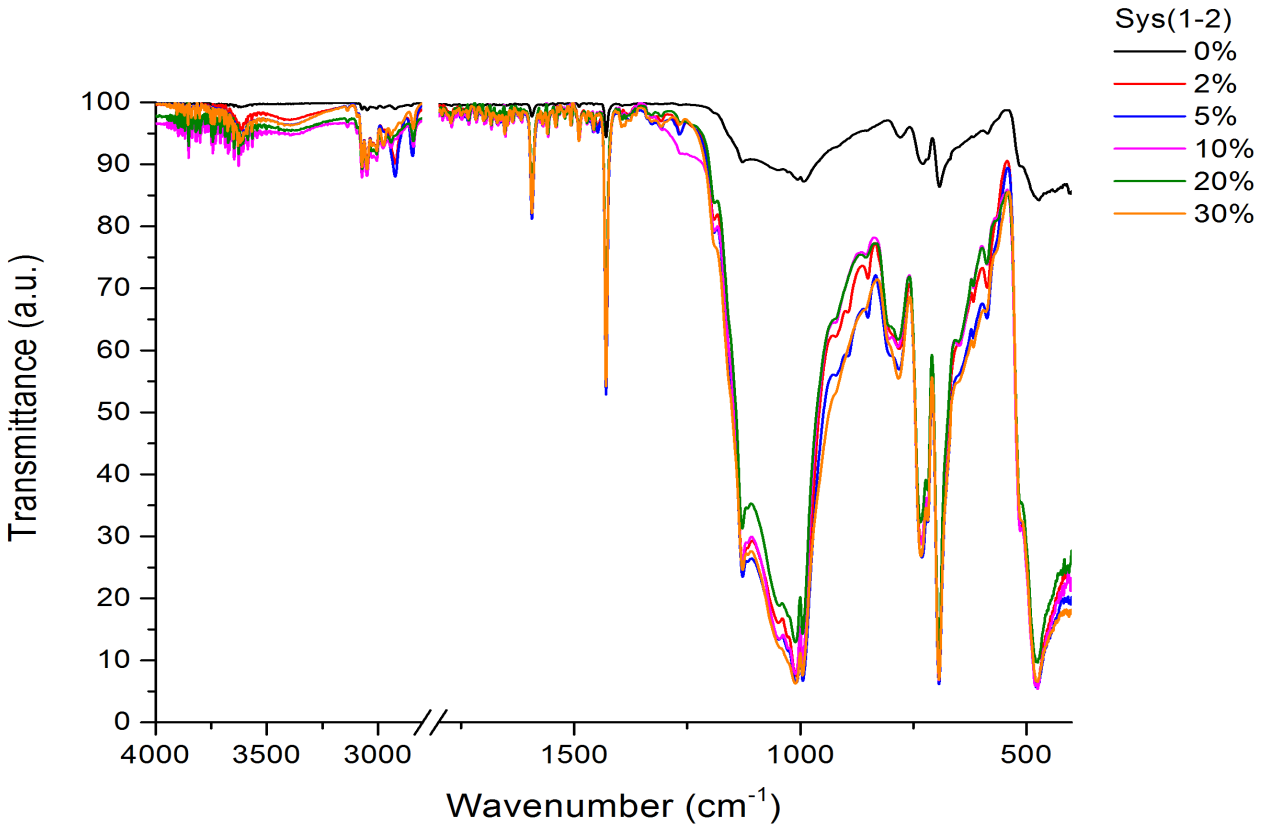
Sys(1-2)
0%
2%
5%
10%
20%
30%
Transmittance (a.u.)
Wavenumber (cm-1)
100
90
80
70
60
50
40
30
20
10
0
4000
3500
3000
1500
1000
500

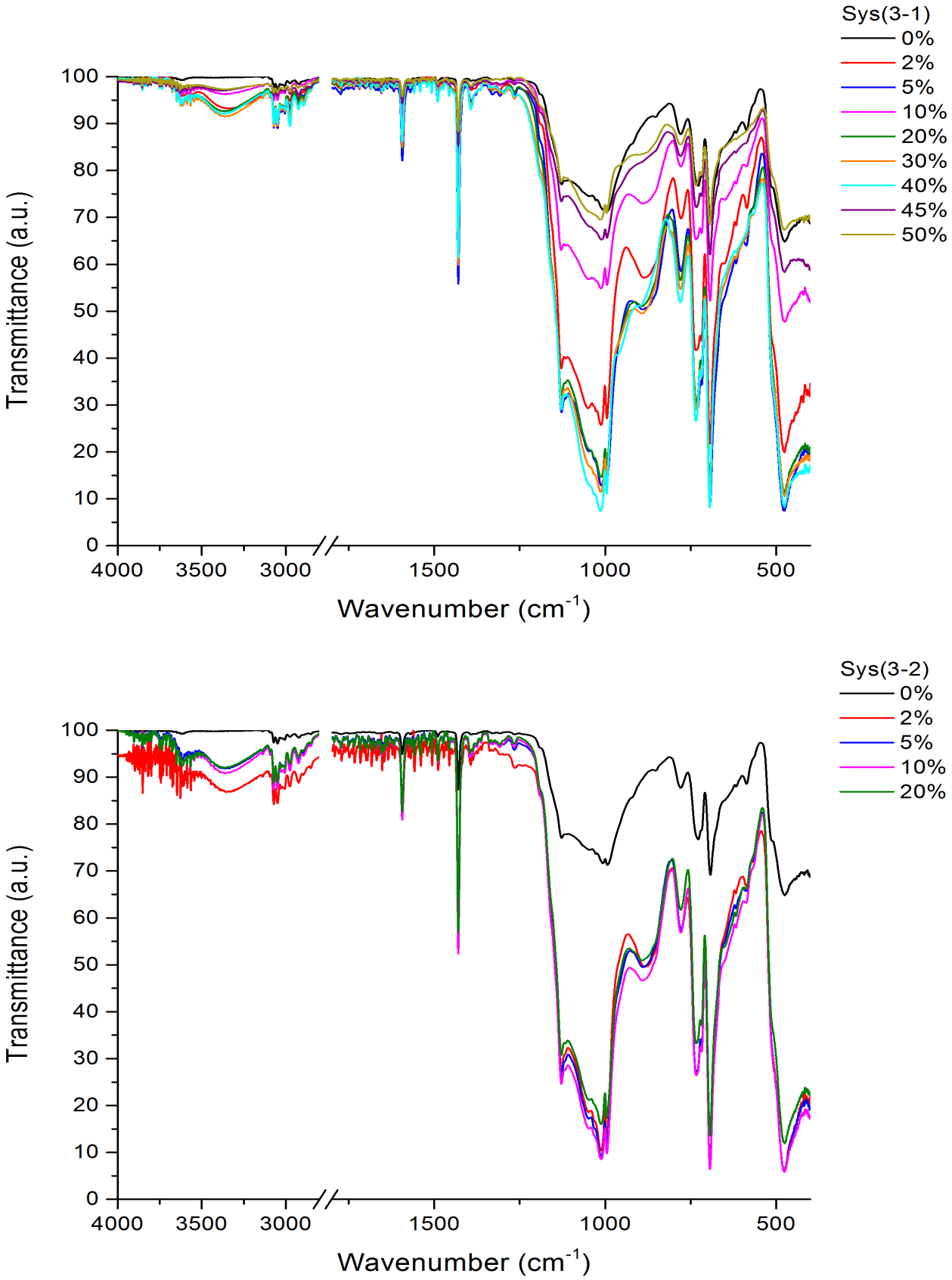

Figure 4.12: The FT-IR spectra of the melting gels after their consolidation for sys (1-1), (1-2), (3-1), and (3-2) with TEOS.

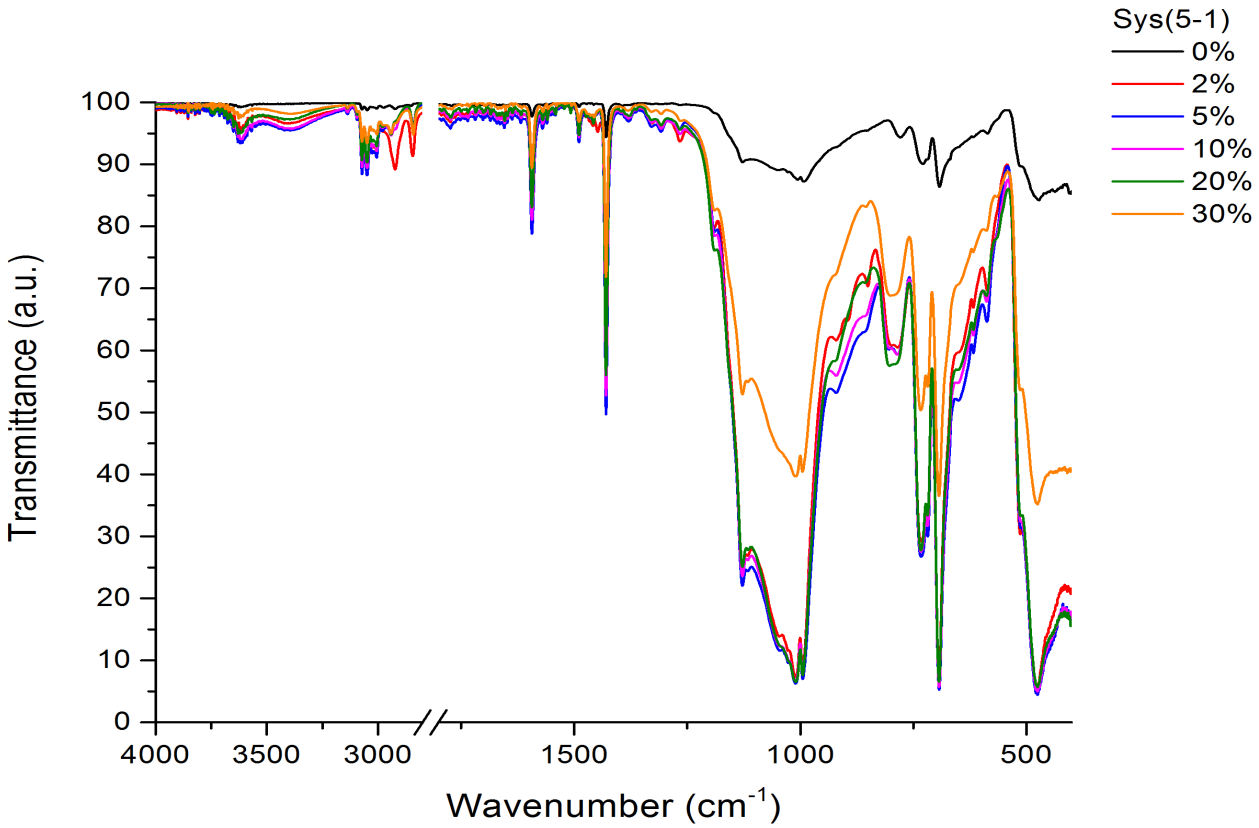
Sys(5-1)
0%
2%
5%
10%
20%
30%
Transmittance (a.u.)
Wavenumber (cm-1)
100
90
80
70
60
50
40
30
20
10
0
4000
3500
3000
1500
1000
500

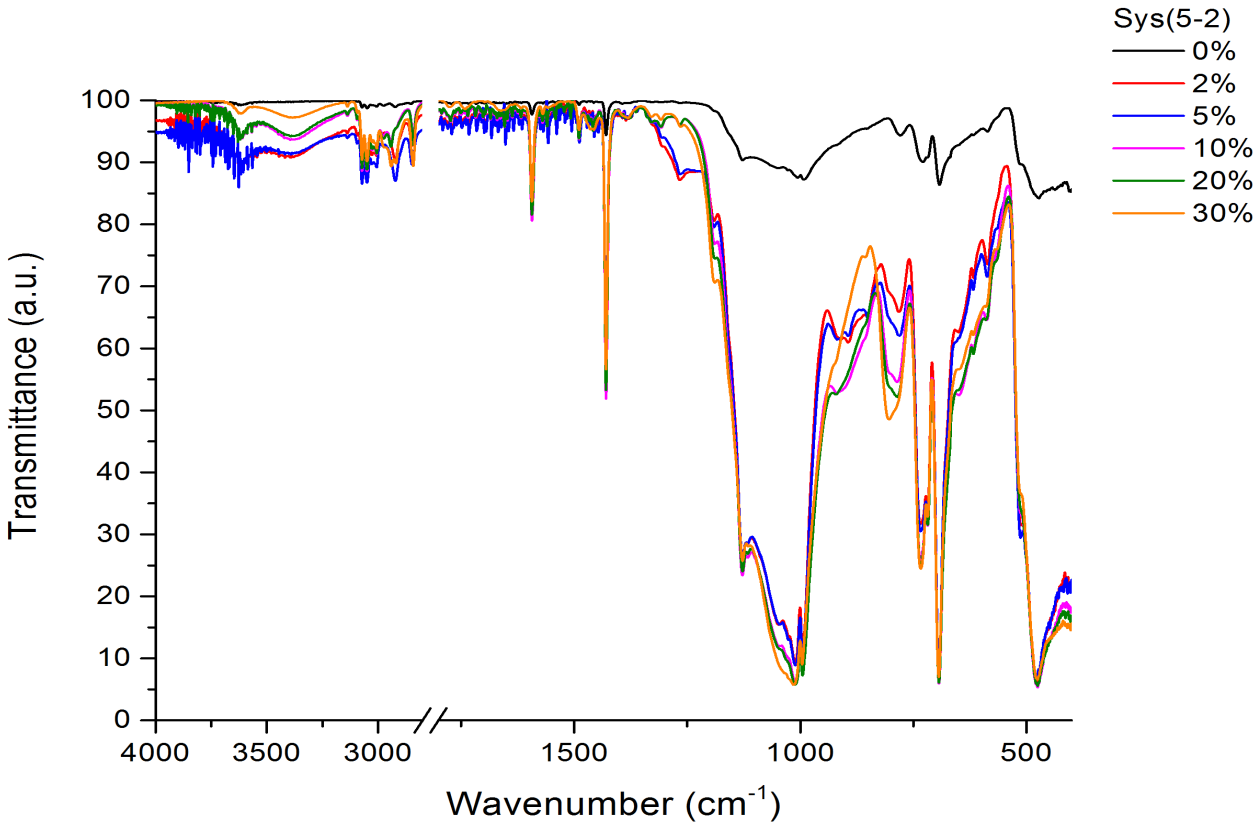
Sys(5-2)
0%
2%
5%
10%
20%
30%
Transmittance (a.u.)
Wavenumber (cm-1)
100
90
80
70
60
50
40
30
20
10
0
4000
3500
3000
1500
1000
500

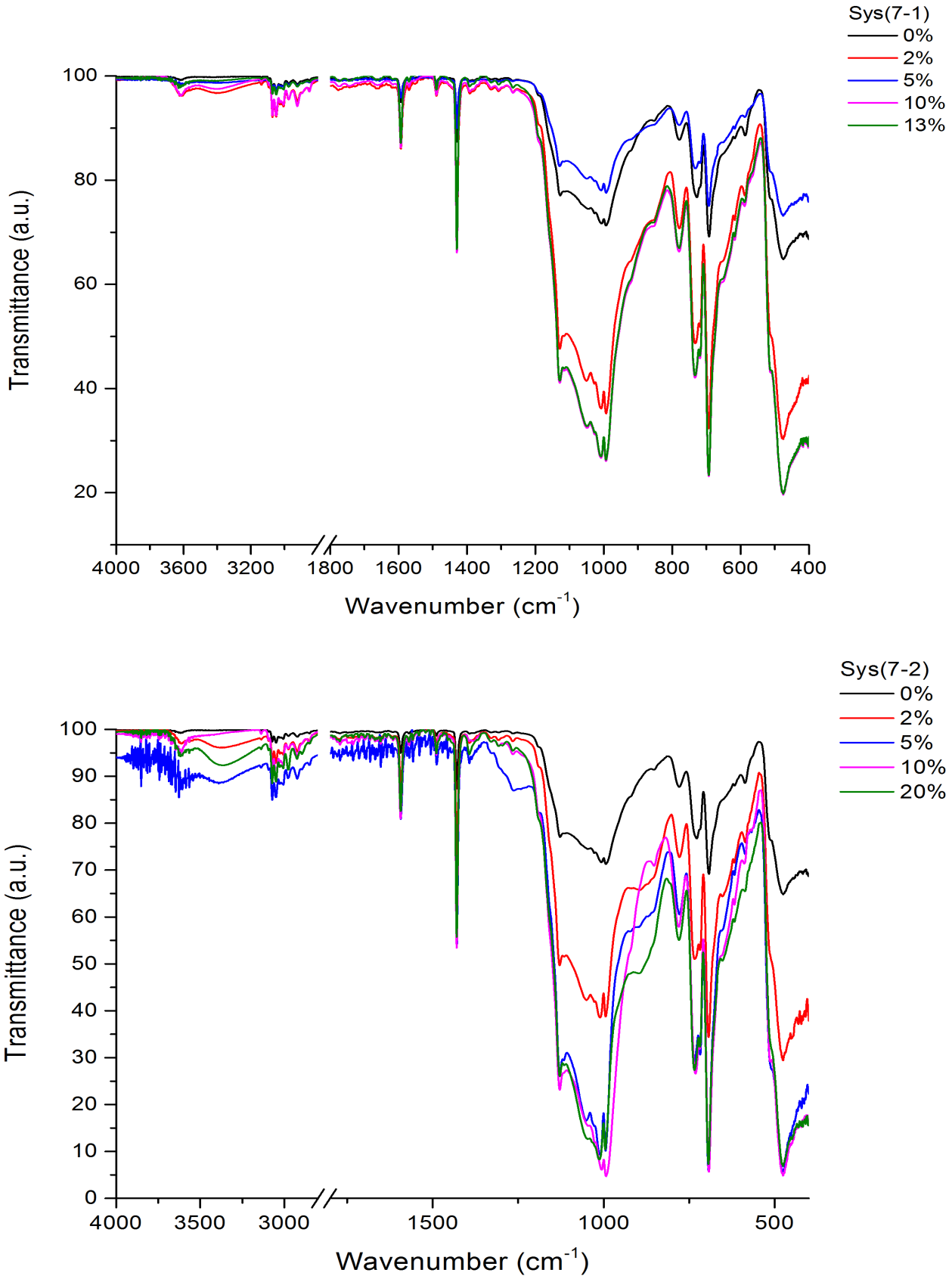

Figure 4.13: The FT-IR spectra of the melting gels after their consolidation for sys (5-1), (5-2), (7-1), and (7-2) with TMOS.

Table 4.2: Peak Assignments of FTIR Spectra for sys (1-1).

System ID	Sys (1-1)	Sys (1-1)	Sys (1-1)	Sys (1-1)	Sys (1-1)	**Assignments**	**Ref.**
TEOS%	0	2	3	4	5		
Peaks (cm^{-1})	3627	3629	3629	3629	3629	νO-H from free OH/ alcoholic	
	-	3383	3386	3390	3391	νO-H associated with hydrogen bonding on the organic modified silica surface	136
	-	3138	3138	3138	3138	-	
	3093	3093	3093	3093	3093	ν (CH)ring	
	3073	3073	3073	3073	3073	ν_{as} (CH)ring	137,138,139
	3050	3050	3050	3050	3050	ν_{s} (CH)ring	137,138,139
	3006	3006	3006	3006	3006	ν (CH)ring	
	2977	2977	2977	2977	2977	ν_{as} CH_3	137,138,139
	-	2939	2939	2939	2941		
	2924	2940	2919	2919	2917	ν_{as} CH_2	136,140,141
	2852	2842	2842	2842	2842	ν_{s} CH_2	136,140,141
	1593	1593	1593	1593	1593	γ CH (C_6H_5)	142
	1489	1489	1489	1489	1489	ν C=C (C_6H_5)	143
	1429	1429	1429	1429	1429	ν C-C (C_6H_5)	144,145,146
	1265	1265	1265	1265	1265	δ_{s} CH_3(Si-CH_3)	137,138,147
	1128	1128	1128	1128	1128	ν Si-C (from Si-C_6H_5)	148
	1050	1050	1050	1050	1050	ν_{as} Si-O-Si (LO Mode)	137,149
	1004	1011	1007	1007	1011	ν_{as} Si-O-Si (TO Mode)	137,149
	994	994	994	994	994	ν Si-O(H)	

	853	857	854	854	853	δ Si-O-C from alkoxy This should be correlated with the presence of CH_2	137,149
	-	806	805	805	806	-	
	780	782	780	780	780	ν_s Si-O-Si	29
	730	730	730	730	730	ρCH_3+the C_6H_5 ring breathing	150
	716	716	716	716	716	σ CH_3	
	692	692	692	692	692	The C_6H_5 ring plane deformation + τ C-C from C_6H_5 ring	151,152, 145,146
	668	648	648	648	648	ν_s Si-O???	
	-	617	617	617	617	$\sigma(\text{ring})_{in}$	
	584	586	586	586	586	δ_s O-Si-O	
	473	477	477	477	477	δ Si-O-Si	141,153,154

ν, stretching vibration; $\boldsymbol{\nu_s}$, symmetric stretching vibration; $\boldsymbol{\nu_{as}}$, antisymmetric stretching vibration; **δ**, deformation vibration; $\boldsymbol{\delta_s}$, symmetric deformation vibration (bending); $\boldsymbol{\delta_{as}}$, antisymmetric deformation vibration (bending); **τ**, out-of-plane bending (twisting); **ρ,** rocking; **γ**, out-of-plane deformation vibration; **σ,** out-of-plane ring deformation vibration; LO, longitudinal optical; TO, transversal optical.

Table 4.3: Peak Assignments of FTIR Spectra for sys (1-2).

System ID	Sys (1-2)	Sys (1-2)	Sys (1-2)	Sys (1-2)	Sys (1-2)	Sys (1-2)	Assignments	Ref.
TEOS%	**0**	**2**	**5**	**10**	**20**	**30**		
	3627	3629	3629	3627	3627	3629	νO-H from free OH/ alcoholic	
	-	3393	3393	3390	3391	3393	νO-H associated with hydrogen bonding on the organic modified silica surface	136
	-	3138	3138	3138	3138	3138	-	
	3093	3093	3093	3093	3093	3093	ν (CH)ring	
	3073	3072	3072	3072	3072	3072	ν_{as} (CH)ring	137,138,139
	3050	3049	3049	3049	3049	3049	ν_{s} (CH)ring	137,138,139
	3006	3006	3006	3006	3006	3006	ν (CH)ring	
	2977	2977	2977	2977	2977	2977	ν_{as} CH_3	137,138,139
	-	-	-	2942	2942	2940	ν_{s} C-H???	
	2924	2924	2924	2918	2918	2924	ν_{as} CH_2	136,140,141
	2895	-	-	2896	2898	2898	ν_{s} CH_3	
	2852	2844	2844	2841	2841	2841	ν_{s} CH_2	136,140,141
	1593	1593	1593	1593	1593	1593	γ CH (C_6H_5)	142
	1489	1490	1490	1490	1490	1490	ν C=C (C_6H_5)	143
	1429	1429	1429	1429	1429	1429	ν C-C (C_6H_5)	144,145,146
	1266	1266	1264	1266	1267	1267	δ_{s} CH_3(Si-CH_3)	137,138,147
	-	1190	1190	1190	1190	1190	-	
	1128	1128	1128	1128	1128	1128	ν Si-C (from Si-C_6H_5)	148
	1050	1049	1049	1048	1048	1047	ν_{as} Si-O-Si (LO	137,149

						Mode)	
1004	1008	1008	1011	1011	1011	ν_{as} Si-O-Si (TO Mode)	137,149
994	994	994	994	994	994	ν Si-O(H)	
853	850	851	856	855	853	δ Si-O-C from alkoxi	137,149
780	780	780	780	780	780	ν_s Si-O-Si	29
730	732	732	732	732	732	ρCH_3+the C_6H_5 ring breathing	150
716	717	717	717	717	717	Ø C-H???	
692	694	694	694	694	694	The C_6H_5 ring plane deformation + τ C-C from C_6H_5 ring	151,152 145,146
668	646	646	646	646	646	ν_s Si-O???	
584	586	586	586	586	586	δ_s O-Si-O	
473	477	477	477	477	477	δ Si-O-Si	141,153,154

ν, stretching vibration; **ν_s**, symmetric stretching vibration; **ν_{as}**, antisymmetric stretching vibration; **δ**, deformation vibration; **δ_s**, symmetric deformation vibration (bending); **δ_{as}**, antisymmetric deformation vibration (bending); **τ**, out-of-plane bending (twisting); **ρ,** rocking; **γ**, out-of-plane deformation vibration; **σ,** out-of-plane ring deformation vibration; LO, longitudinal optical; TO, transversal optical.

Table 4.4: Peak Assignments of FTIR Spectra for sys (3-1).

System ID	Sys (3-1)	Sys (3-1)	Sys (3-1)	Sys (3-1)	Sys (3-1)	Sys (3-1)	Sys (3-1)	Sys (3-1)	Sys (3-1)	**Assignments**	**Ref.**
TEOS%	0	2	5	10	20	30	40	45	50		
	3617	3613	3614	3619	3619	3618	3617	3620	3620	νO-H from free OH/ alcoholic	
	-	3335	3366	3356	3362	3356	3366	3376	3356	νO-H associated with hydrogen bonding on the organic modified silica surface	136
	3140	3140	3140	3140	3140	3140	3140	3135	3135	-	
	3094	3094	3094	3094	3094	3094	3094	3092	3094	ν (CH)ring	
	3072	3072	3072	3072	3072	3072	3072	3071	3072	ν_{as} (CH)ring	137,138,139
	3049	3049	3049	3049	3049	3050	3050	3048	3049	ν_{s} (CH)ring	137,138,139
	3006	3006	3006	3006	3006	3006	3006	3006	3006	ν (CH)ring	
Peaks	2977	2977	2977	2977	2977	2977	2977	2974	2975	ν_{as} CH_3	137,138,139
	2924	2924	2924	2924	2925	2925	2925	2923	2925	ν_{as} CH_2	136,140,141
	2895	2895	2895	2895	2895	2895	2895	2894	2895	ν_{s} CH_3	
	2850	2850	2850	2850	2850	2850	2850	2848	2850	ν_{s} CH_2	136,140,141
	1593	1593	1593	1593	1593	1593	1593	1593	1593	γ CH (C_6H_5)	142
	1490	1490	1490	1490	1490	1490	1490	1490	1490	ν C=C (C_6H_5)	143
	1429	1429	1429	1429	1429	1429	1429	1429	1429	ν C-C (C_6H_5)	144,145,146
	1394	1394	1394	1394	1394	1394	1394	1389	1389	δ_{as} CH_3	136

	1329	1329	1329	1329	1329	1329	1328	1329	1329	-	
	1266	1266	1266	1266	1266	1266	1266	1266	1264	δ_s CH_3(Si-CH_3)	137,138,147
	1128	1128	1128	1128	1128	1128	1128	1128	1128	ν Si-C (from Si-C_6H_5)	148
	1053	1049	1050	1051	1050	1051	1050	1051	1051	ν_{as} Si-O-Si (LO Mode)	137,149
	1006	1012	1011	1012	1012	1012	1014	1010	1014	ν_{as} Si-O-Si (TO Mode)	137,149
	994	994	994	994	994	994	994	994	994	ν Si-O(H)	
	853	887	891	888	892	892	895	849	878	δSi-O-C from alkoxy This should be correlated with the presence of CH2	137,149
	778	778	778	778	778	778	778	778	778	ν_s Si-O-Si	29
	730	734	734	734	734	736	736	734	734	ρCH_3+the C_6H_5 ring breathing	150
	693	693	693	693	693	693	693	693	694	The C_6H_5 ring plane deformation + τ C-C from C_6H_5 ring	151,152,145,146
	585	585	585	585	585	585	588	586	586	δ_s O-Si-O	
	477	477	477	477	477	477	477	477	477	δ Si-O-Si	141,153,154

Table 4.5: Peak Assignments of FTIR Spectra for sys (3-2).

System ID	Sys (3-2)	Sys (3-2)	Sys (3-2)	Sys (3-2)	Sys (3-2)	Assignments	Ref.
TEOS %	**0**	**2**	**5**	**10**	**20**		
Peaks	3617	3627	3627	3613	3618	νO-H from free OH/ alcoholic	
	-	3353	3361	3360	3365	νO-H associated with hydrogen bonding on the organic modified silica surface	136
	3140	3140	3140	3140	3140	-	
	3094	3095	3095	3095	3095	ν (CH)ring	
	3072	3073	3073	3073	3073	ν_{as} (CH)ring	137,138, 139
	3049	3049	3049	3049	3049	ν_{s} (CH)ring	137,138, 139
	3006	3007	3007	3007	3007	ν (CH)ring	
	2977	2976	2976	2976	2976	ν_{as} CH_3	137,138, 139
	2924	2924	2924	2924	2924	ν_{as} CH_2	136,140, 141
	2895	2895	2895	2895	2895	ν_{s} CH_3	
	2850	2851	2851	2851	2851	ν_{s} CH_2	136,140, 141
	1593	1593	1593	1593	1593	γ CH (C_6H_5)	142
	1490	1489	1489	1489	1489	ν C=C (C_6H_5)	143
	1429	1429	1429	1429	1429	ν C-C (C_6H_5)	144,145, 146
	1394	1394	1394	1394	1394	δ_{as} CH_3	136
	1329	1329	1329	1329	1329	-	

1266	1266	1266	1266	1266	δ_s CH_3(Si-CH_3)	137,138, 147
1128	1128	1128	1128	1128	ν Si-C (from Si-C_6H_5)	148
1053	1051	1051	1051	1051	ν_{as} Si-O-Si (LO Mode)	137,149
1006	1012	1011	1011	1012	ν_{as} Si-O-Si (TO Mode)	137,149
994	995	995	995	995	ν Si-O(H)	
853	882	888	891	891	δSi-O-C from alkoxy This should be correlated with the presence of CH2	137,149
778	778	778	778	778	ν_s Si-O-Si	29
730	733	734	734	734	ρCH_3+the C_6H_5 ring breathing	150
693	694	694	694	694	The C_6H_5 ring plane deformation + τ C-C from C_6H_5 ring	151,152, 145,146
585	586	586	586	586	δ_s O-Si-O	
477	477	477	477	477	δ Si-O-Si	141,153, 154

ν, stretching vibration; **ν_s**, symmetric stretching vibration; **ν_{as}**, antisymmetric stretching vibration; **δ**, deformation vibration; **δ_s**, symmetric deformation vibration (bending); **δ_{as}**, antisymmetric deformation vibration (bending); **τ**, out-of-plane bending (twisting); **ρ,** rocking; **γ**, out-of-plane deformation vibration; **σ,** out-of-plane ring deformation vibration; LO, longitudinal optical; TO, transversal optical.

Table 4.6: Peak Assignments of FTIR Spectra for sys (5-1).

System ID	Sys (5-1)	Sys (5-1)	Sys (5-1)	Sys (5-1)	Sys (5-1)	Sys (5-1)	**Assignments**	**Ref.**
TMOS%	0	2	5	10	20	30		
	3625	3625	3620	3617	3625	3627	νO-H from free OH/ alcoholic	
	-	3395	3395	3395	3395	3395	νO-H associated with hydrogen bonding on the organic modified silica surface	136
	-	3139	3139	3139	3139	3137	-	
	3094	3094	3094	3094	3094	3094	ν (CH)ring	
	3073	3073	3073	3073	3073	3073	ν_{as} (CH)ring	137,138,139
	3050	3050	3050	3050	3050	3050	ν_{s} (CH)ring	137,138,139
	-	3028	3028	3028	3028	3026	-	
	3006	3006	3006	3006	3006	3005	ν (CH)ring	
Peaks (cm^{-1})	2977	2980	2980	2980	2980	2980	ν_{as} CH_3	137,138,139
	2924	2922	2941	2942	2941	2942	ν_{as} CH_2	136,140,141
	2852	2844	2842	2842	2842	2841	ν_{s} CH_2	136,140,141
	1593	1593	1593	1593	1593	1593	γ CH (C_6H_5)	142
	1489	1489	1489	1489	1489	1489	ν C=C (C_6H_5)	143
	1429	1429	1429	1429	1429	1429	ν C-C (C_6H_5)	144,145,146
	-	1380	1380	1380	1380	1380	δ_{as} CH_3	136
	1266	1266	1266	1266	1266	1265	δ_{s} CH_3(Si-CH_3)	137,138,147
	1190	1190	1190	1190	1190	1190	-	
	1128	1128	1128	1128	1128	1128	ν Si-C (from Si-C_6H_5)	148
	1050	1047	1045	1048	1047	1047	ν_{as} Si-O-Si (LO Mode)	137,149
	1008	1010	1010	1010	1010	1010	ν_{as} Si-O-Si (TO Mode)	137,149
	994	994	994	994	994	994	ν Si-O(H)	

	853	850	853	855	855	855	δSi-O-C	137,149
	-	802	805	805	805	-	-	
	780	784	785	785	785	795	ν_s Si-O-Si	29
	730	733	733	733	733	733	ρCH_3+the C_6H_5 ring breathing	150
	716	718	718	718	718	718	Ø C-H???	
	692	692	692	692	692	693	The C_6H_5 ring plane deformation + τ C-C from C_6H_5 ring	151,152 145,146
	668	645	648	648	650	647	ν_s Si-O???	
	-	617	617	617	617	617	-	
	584	587	587	587	587	587	δ_s O-Si-O	
	515	513	513	513	513	513	-	
	473	477	477	477	477	476	δ Si-O-Si	141,153,154

ν, stretching vibration; **ν_s**, symmetric stretching vibration; **ν_{as}**, antisymmetric stretching vibration; **δ**, deformation vibration; **δ_s**, symmetric deformation vibration (bending); **δ_{as}**, antisymmetric deformation vibration (bending); **τ**, out-of-plane bending (twisting); **ρ,** rocking; **γ**, out-of-plane deformation vibration; **σ,** out-of-plane ring deformation vibration; LO, longitudinal optical; TO, transversal optical.

Table 4.7: Peak Assignments of FTIR Spectra for sys (5-2).

System ID	Sys (5-2)	Sys (5-2)	Sys (5-2)	Sys (5-2)	Sys (5-2)	Sys (5-2)	Assignments	Ref.
TMOS%	0	2	5	10	20	30		
Peaks (cm^{-1})	-	3852	3852	3854	3854	-	ν_s(O-H) or ν_s(CH) ???	
	3625	3628	3628	3628	3628	3627	νO-H from free OH/ alcoholic	
	-	3412	3390	3393	3393	3384	νO-H associated with hydrogen bonding on the organic modified silica surface	136
	-	3138	3138	3138	3138	3137	-	
	3094	3093	3093	3093	3093	3093	ν (CH)ring	
	3073	3073	3073	3073	3073	3072	ν_{as} (CH)ring	137,138,139
	3050	3050	3050	3050	3050	3049	ν_s (CH)ring	137,138,139
	-	3027	3027	3027	3027	3027	-	
	3006	3007	3007	3007	3007	3005	ν (CH)ring	
	2977	3983	3980	2978	2978	2975	ν_{as} CH_3	137,138,139
	-	-	-	2941	2942	2942	-	
	2924	2922	2922	2916	2916	2918	ν_{as} CH_2	136,140,141
	2852	2848	2846	2841	2843	2843	ν_s CH_2	136,140,141
	1593	1593	1593	1593	1593	1593	γ CH (C_6H_5)	142
	1489	1489	1489	1489	1489	1489	ν C=C (C_6H_5)	143
	1429	1429	1429	1429	1429	1429	ν C-C (C_6H_5)	144,145,146
	-	1385	1385	1387	1387	1381	δ_{as} CH_3	136
	1266	1266	1266	1266	1266	1265	δ_s CH_3(Si-CH_3)	137,138,147
	1190	1190	1190	1190	1190	1190	-	
	1128	1128	1128	1128	1128	1128	ν Si-C (from Si-C_6H_5)	148

1050	1048	1046	1047	1047	1035	ν_{as} Si-O-Si (LO Mode)	137,149
1008	1011	1011	1011	1011	1014	ν_{as} Si-O-Si (TO Mode)	137,149
994	994	994	994	994	996	ν Si-O(H)	
-	913	916	919	919	921	νβ Si-O???	
853	850	850	853	853	855	δSi-O-C	137,149
-	806	806	807	807	806	-	
780	781	781	784	784	784	ν_s Si-O-Si	29
730	733	733	733	733	733	ρCH_3+the C_6H_5 ring breathing	150
716	718	718	718	718	718	Ø C-H???	
692	693	693	693	693	693	The C_6H_5 ring plane deformation + τ C-C from C_6H_5 ring	151,152 145,146
668	649	649	647	647	644	ν_s Si-O???	
-	617	617	617	617	617	-	
584	587	587	587	587	588	δ_s O-Si-O	
515	513	513	513	513	514	-	
473	475	475	475	478	477	δ Si-O-Si	141,153,154

ν, stretching vibration; **ν_s**, symmetric stretching vibration; **ν_{as}**, antisymmetric stretching vibration; **δ**, deformation vibration; **δ_s**, symmetric deformation vibration (bending); **δ_{as}**, antisymmetric deformation vibration (bending); **τ**, out-of-plane bending (twisting); **ρ,** rocking; **γ**, out-of-plane deformation vibration; **σ,** out-of-plane ring deformation vibration; LO, longitudinal optical; TO, transversal optical.

Table 4.8: Peak Assignments of FTIR Spectra for sys (7-1).

System ID	Sys (7-1)	Sys (7-1)	Sys (7-1)	Sys (7-1)	Sys (7-1)	Assignments	Ref.
TEOS%	**0**	**2**	**5**	**10**	**13**		
Peaks (Cm^{-1})	3617	3616	3624	3616	3619	νO-H from free OH/ alcoholic	
	-	3395	3390	3391	3396	νO-H associated with hydrogen bonding on the organic modified silica surface	136
	3140	3138	3138	3138	3138	-	
	3094	3092	3095	3092	3095	ν (CH)ring	
	3072	3073	3073	3073	3073	ν_{as} (CH)ring	137,138, 139
	3049	3049	3049	3049	3049	ν_{s} (CH)ring	137,138, 139
	3006	3006	3006	3006	3006	ν (CH)ring	
	2977	2974	2976	2974	2976	ν_{as} CH_3	137,138, 139
	2924	2924	2924	2924	2924	ν_{as} CH_2	136,140, 141
	2895	2895	2895	2895	2895	ν_{s} CH_3	
	2850	2851	2852	2852	2851	ν_{s} CH_2	136,140, 141
	1593	1593	1593	1593	1593	γ CH (C_6H_5)	142
	1490	1489	1489	1489	1489	ν C=C (C_6H_5)	143
	1429	1429	1429	1429	1429	ν C-C (C_6H_5)	144,145, 146
	1394	1392	1389	1392	1389	δ_{as} CH_3	136
	1329	1329	1329	1329	1329	-	

1307	1307	1307	1307	1307	-	
1266	1266	1266	1266	1266	δ_s CH_3(Si-CH_3)	137,138, 147
1128	1128	1128	1130	1130	ν Si-C (from Si-C_6H_5)	148
1053	1051	1051	1051	1051	ν_{as} Si-O-Si (LO Mode)	137,149
1006	1009	1009	1009	1009	ν_{as} Si-O-Si (TO Mode)	137,149
994	992	992	992	992	ν Si-O(H)	
918	920	919	920	921	-	
852	852	850	854	853	δSi-O-C	137,149
778	780	780	780	780	ν_s Si-O-Si	29
730	733	733	733	733	ρCH_3+the C_6H_5 ring breathing	150
693	694	694	694	694	The C_6H_5 ring plane deformation + τ C-C from C_6H_5 ring	151,152 145,146
585	586	586	586	586	δ_s O-Si-O	
477	477	476	475	475	δ Si-O-Si	141,153, 154

ν, stretching vibration; **ν_s**, symmetric stretching vibration; **ν_{as}**, antisymmetric stretching vibration; **δ**, deformation vibration; **δ_s**, symmetric deformation vibration (bending); **δ_{as}**, antisymmetric deformation vibration (bending); **τ**, out-of-plane bending (twisting); **ρ,** rocking; **γ**, out-of-plane deformation vibration; **σ,** out-of-plane ring deformation vibration; LO, longitudinal optical; TO, transversal optical.

Table 4.9: Peak Assignments of FTIR Spectra for sys (7-2).

System ID	Sys (7-2)	Sys (7-2)	Sys (7-2)	Sys (7-2)	Sys (7-2)	**Assignments**	**Ref.**
TMOS %	**0**	**2**	**5**	**10**	**20**		
Peaks (cm^{-1})	3617	3616	3616	3617	3617	νO-H from free OH/ alcoholic	
	-	3385	3390	3395	3376	νO-H associated with hydrogen bonding on the organic modified silica surface	136
	3140	3137	3139	3137	3137	-	
	3094	3094	3094	3094	3094	ν (CH)ring	
	3072	3072	3071	3072	3072	ν_{as} (CH)ring	137,138,139
	3049	3049	3049	3049	3049	ν_{s} (CH)ring	137,138,139
	3006	3006	3006	3006	3006	ν (CH)ring	
	2977	2975	2976	2979	2979	ν_{as} CH_3	137,138,139
	2924	2924	2924	2924	2924	ν_{as} CH_2	136,140,141
	2895	2895	2895	2895	2895	ν_{s} CH_3	
	2850	2853	2852	2852	2852	ν_{s} CH_2	136,140,141
	1593	1592	1593	1593	1593	γ CH (C_6H_5)	142
	1490	1491	1488	1489	1489	ν C=C (C_6H_5)	143
	1429	1429	1429	1429	1429	ν C-C (C_6H_5)	144,145,146
	1394	1393	1389	1392	1394	δ_{as} CH_3	136
	1329	1329	1329	1329	1329	-	
	1266	1266	1264	1266	1266	δ_{s} CH_3(Si-CH_3)	137,138,147
	1128	1128	1128	1130	1130	ν Si-C (from Si-	148

					C_6H_5)	
1053	1053	1053	1054	1051	ν_{as} Si-O-Si (LO Mode)	137,149
1006	1011	1011	1005	1012	ν_{as} Si-O-Si (TO Mode)	137,149
994	994	994	993	994	ν Si-O(H)	
852	855	851	852	850	δSi-O-C	137,149
778	780	780	780	780	ν_s Si-O-Si	29
730	733	735	730	735	ρCH_3+the C_6H_5 ring breathing	150
693	694	693	693	693	The C_6H_5 ring plane deformation + τ C-C from C_6H_5 ring	151,152 145,146
585	586	586	586	586	δ_s O-Si-O	
477	477	476	475	475	δ Si-O-Si	141,153,154

4.6 Hydroxyl Species Concentration

The IR absorption spectra of O–H stretching vibrations include different types of contributions in the region between 2800–4000 cm^{-1}. In general, this band is very broad and intense in silica xerogels and decreases in intensity with increasing the treatment temperature. Also, it is strongly dependent on the atmosphere of treatment and humidity of the environment.

On the basis of the literature two main groups of bands can be assigned in this interval: (a) stretching modes of OH groups not involved or partially involved in hydrogen

bonding, which include isolated OH and terminal OH (3800–3650 cm^{-1}); (b) stretching modes of hydrogen-bonded OH groups (3650–3200 cm^{-1}) [155].

The first group appears as a sharp narrow peak at around 3620 cm^{-1} in all systems which is assigned to isolated silanol groups, and also due to terminal silanols. This group is found at higher frequency than the other group [156-158].

The second group associated with hydrogen bonded silanols in chains on the organically modified silica surface, containing more than one pair of mutually H-bonded OH groups, are observed as a broad band between 3500–3200 cm^{-1} region in all systems as well. These H–bonded surface silanols can form chains of different lengths and shapes and this diversity explains the broadness of this band [155]. However, what is most interesting is that this group does not appear in melting gels with only two components. In other words, the H-bonded surface silanols are associated with the addition of the tetra alkoxide, both TEOS and TMOS.

Figures 4.15 and 4.16 show the absorbance intensity of the two groups for systems with TEOS and systems with TMOS respectively. In all systems, the intensity of the free OH group and OH associated with hydrogen bonding on the organically modified silica surface group seem to be coincident with each other along the tetra-alkoxide weight percent axis. The concentration of the two-hydroxyl species increases with increasing tetra-alkoxide concentration due to unreacted Si–O–R groups and residual alcoholic co-solvent within the film. Afterword the intensity starts to decrease near the systems limit due to the formation of siloxane bridges and an increase of the isolated species. The intensity is higher when the tetra-alkoxide is diluted with ethanol sys (x-2) rather than methanol as seen in Figure 4.15 and 4.16.

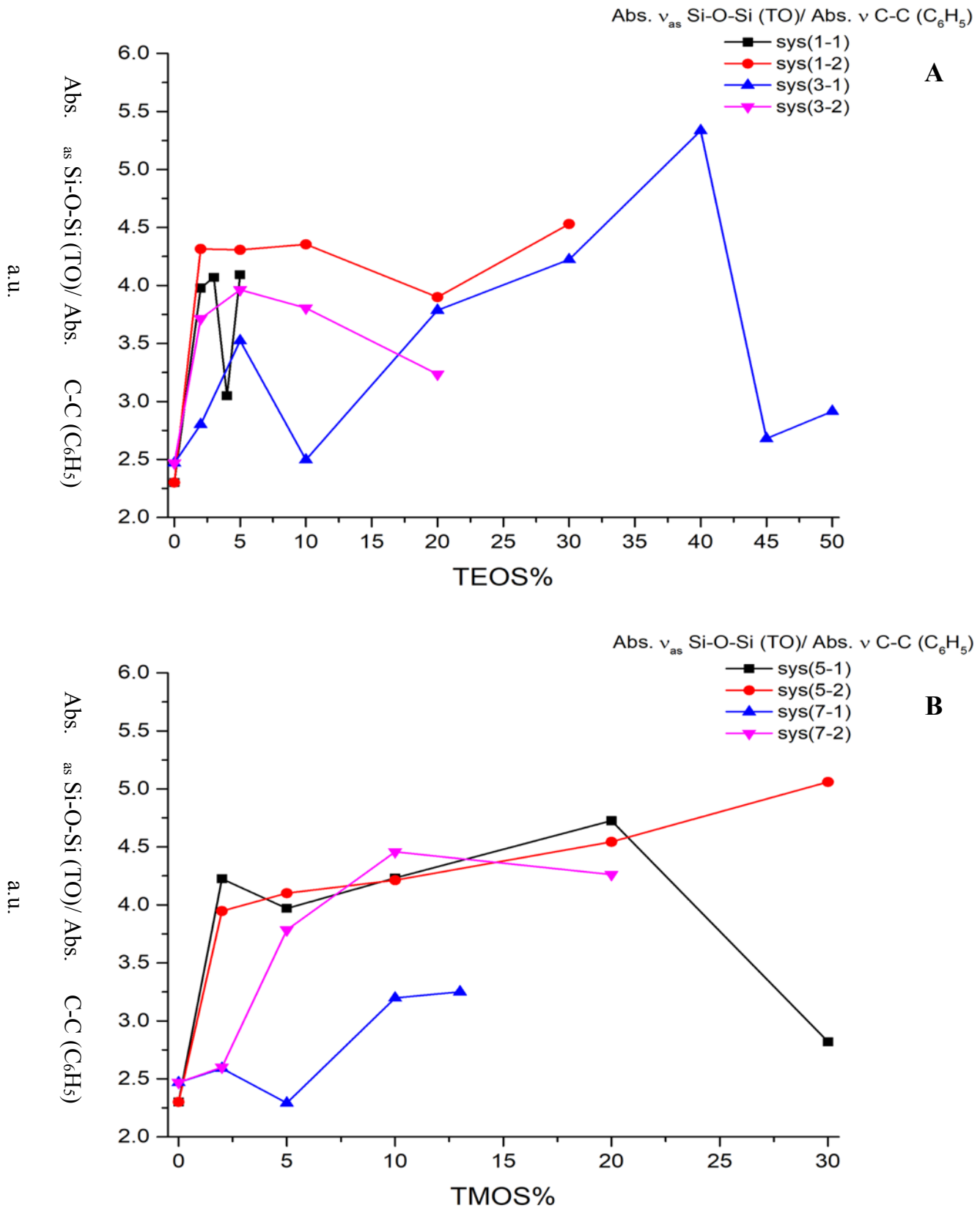

Fig. 4.14: Comparative FTIR ratios of Si-O-Si to C-C bond as a function of tetra-alkoxide weight percent **(A)** systems with TEOS, **(B)** systems with TMOS.

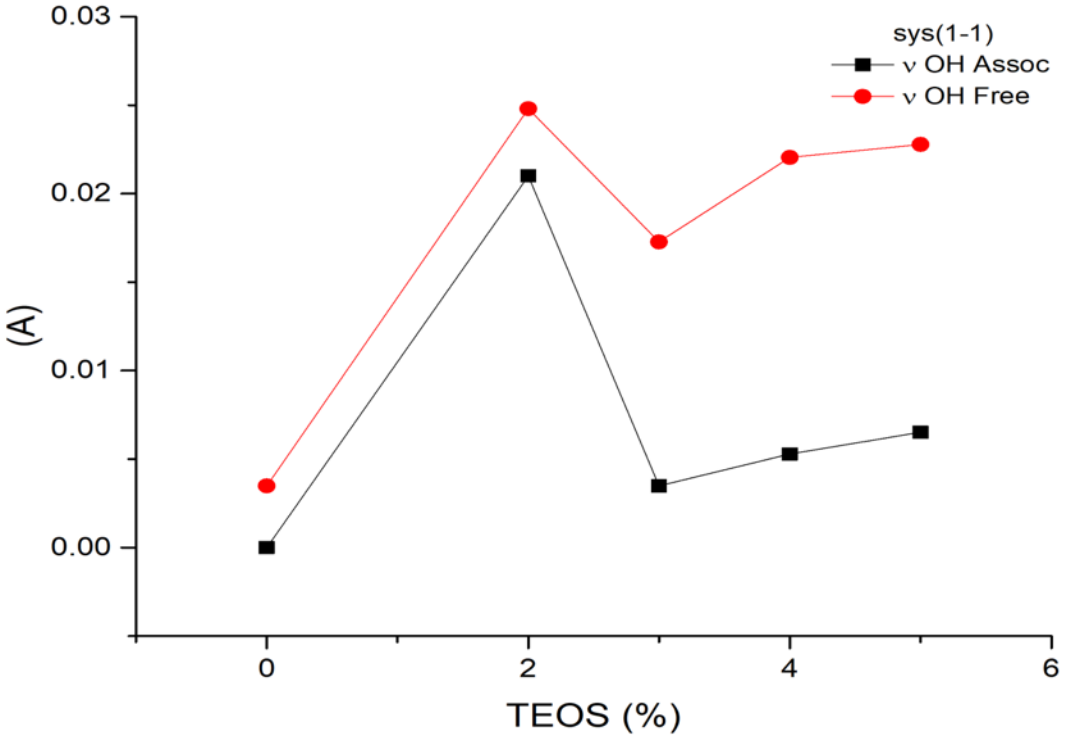
sys(1-1)
ν OH Assoc
ν OH Free
0.03
0.02
0.01
0.00
(A)
0
2
4
6
TEOS (%)

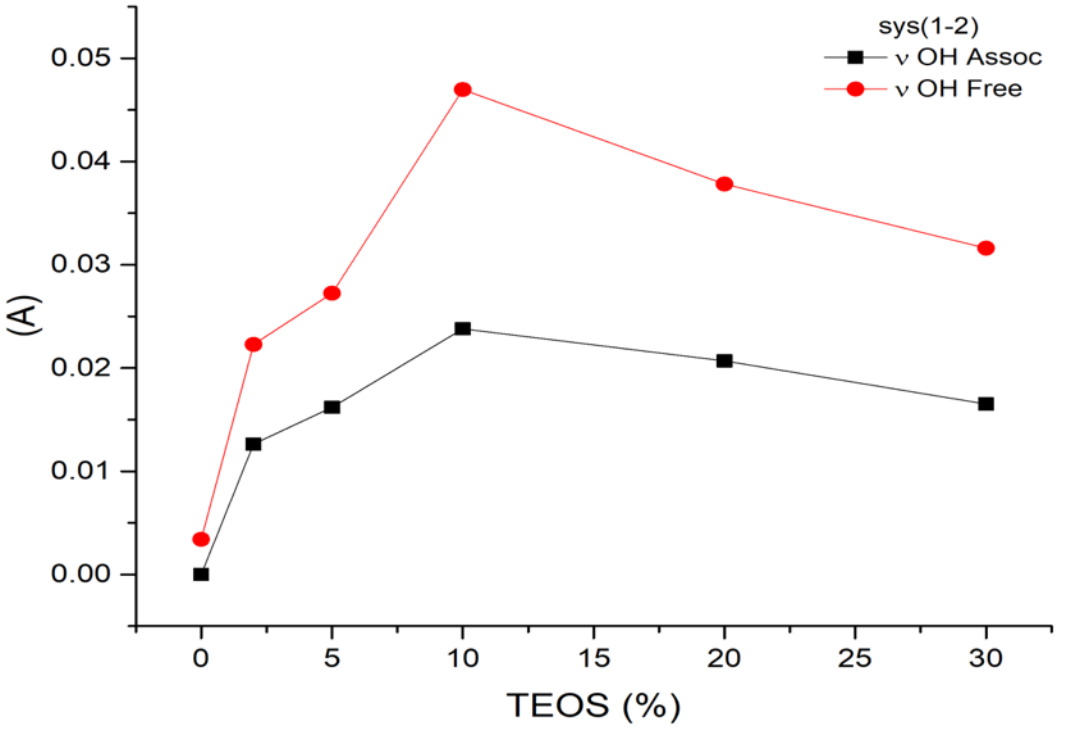
sys(1-2)
ν OH Assoc
ν OH Free
0.05
0.04
0.03
0.02
0.01
0.00
(A)
0
5
10
15
20
25
30
TEOS (%)

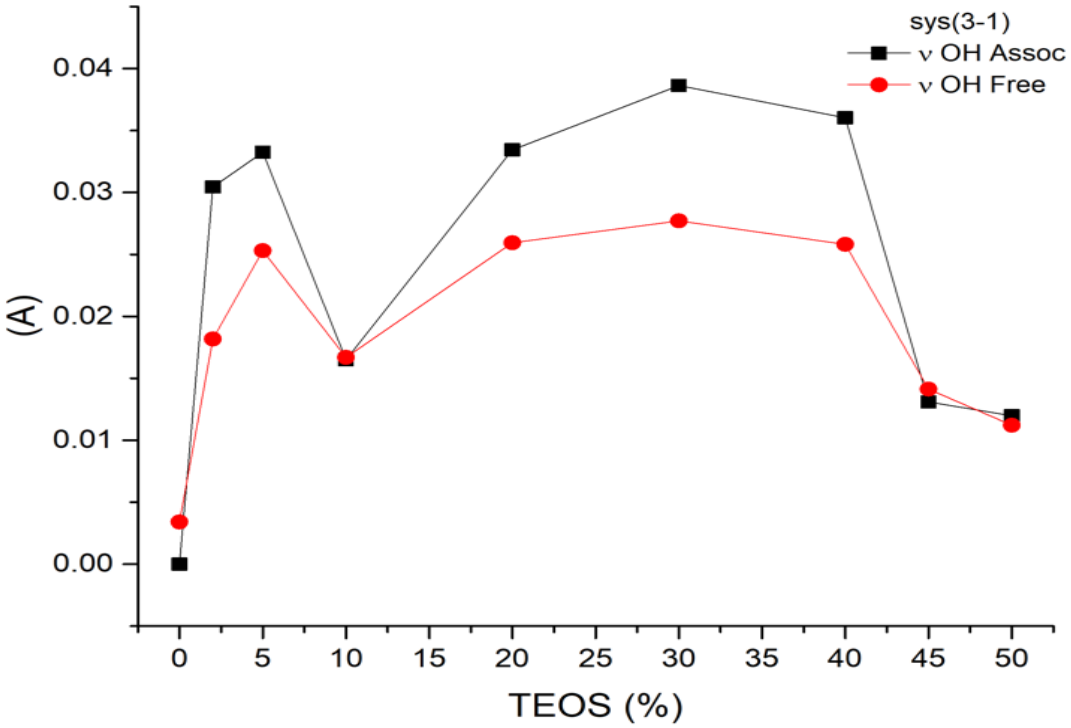

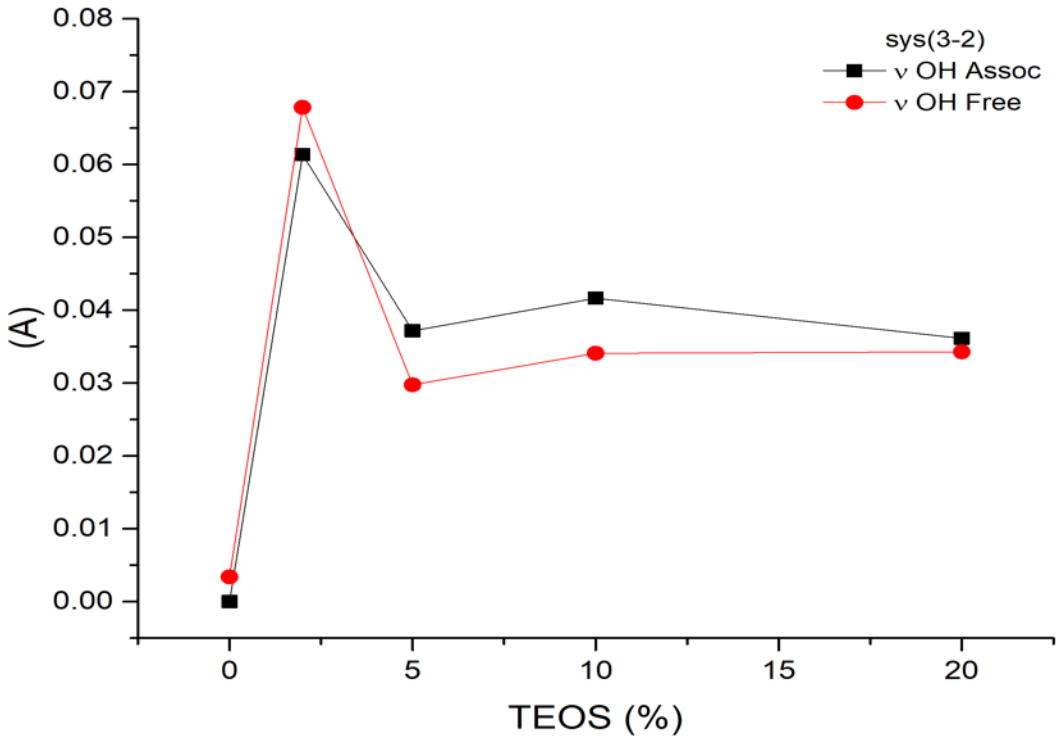

Figure 4.15: Absorbance intensity of hydroxyl goups vs. TEOS concentration for sys (1-1), (1-2), (3-1), and (3-2)

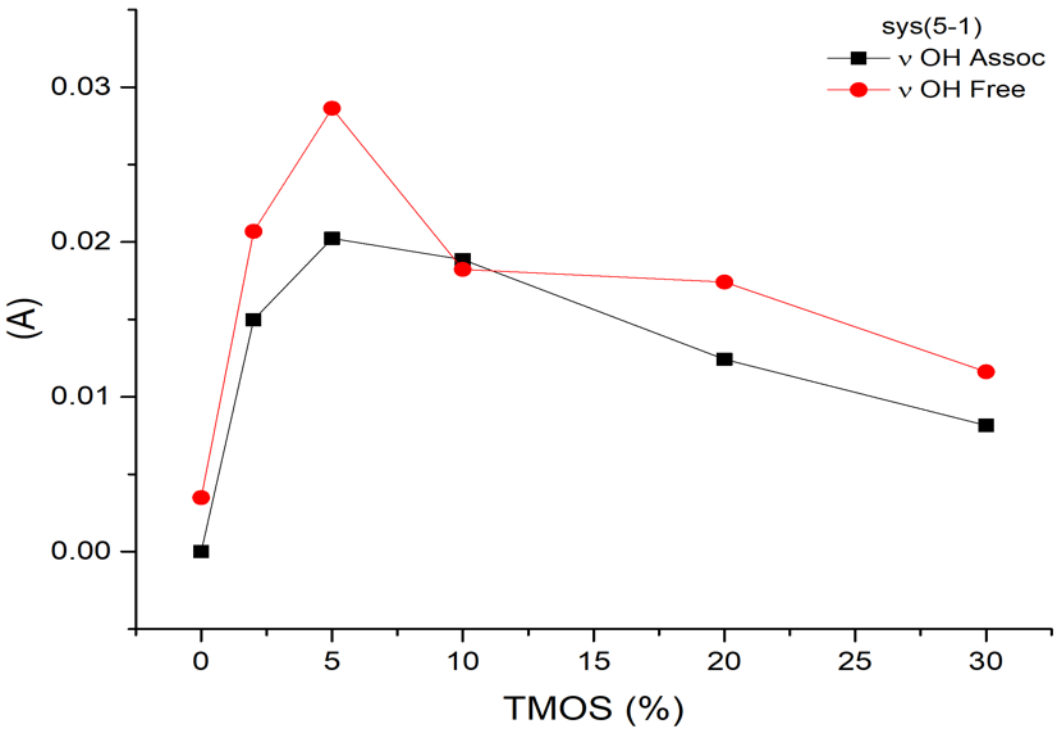
sys(5-1)
ν OH Assoc
ν OH Free
0.03
0.02
0.01
0.00
(A)
0
5
10
15
20
25
30
TMOS (%)

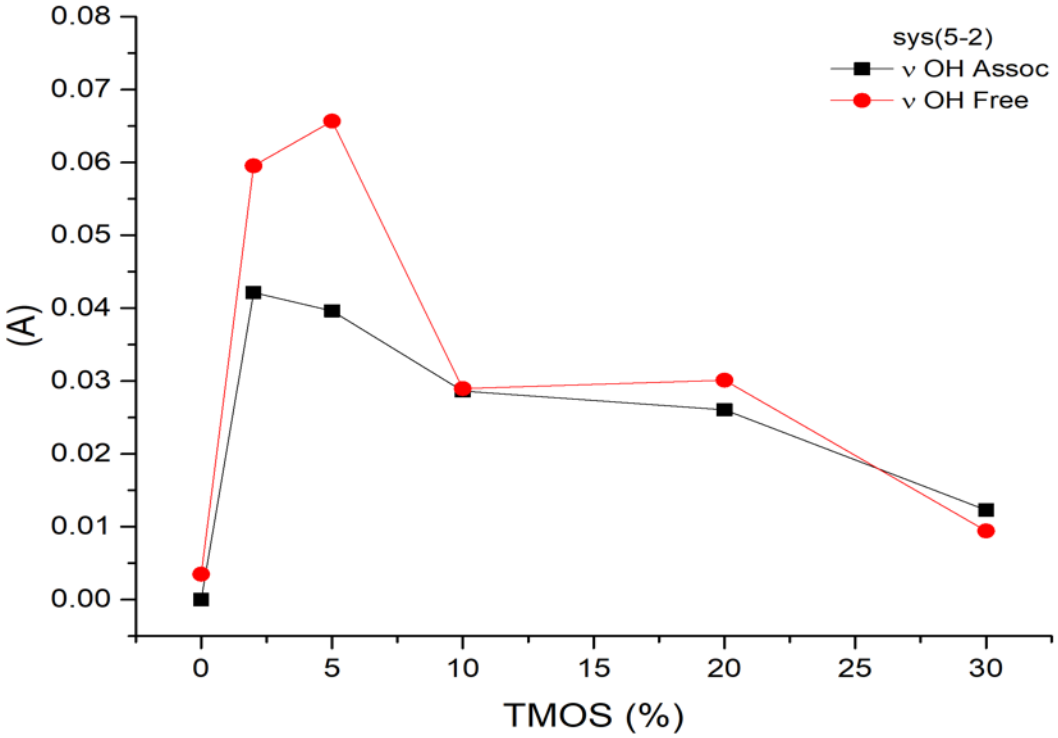
sys(5-2)
ν OH Assoc
ν OH Free
0.08
0.07
0.06
0.05
0.04
0.03
0.02
0.01
0.00
(A)
0
5
10
15
20
25
30
TMOS (%)

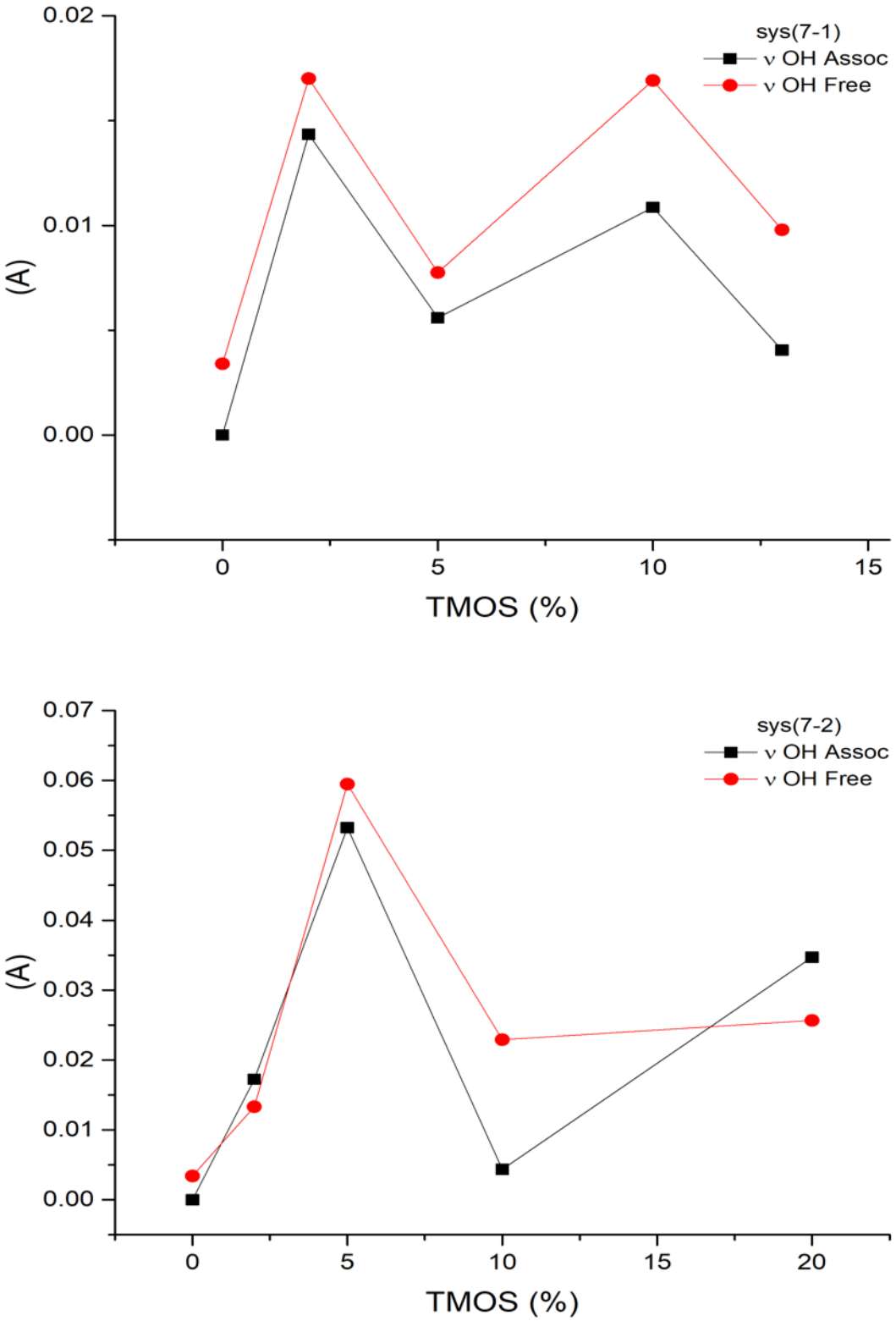

Figure 4.16: Absorbance intensity of hydroxyl goups vs. TEOS concentration for sys (5-1), (5-2), (7-1), and (7-2)

4.7 Contact Angle Measurements

Contact angles were measured on samples that had been fully consolidated for 24 h at their indicated consolidation temperatures in Table 4.1. Five measurements were made for each composition and averaged. Contact angle measurements are listed in Table 4.10. Contact angles are an indication of the hydrophobicity of the consolidated coatings on mica substrates, by using droplets of water as the wetting liquid.

Figure 4.17 shows contact angles for systems with TEOS while Figure 4.18 shows contact angles for systems with TMOS. The highest contact angles were obtained for systems with PhTMS:DPhDMS, which are systems 1 and 5, for both TMOS and TEOS. Both have almost the same contact angles in the range between θ= 86-94°. However systems with PhTES:DPhDES, which are systems 3 and 7, have more hydrophilic properties with contact angles between θ= 82-90°. These results are supported by the FTIR which confirm the presence of hydroxyl groups on the surface of three component systems with higher intensity especially when the mixture contain ethanol and/or ethoxy substituents alkoxide.

When silanol groups on the surface are replaced by alkyl and phenyl groups, which have a poor affinity for water, the gel surface is hydrophobic. In melting gels, the presence of organic groups contributes to melting gels having contact angle values that are greater than 90°, with respect to water [124]. All the melting gels systems studied before, without the additional of a tetrafunctional alkoxysilane, were hydrophobic.

sys(1-1) Contact Angle

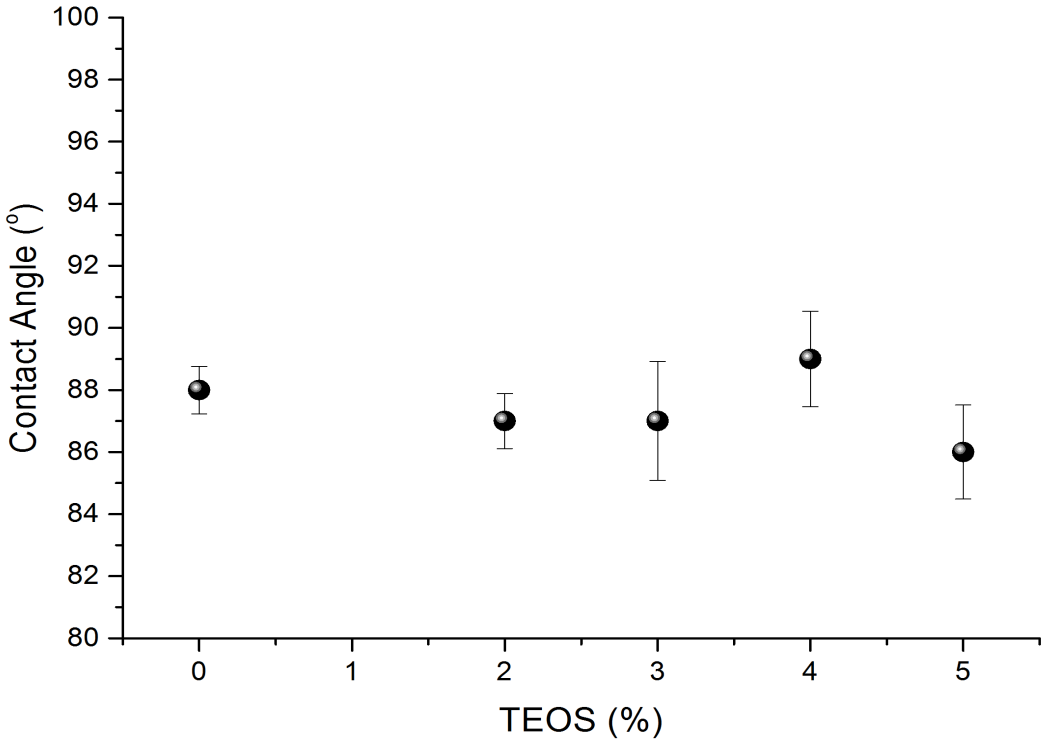

sys(1-2) Contact Angle

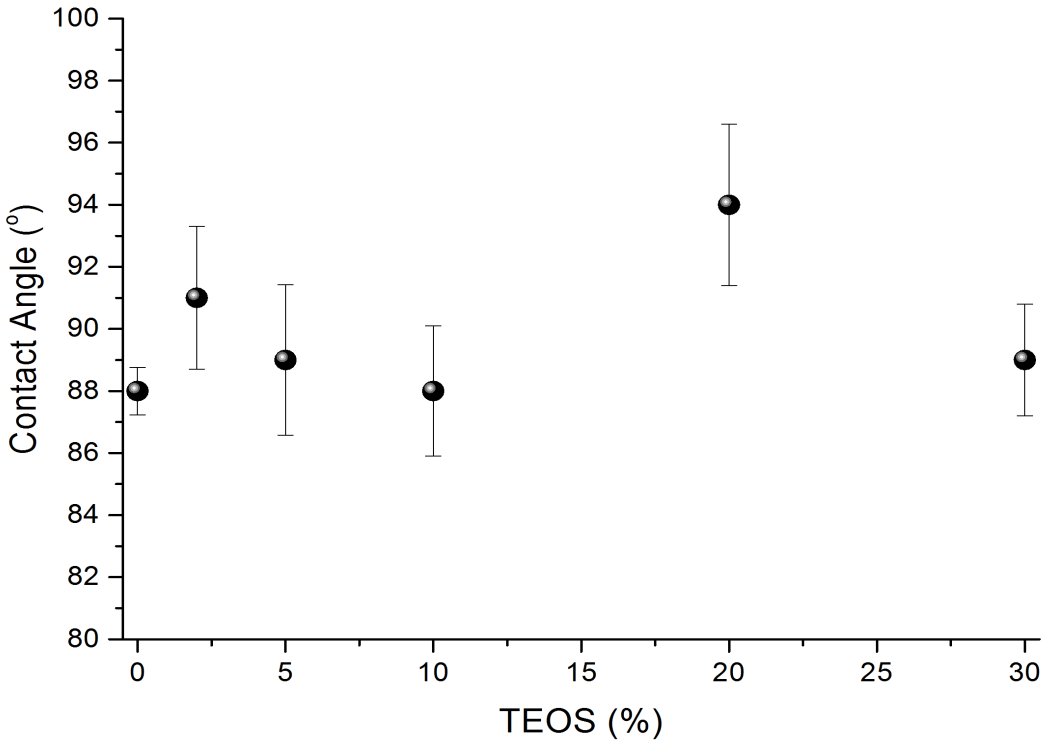

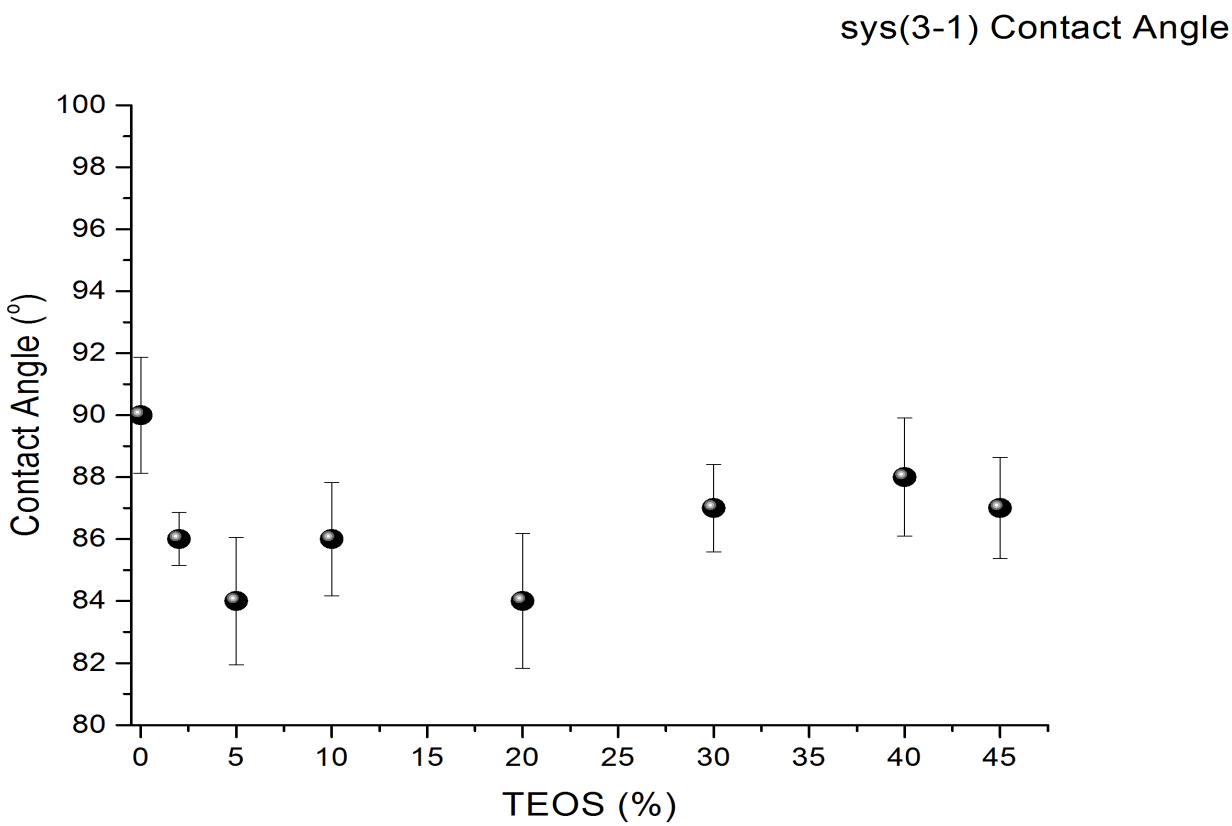

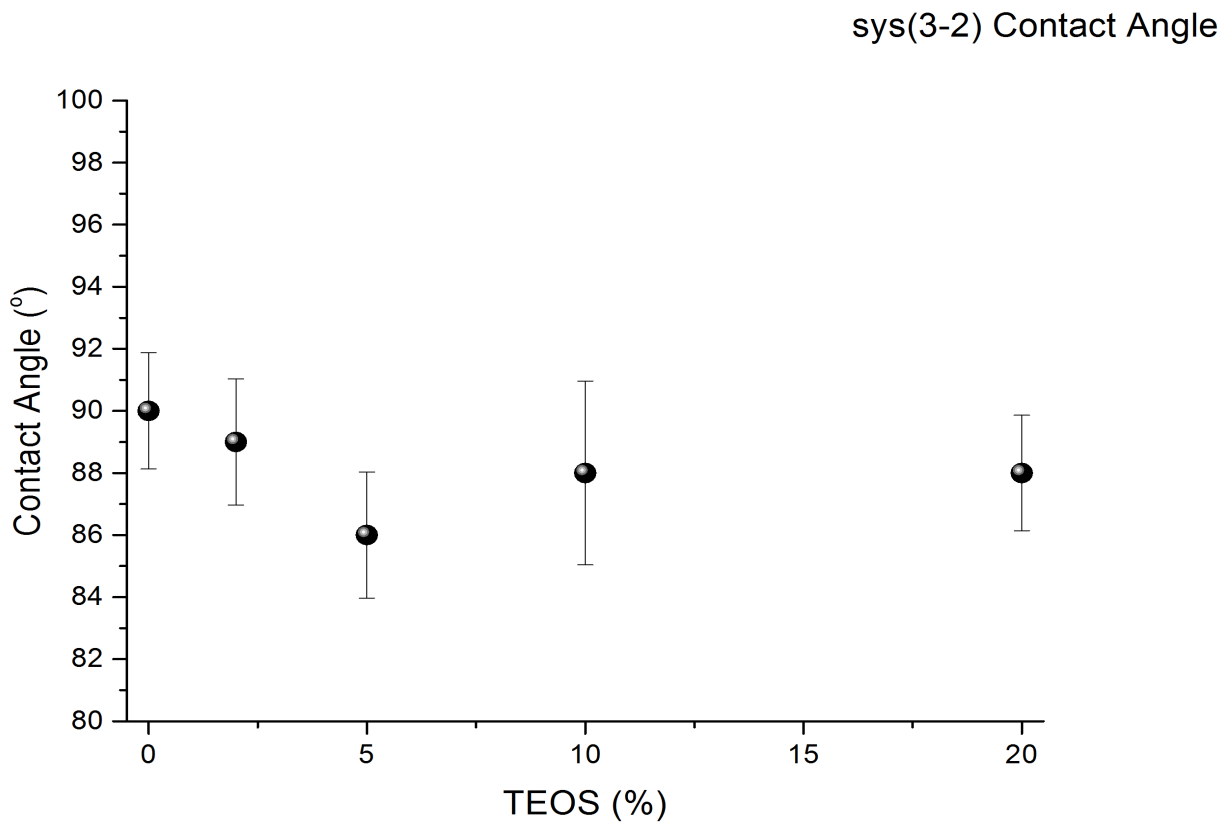

Figure 4.17: Contact Angles Measurements with respect to TEOS weight percent for systems (1-1), (1-2), (3-1) and (3-2).

sys(5-1) Contact Angle

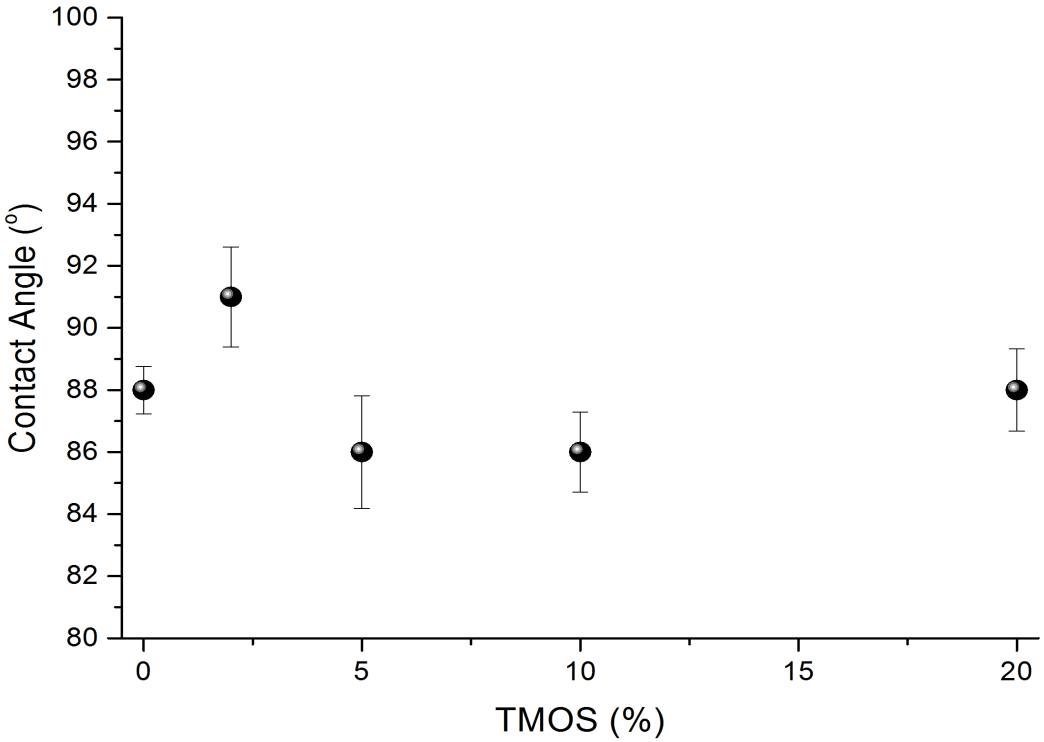

sys(5-2) Contact Angle

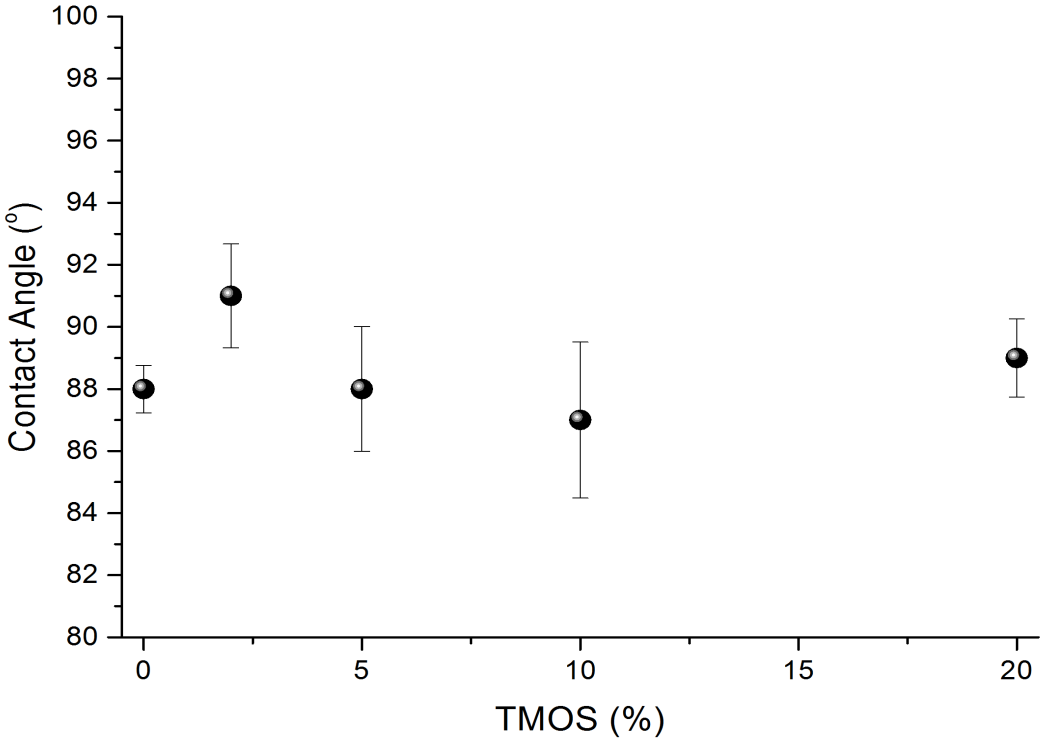

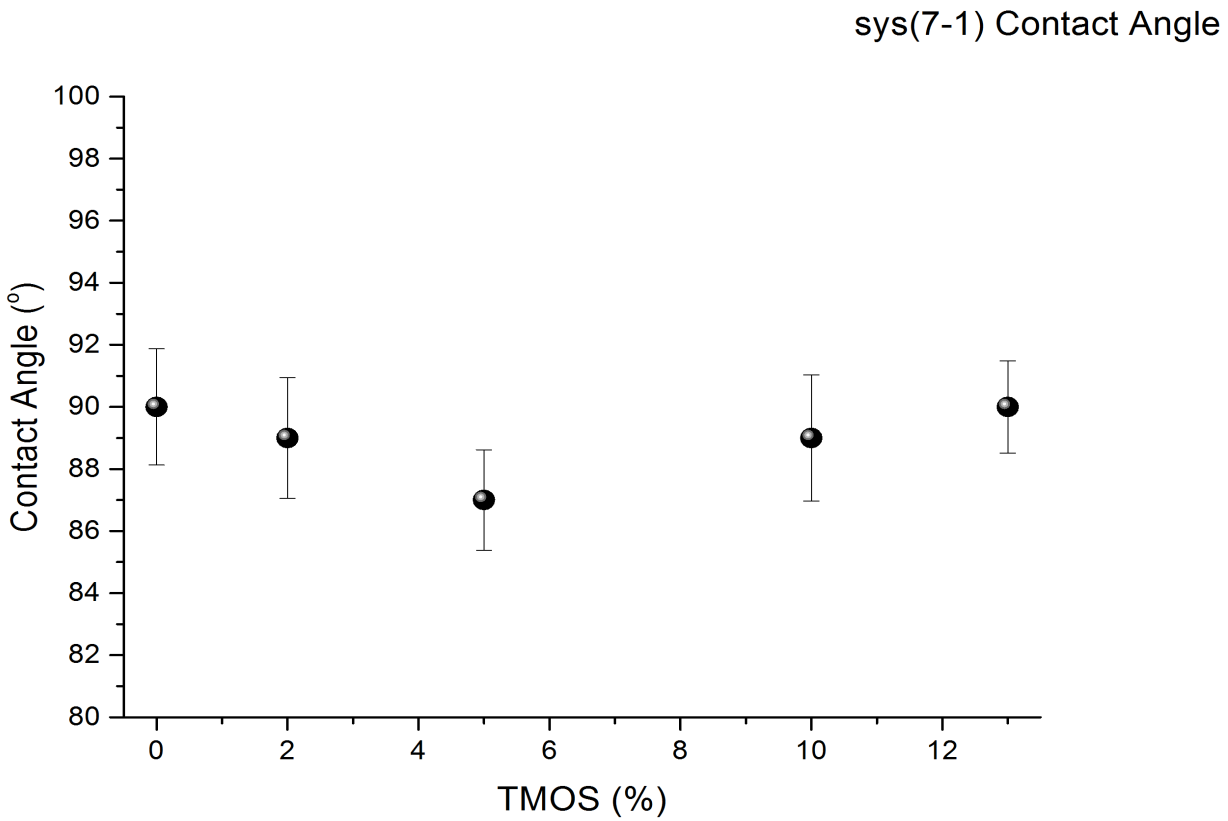

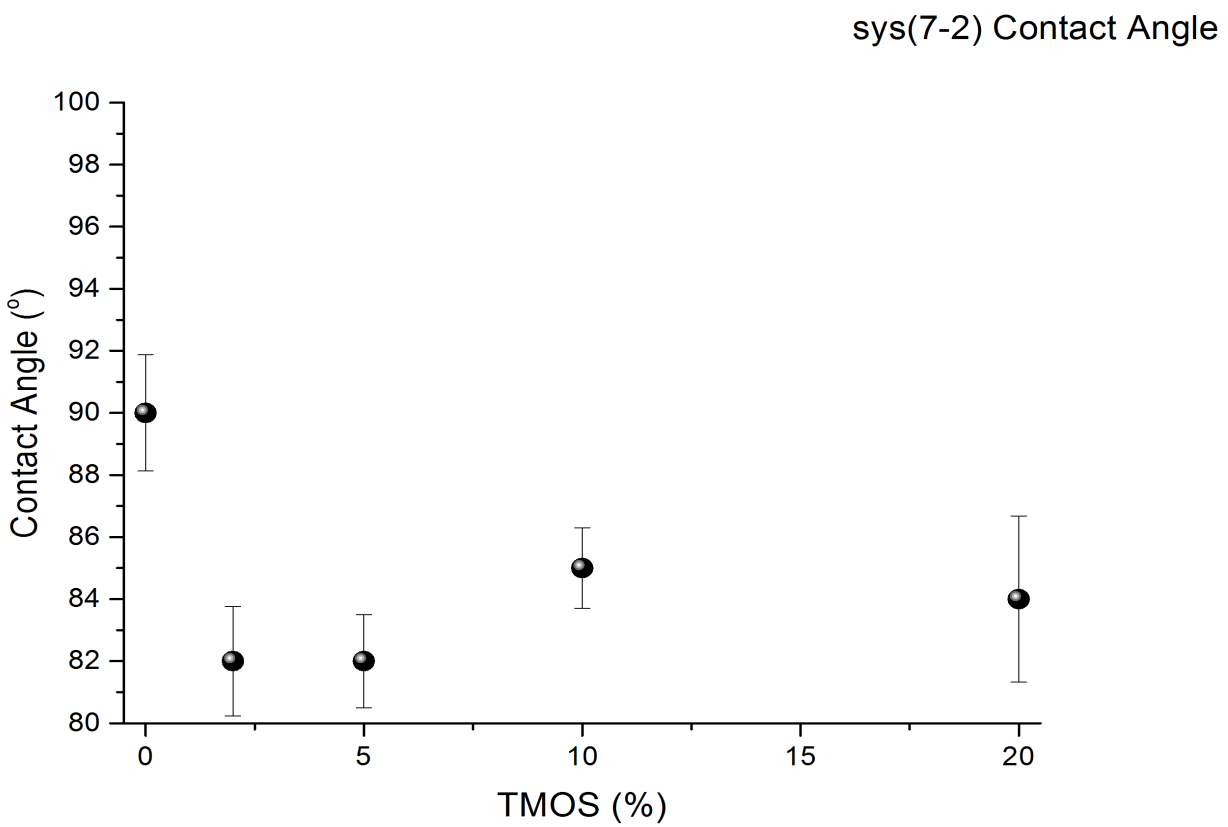

Figure 4.18: Contact Angles Measurements with respect to TMOS weight percent for systems (5-1), (5-2), (7-1) and (7-2).

4.8 Vickers Micro-Indentation Hardness

There is a direct relation between mechanical properties and glass transition temperature in sol gel material through their ability to form a 3D network [159]. The degree of cross linking of TEOS based sol gel coating is influenced by the ratio of hydroxyl and alkoxy groups on the Si atoms. More hydroxyl groups lead to a higher degree of cross linking, and consequently higher mechanical properties. The higher amount of inorganic network structure gives higher hardness as well [160]. Hardness measurements are listed in Table 4.10. The hardness measurements correlate well with the glass transition temperatures. Hardness of the samples increased in systems with increasing tetra-alkoxide component when diluted with the parent alcohol as shown in Figure 4.19, 4.20, and 4.21. Only system (1-1) did not show this trend. As a general rule, systems with ethoxy substituents have higher hardness than systems with methoxy substituents when they have the same tetraalkoxy (alcohol) substituent as shown in Figure 4.22. That is because systems with more ethoxy substituents have longer gelling times than methoxy systems, allowing more cross-linking in the network and subsequently an increase in the hardness. However, the all ethoxy system sys (3-2) appeared to have lower hardness than the comparable system sys (1-2). The reason for this exception is likely the dilution effect. Adding TEOS decreased the viscosity, while adding TMOS increased it. For the same reason, the system with all ethoxy substituents system (3-2) had lower hardness than all methoxy substituents system (5-1), as shown in Figure 4.23.

Most of the samples show radial cracks under the microscope. At higher loads, this is followed by delamination and chipping, as shown in Figure 4.24. Such radial cracks appear to emanate from the indent as a result of residual tensile stresses that develop during

unloading. Measured crack lengths can be correlated to the material toughness, Kc, through the semi-empirical relationship [161]. These elongated cracks prove that most of the systems are durable for plastic deformation to some extent.

4.9 True Density

To measure the density, it was necessary to remove the coatings from the mica substrates. This was accomplished by immersing the samples in liquid nitrogen for 5 min followed by exposure at room temperature. Due to the difference in thermal expansion coefficients, the coatings immediately peeled off. Subsequently, the samples were placed under liquid nitrogen for ease of grinding. The densities were measured on the ground powders. True density results from He pycnometry are listed in Table 4.10. The trend in the data reveals that increasing the tetra-alkoxide mole ratio increases the measured density. In addition, samples with TMOS had higher density than those with TEOS. The higher density with TMOS reflects the fact that TMOS is more reactive than TEOS. The hydrolysis of TMOS is, in fact, around six times faster. The decrease in the hydrolysis rate with an increase of the organic group size is attributed to steric hindrance [162].

Generally, the reactions are faster in the methoxy containing systems than in the ethoxy systems. The higher reactivity of the methoxy groups is said to give a more disordered three-dimensional network with shorter methyl modified silica chains. This leads to lower weight loss percentage for the samples prepared with the methoxy groups, as well as lower skeletal densities [64]. Moreover, mixtures of TEOS or TMOS with substituted methoxysilanes generate low-density xerogels due to a nucleation mechanism involving the substituted alkoxysilane. [163]

4.10 Consolidation Temperature

Before consolidation, the gels contain linear molecular chains, which allow those gels to soften. Upon thermal treatment to the consolidation temperature, the linear molecular chains are mobile and hydroxyl groups from different chains come into a favorable position so that hydrolysis reactions between molecular chains can occur. In this way, a three-dimensional network forms, preventing the re-softening of the gels.

The coatings were deposited by pouring the softened gel onto the substrates. The apparent viscosity of the melting gels decreased with increasing TEOS mole percentage. In contrast, the viscosity increased with increasing TMOS mole percentage. These trends are reflected in the higher consolidation temperatures for systems with TEOS, compared to those with TMOS.

Systems with TMOS have high transparency. The clarity improves with increased amount of tetra-alkoxide. Systems with TEOS are less transparent and became more yellowish by increasing the tetra-alkoxides percentage. In addition, systems with methoxy groups have higher consolidation temperature than comparable systems with ethoxy groups. For example, sys (1-2) with methoxy has higher consolidation temperatures compared with sys (3-2) with ethoxy, as listed in table 4.1.

4.11 Melting Gel Limits

Adding tetra-alkoxide to the mono-substituted and di-substituted mixtures does not prevent melting, up to a certain limit of mol % of TROS. In comparison, mixtures of TEOS and mono-substituted alkoxysilanes do not form melting gels. The limits vary with co-solvent used in the mixture of the three components and the nature of the substitution. The

limit of the systems was determined either by finding when the gel lost its ability to soften or, when a visible phase separation indicated by cloudiness was observed.

In alkoxy-derived sol-gel systems, various macroporous morphologies can be obtained by inducing the phase separation parallel to the sol-gel transition. This principle of macroporous morphology control can be best applied to pure silica and silica-based multicomponent oxide systems that have many practical applications [164]. In the case of melting gels, it is desirable to avoid phase separation. In other words, this study did not try to induce phase separation by the use of solvents. In fact, the goal of this study was to maintain a single liquid during the synthesis stage. Nevertheless, there is a limit to how much of the third component can be added to the melting gel. Recognizing that there are competing reactions with regard to hydrolysis, condensation, and esterification, and that there are competing roles of hydrophobic and hydrophilic groups in the gel, it is expected that there is a limit. By making controlled additions of the third component, it was possible to determine the system limits, which are listed in table 4.11. The limits are given to the nearest 5% of TROS, as a weight per cent of mono-substituent. For example, in system (1-1) the limit was 5%, which means that using 5g of mono-substituent (PhTMS), the limit was found by using 0.25g of TEOS diluted with methanol. The mono-substituted to di-substituted ratio is constant 1:0.25 mole%. The lowest limit was obtained for system (1-1), which was 5%. The highest limit was for system (3-1) near 50% of TEOS before the gel no longer re-softened.

A simplified ternary diagram among the three components was plotted using Origin Lab 2016 software showing the border along that we can prepare melting gel as presented in Figure 4.25 for systems with TEOS and Figure 4.26 for systems with TMOS.

Table 4.10: Physical properties of melting gel (density, contact angle, Vickers hardness and time to gel).

Sample ID	*Composition Monosub./Disub./TROS*	*TROS W% of (Mono)*	*Glass transition Tg (˚C)*	*Contact Angle ^{o}*	*Density (g/cm3)*	*Density Standard Deviation*	*Hardness (g/um^2)*	*Hardness (GPa)*	*Time to Gel (hrs.)*
Sys (1-1)	*PhTMS/ DPhDMS/TEOS (MeOH)*	2	19.4	87	1.2876	0.0018	4.3	42.17	12
=	=	3	24.09	87	1.2837	0.0063	4.8	47.07	12
=	=	4	23.09	89	1.2845	0.0016	8.9	87.28	12
=	=	5	2.89	86	1.2921	0.0042	8.5	83.36	12
Sys (1-2)	*PhTMS/ DPhDMS/TEOS (EtOH)*	2	13.02	91	1.2892	0.003	8.1	79.43	12
=	=	5	4.97	89	1.2924	0.0033	8.6	84.34	12
=	=	10	24.48	88	1.2943	0.0006	8.8	86.3	13
=	=	20	25.24	94	1.2910	0.0018	9	88.26	13
=	=	30	30.94	89	1.3012	0.0037	8.5	83.36	13
Sys (5-1)	*PhTMS/ DPhDMS/TMOS (MeOH)*	2	19.91	91	1.2867	0.001	7.9	77.47	10
=	=	5	36.93	86	1.2859	0.0016	10.7	104.93	10
=	=	10	41.3	86	1.2882	0.0006	10.4	101.99	10
=	=	20	40.9	88	1.2924	0.0002	10.3	101.01	10
=	=	30	26.63	-	1.295	0.007	9.4	92.18	10
Sys (5-2)	*PhTMS/ DPhDMS/TMOS (EtOH)*	2	38.13	91	1.2956	0.002	9.6	94.14	10
=	=	5	37.17	88	1.2978	0.0043	9.1	89.24	11
=	=	10	26.51	87	1.2989	0.0071	7.3	71.59	11
=	=	20	16.46	89	1.3075	0.0026	6.8	66.68	11
=	=	30	-8.85	-	1.331	0.0006	8.8	86.3	10
Sys (3-1)	*PhTES/ DPhDES/TEOS (MeOH)*	2	40.94	86	1.2819	0.0003	10.2	100.03	15
=	=	5	28.12	84	1.2825	0.001	9.4	92.18	15
=	=	10	38.84	86	1.2942	0.0035	10.3	101.01	15
=	=	20	10.82	84	1.2954	0.0027	7.3	71.59	16
=	=	30	12.44	87	1.3009	0.0022	6.6	64.72	16
=	=	40	-2.51	88	1.3111	0.003	3.4	33.34	16
=	=	45	22.1	90	1.341	0.0062	10	98.07	17
=	=	50	28.25	-	-	-	9.8	96.1	16
Sys (3-2)	*PhTES/ DPhDES/TEOS (EtOH)*	2	30.95	89	1.2832	0.0006	4.6	45.11	17
=	=	5	25.23	86	1.2865	0.0041	6.7	65.70	18
=	=	10	58.57	88	1.2948	0.002	10.1	99.05	18
=	=	20	49.00	88	1.2963	0.0052	9.5	93.16	19
Sys (7-1)	*PhTES/ DPhDES/TMOS (MeOH)*	2	37.9	89	1.2988	0.0036	10.2	100.03	15
=	=	5	45.89	87	1.2993	0.0006	11.1	108.85	15
=	=	10	47.92	89	1.3031	0.0017	10.5	102.97	15

=	=	13	43.74	90	1.3072	0.002	10	98.07	16
Sys (7-2)	*PhTES/ DPhDES/TMOS (EtOH)*	2	41.09	82	1.2991	0.0008	10.9	106.89	16
=	=	5	32.58	82	1.2980	0.0022	10.7	104.93	16
=	=	10	41.34	85	1.3133	0.001	11.0	107.87	17
=	=	20	42.55	84	1.3216	0.0025	11.5	112.78	17
=	=	30	54.14	-	1.3314	0.0068	-	-	16
Sys1 or 5	*PhTMS/ DPhDMS*	0	25.97	88	1.2843	0.0037	6.3	61.78	16
Sys 3 or 7	*PhTES/ DPhDES*	0	1.24	90	1.2837	0.0041	8.8	86.30	16

Table 4.11: Compositions of the investigated melting gels systems and their limits.

System ID	***Composition***			***System limit%, TROS W% of (Mono.)***
	TROS	***Mono. Sub.***	***Di.Sub.***	
Sys (1-1)	TEOS (MeOH)	PhTMS	DPhDMS (MeOH)	5
Sys (1-2)	TEOS (EtOH)	PhTMS	DPhDMS (MeOH)	30
Sys (3-1)	TEOS (MeOH)	PhTES	DPhDES (EtOH)	45
Sys (3-2)	TEOS (EtOH)	PhTES	DPhDES (EtOH)	20
Sys (5-1)	TMOS (MeOH)	PhTMS	DPhDMS (MeOH)	30
Sys (5-2)	TMOS (EtOH)	PhTMS	DPhDMS (MeOH)	30
Sys (7-1)	TMOS (MeOH)	PhTES	DPhDES (EtOH)	13
Sys (7-2)	TMOS (EtOH)	PhTES	DPhDES (EtOH)	30
Sys 1 or Sys 5	-	PhTMS	DPhDMS (MeOH)	-
Sys 3 or Sys 7	-	PhTES	DPhDES (EtOH)	-

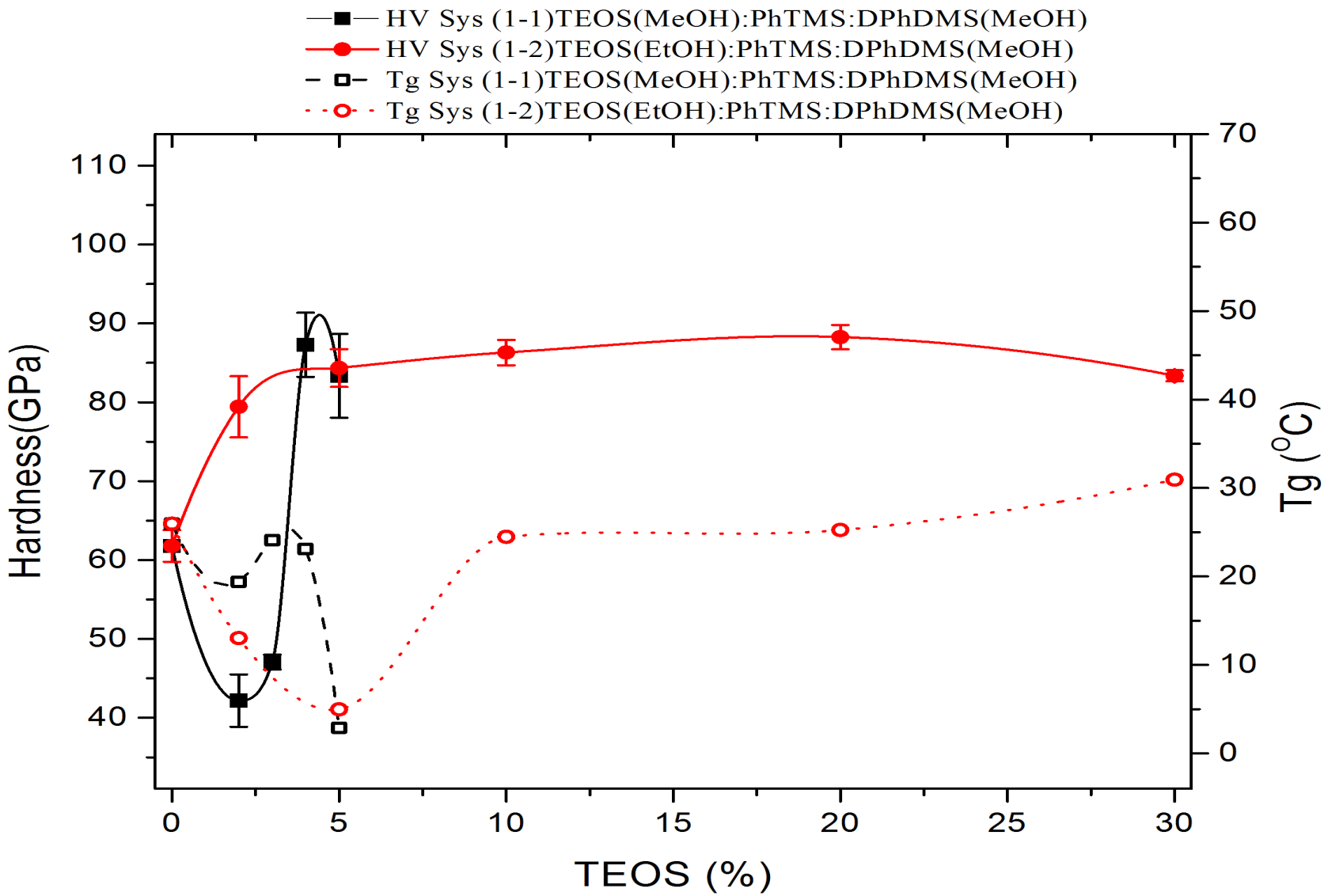

Fig 4.19: Vickers hardness vs. glass transition temperature for sys (1-1), and sys (1-2).

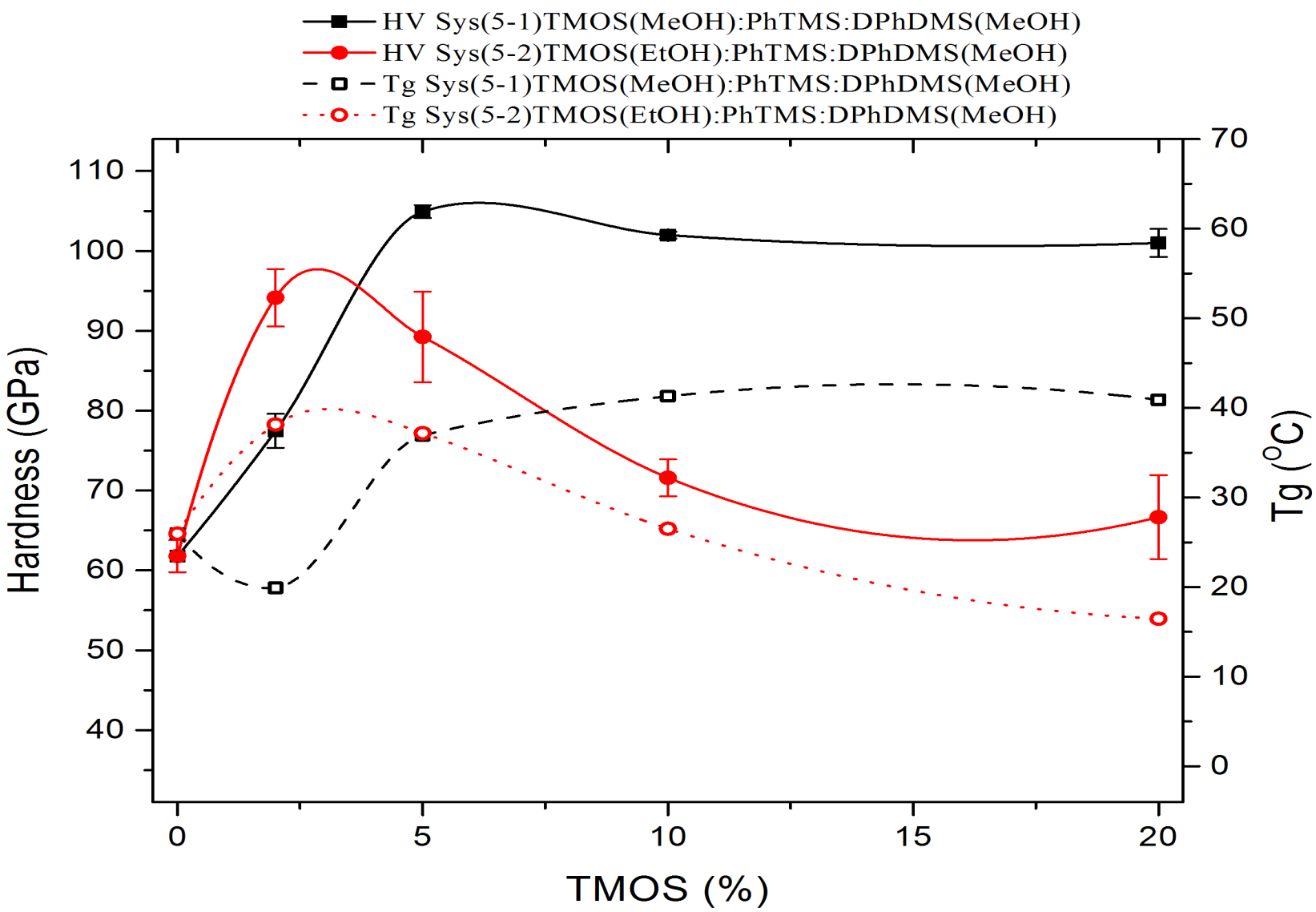

Fig 4.20: Vickers hardness vs. glass transition temperature for sys (5-1), and sys (5-2).

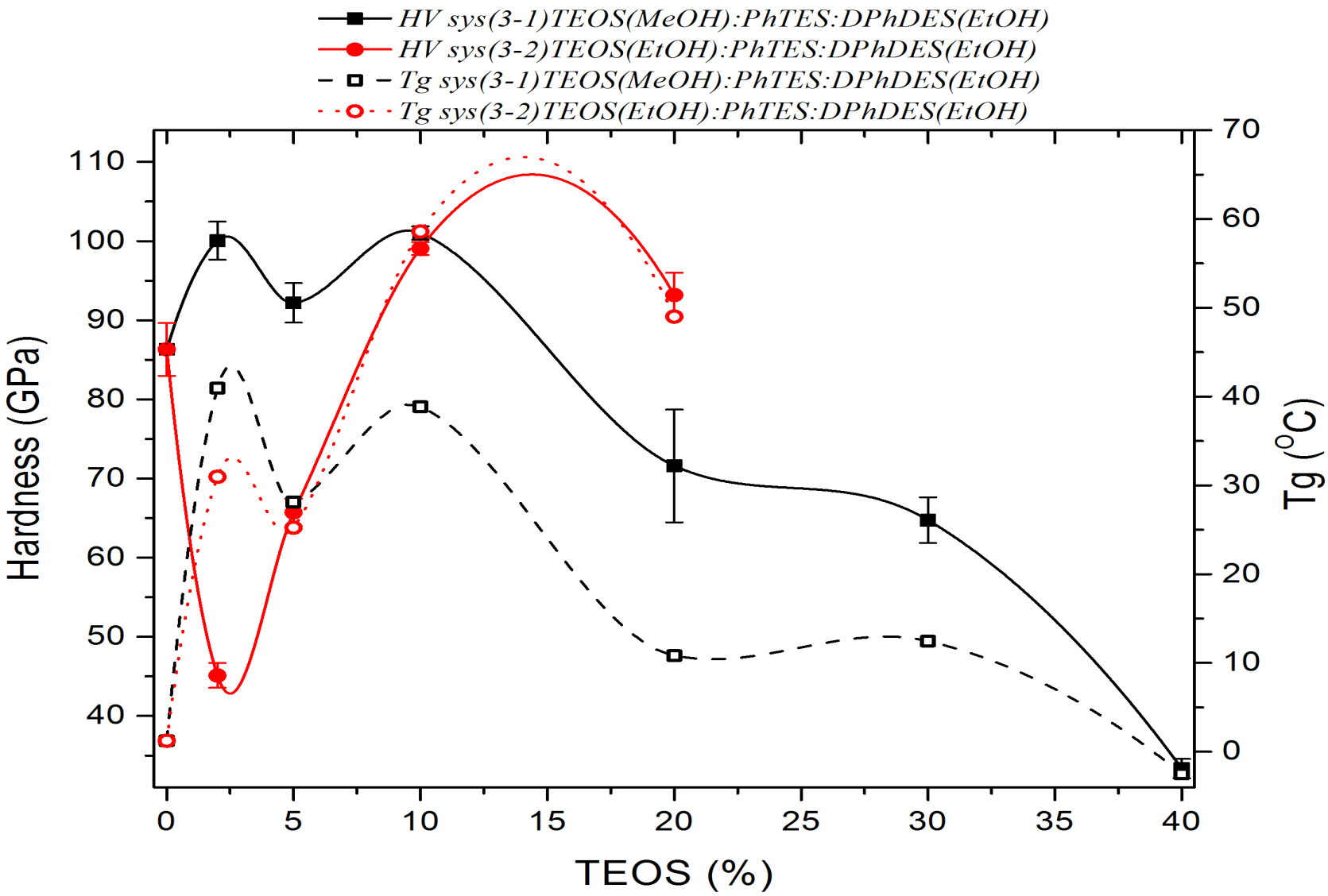

Fig 4.21: Vickers hardness vs. glass transition temperature for sys (3-1), and sys (3-2).

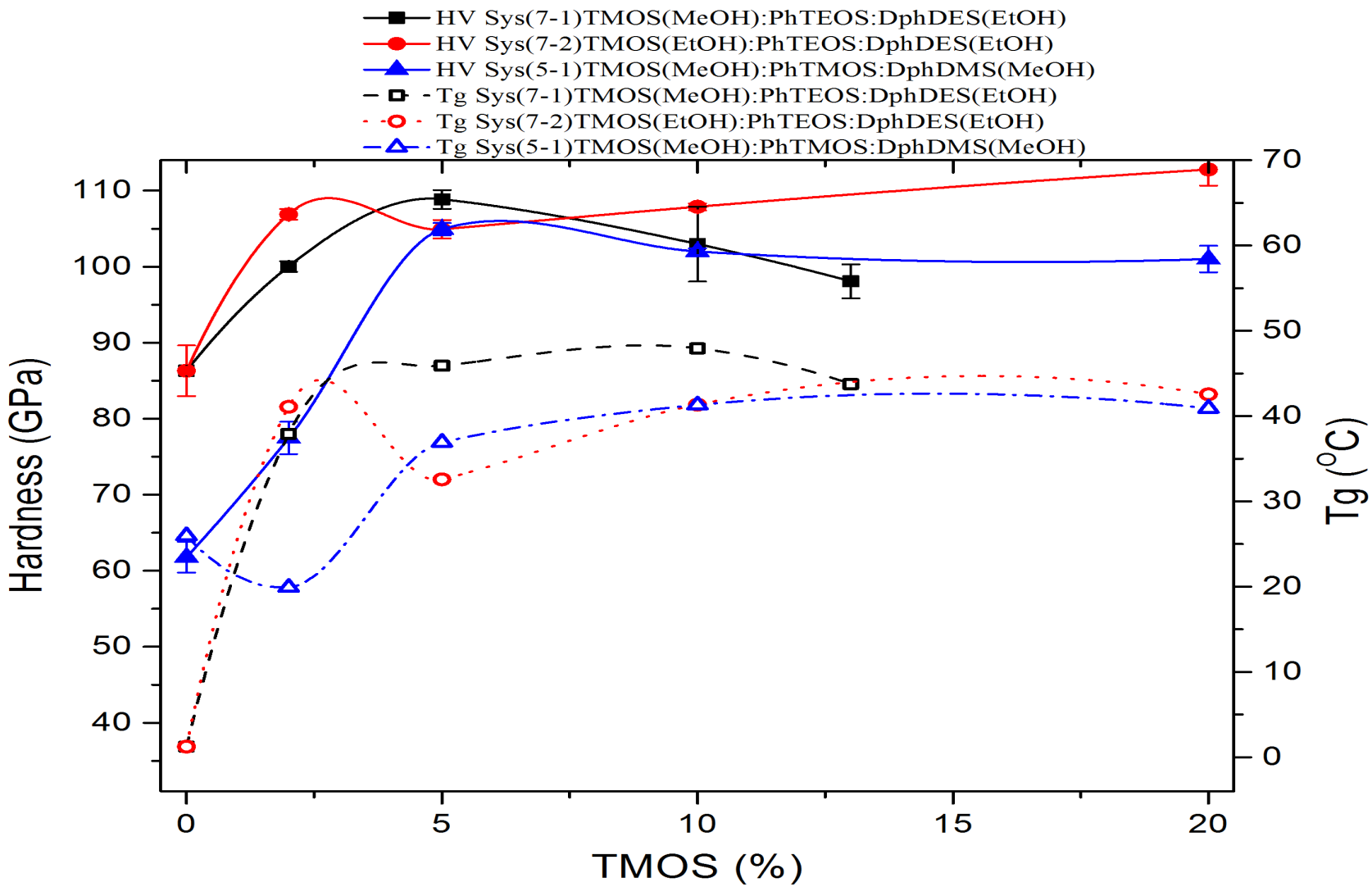

Fig 4.22: Vickers hardness vs. glass transition temperature for sys (7-1), (7-2), and (5-1).

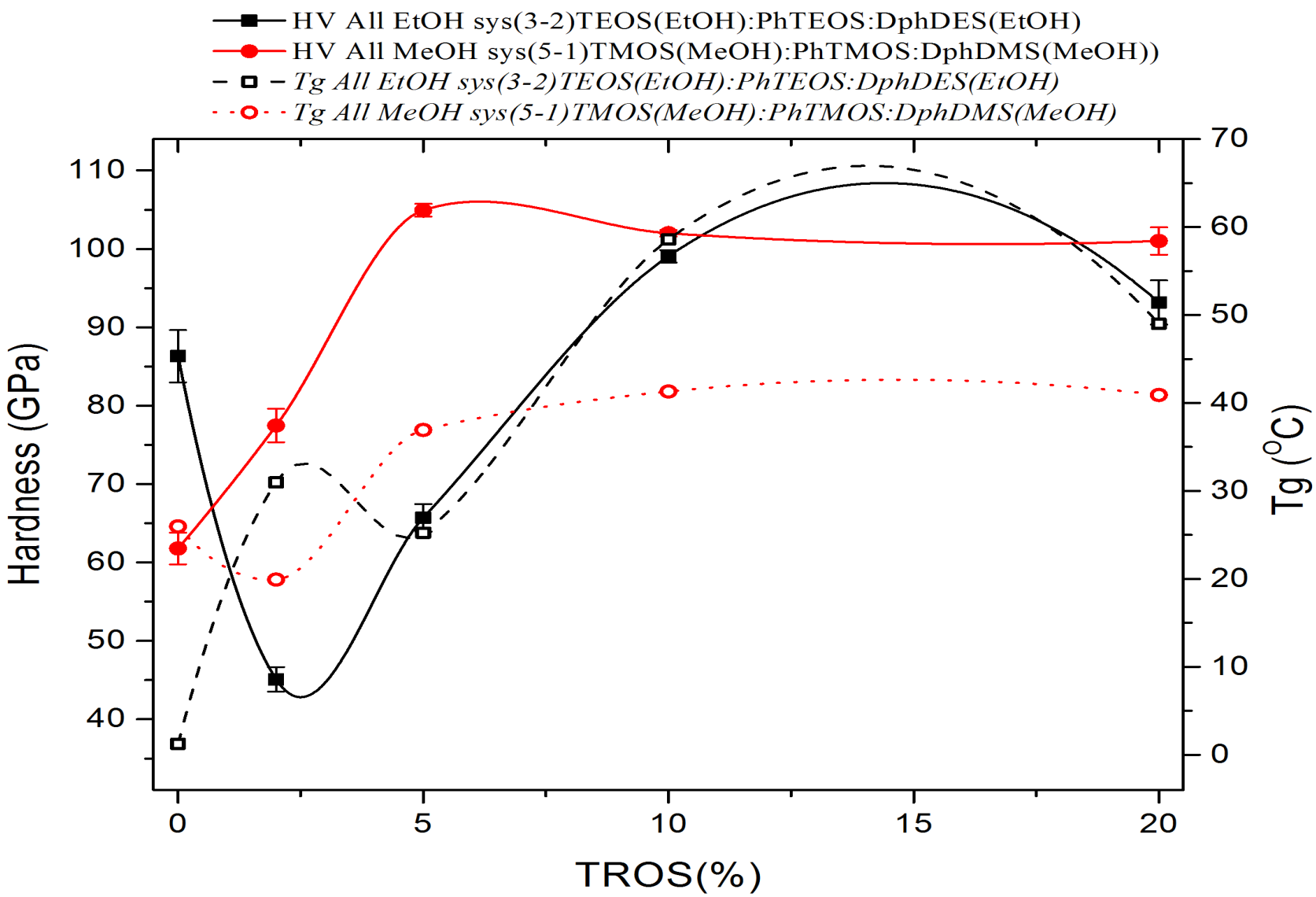

Fig 4.23: Vickers hardness vs. glass transition temperature for all Ethoxy system (3-2) and all Methoxy system (5-1).

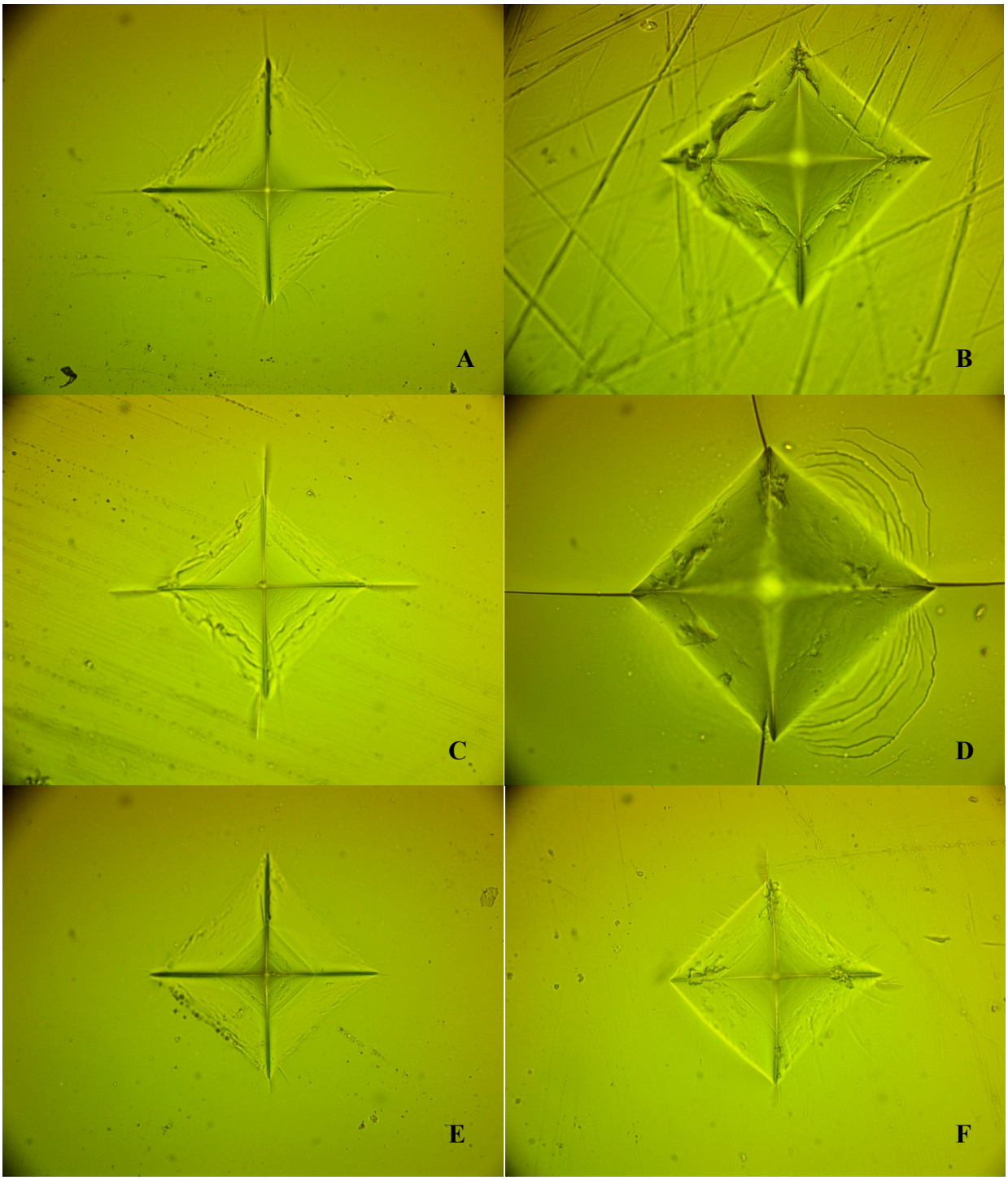

Figure 4.24: Optical micrograph of a Vickers indentation for **A** sys (1-1)5%, **B** sys (3-1)20%, **C** sys (5-1)20%, **D** sys (7-1)13%, **E** (PhTMS/DPhDMS), **F** (PhTES/DPhDES).

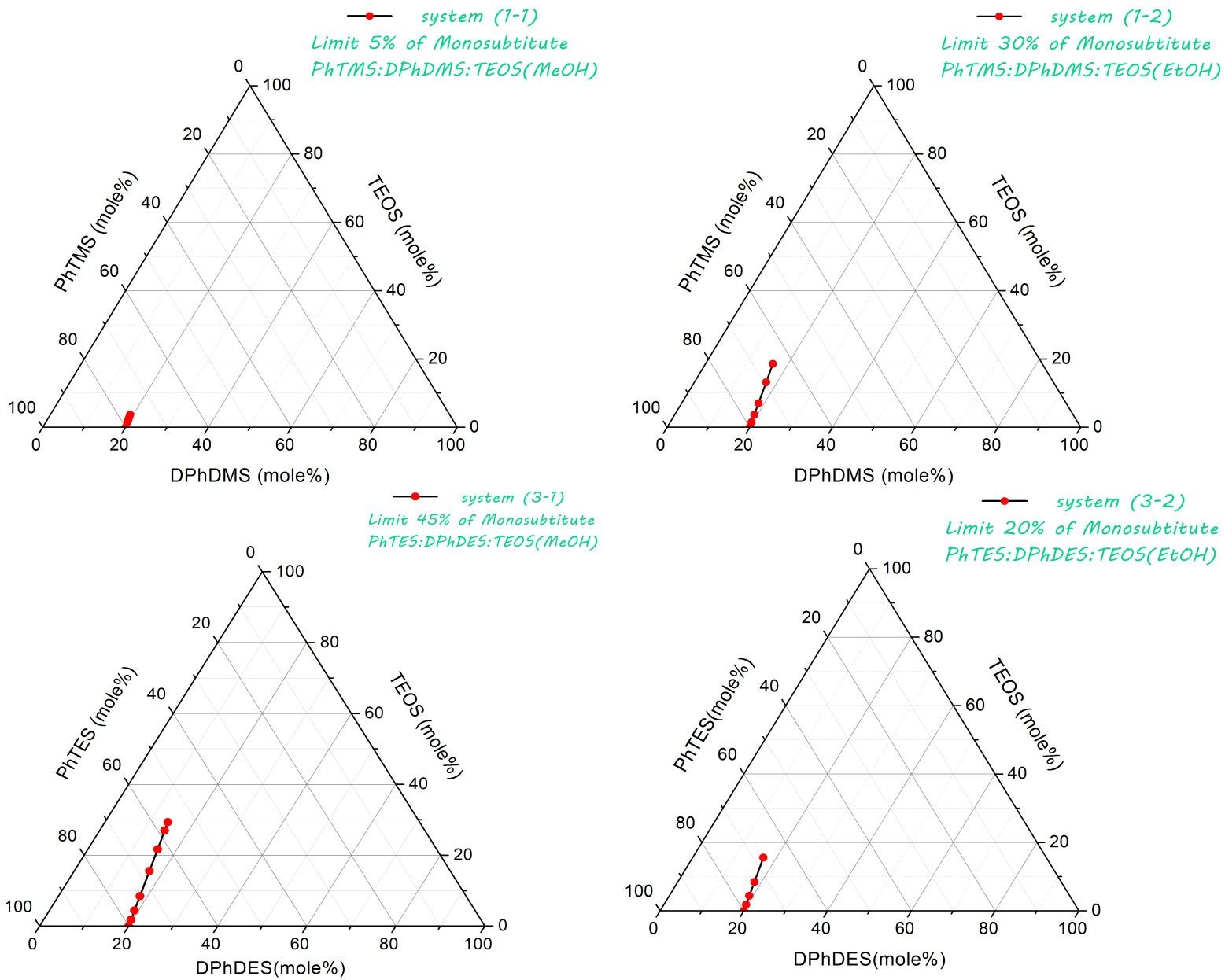

Figure 4.25: Ternary expression of composition region in which melting gel can be process with TEOS.

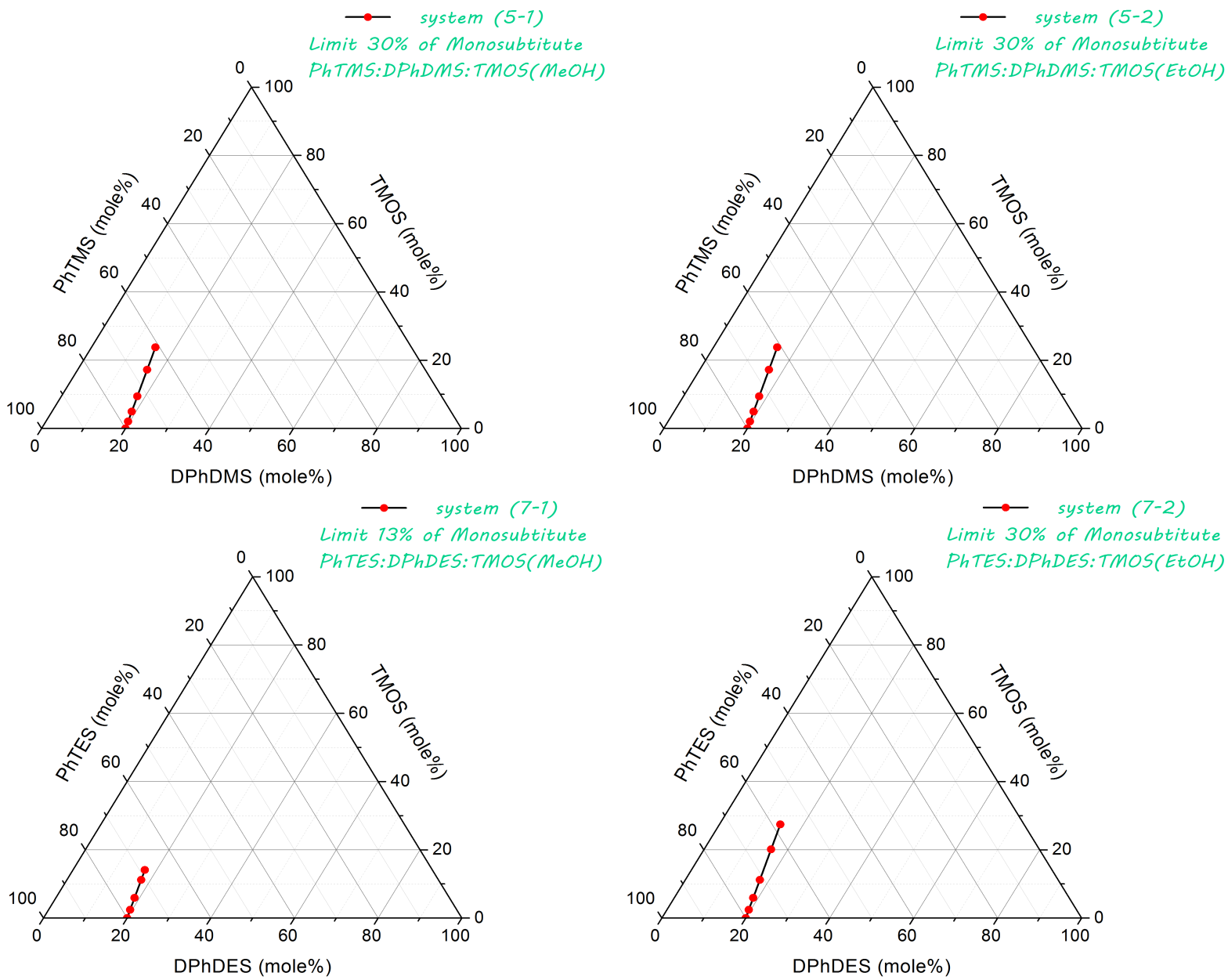

Figure 4.26: Ternary expression of composition region in which melting gel can be process with TMOS.

Chapter Five

Conclusions and Future Work

5.1 Conclusions

This dissertation is based on the preparation of melting gel materials, which are a class of organic-inorganic hybrid materials, also known as "ceramers" or "ormosil". These materials possess both ceramic and polymeric characteristics. Melting gels have the ability to soften upon heating to a temperature around (~110) °C and become rigid again when cooled down to room temperature. This process can be repeated many times. Once melting gels are heated to their consolidation temperature, they do not soften again. They are transformed into hybrid glasses. The consolidation temperature varies with the composition. Organic-inorganic hybrid materials have been developed as coatings for anticorrosion applications. The inorganic component in the coatings, typically prepared from alkoxysilanes via a sol-gel process, functions as both an adhesion promoter and a corrosion inhibitor.

Hybrid melting gels were successfully synthesized using phenyl substituted alkoxides and tetra-alkoxysilane. In general, three components (mono-substituted organo-modified alkoxysilane $\mathrm{R'Si(OR)_3}$, di-substituted organo-modified alkoxysilane $\mathrm{R'_2Si(OR)_2}$, and tetra-alkoxysilane $Si(OR)_4$) were mixed to prepare melting gels. The miscibility limits of adding tetra-alkoxide for all systems were determined and it was maximum for system (3-1) containing PhTES and DPhDES in ethanol with 50% TEOS in methanol, and minimum for sys (1-1) containing PhTMS and DPhDMS in methanol with

5% TEOS in methanol.

Increasing the amount of tetrafunctional alkoxide is intended to increase the number of reactive sites, and, therefore, the number of bridges between the molecular species formed when the tetralkoxysiloxanes hydrolyze. Accordingly, the total weight loss and the consolidation temperature generally decrease with increasing the concentration of the tetralkoxysiloxane. In general, the maximum exothermic peak temperature and total weight loss were higher in systems with TEOS than with TMOS. From the DSC plots, glass transition temperatures showed that it increases gradually with increasing tetra-alkoxysilane when it is diluted with the same alcohol group but decreases when tetra-alkoxysilane is diluted with a different alcohol group. For example, the glass transition temperature increases from about 1 to 60°C in sys (3-1) containing PhTES and DPhDES in ethanol with TEOS in ethanol, while it decreased from about 40 to -2°C in sys (3-2) containing PhTES and DPhDES in ethanol with TEOS in methanol. This is due to the transesterification reactions that compete with condensation polymerization and network formation.

All samples of the consolidated gel on mica substrates for systems with TMOS were smooth and transparent while it became more yellowish with increasing TEOS%. SEM images show that solvent effects are seen in the morphology of the hybrid glass. It appears smoother with uniform structure when the co-solvent used in the mixture has the same parent alcohol group as the tetra alkoxysilane.

The study shows that the hardness measurements correlate well with the glass

transition temperatures. Hardness increased with increasing tetra-alkoxysilane component when diluted with the parent alcohol. The exception was system 1 where the hardness increased with TEOS in both ethanol and methanol solvents. As a general rule, systems with ethoxy substituents have higher hardness than the comparable systems with methoxy substituents.

Melting gels with methoxy substituents were more hydrophobic to water than systems with ethoxy substituents, regardless the solvents. However, melting gels synthesized using only two components have higher contact angles than three components systems.

FTIR spectra of melting gels after consolidation confirm the existence of Si–C direct bonds that are retained as a part of the polymer network in the consolidated hybrid glasses. All of the peaks could be assigned to different groups that are expected in the consolidated gel. Most of the peaks shift to slightly higher wavenumbers in systems with TEOS, while in systems with TMOS the peaks shift to a lower wavenumber. The shifts in wavelength are consistent with ethoxy substituted silanes having longer times of gelation than methoxy substituted silanes. Also, the study found that the intensity of the peaks for free OH and associated OH groups increased with increasing tetra-alkoxide concentration due to unreacted Si–O–R groups, uncondensed Si-O-H groups, and residual alcoholic co-solvent within the films which are not present in two component systems.

He pycnometry density of all samples increases with increasing the tetra-alkoxide content. Samples with TMOS had higher density than those with TEOS due to the higher

reactivity of TMOS. Moreover, methoxy containing systems have lower weight loss percentage and therefor lower skeletal densities than ethoxy containing systems. This is consistent with methoxy containing systems having higher consolidation temperatures than comparable ethoxy containing systems.

5.2 Future Work

The glasses obtained by the melting gel method offer the application not only to electronics but also to photonics by incorporating optically functional molecules. These glasses are indispensable to advanced electronics technology. For example, they are used as insulating, bonding, and passivation materials in a variety of electronics parts [116,123,167]. Linear or nonlinear optical molecules along with metal ions such as rare earth and transition metals can be mixed together in the polysiloxane glasses due to the high solubility and the coexistence of an organic functional group and an inorganic network.

Organic–inorganic hybrid (OIH) coatings produced by sol-gel process exhibited promising properties of adhesion and corrosion protection with many metal substrate [168]. Our melting gel materials were successfully used as corrosion protection for stainless steel [127] and need to be studied further with other metals to prove their effectiveness as corrosion inhibitor by preventing the contact between the corrosive medium and the metallic substrate and preventing ion migration through the coatings. OIHs obtained by sol–gel methods are a new generation of multifunctional materials with a broad spectrum of useful properties and a diversity of application potential that need to be investigate.

Other recommendations that need to be considered in the future in order to fully understand the behavior of melting gel and improve their properties include:

1- Investigate the molecular structure further using Raman and Nuclear magnetic resonance spectroscopy and evaluate the effect of TEOS and TMOS on it.
2- Employ hybrid glass that we obtain in other applications such as microelectronics and dye-sensitized solar cells.
3- Study the effect of changing mono-substituents to di-substituents mole ratio on melting gel properties.
4- Using substituents other than phenyl such as methyl or ethyl or mixture of them with tetra-alkoxide to examine the possibility of producing melting gel.
5- Changing the molar ratio between TROS: alcohol instead of 1:4 that have been used in this study and determine its influence on melting gel properties.
6- Use different method of coating such as spin coating and examine the effect on the properties of melting gel (hardness, FTIR spectra, contact angle, thermal behavior).

References

1. W.D. Callister and D.G. Rethwisch. Materials science and engineering: an introduction; Wiley New York, 2007.

2. K.K. Chawla, Composite materials: science and engineering; Springer Science & Business Media, 2012.

3. J.W. Martin, Concise encyclopedia of the structure of materials; Elsevier, 2006.

4. P. Gómez-Romero and C. Sanchez. "Hybrid materials, functional applications. An introduction," Functional hybrid materials, 1-14 (2004).

5. P. Gomez Romero, "Hybrid organic–inorganic materials—in search of synergic activity," Adv Mater, 13, 163-74 (2001).

6. S. Kuo, C. Huang and F. Chang. "Nanocomposites based on POSS," Recent advances in polymer nanocomposites. Boston: Brill Academic Publishers, 155-91 (2010).

7. B.M. Novak, "Hybrid nanocomposite materials—between inorganic glasses and organic polymers," Adv Mater, 5, 422-33 (1993).

8. A. Deronzier and J. Moutet. "Polypyrrole films containing metal complexes: syntheses and applications," Coord. Chem. Rev., 147, 339-71 (1996).

9. M. Lira-Cantu and P. Gomez-Romero. "Hybrid organic-inorganic functional materials: insertion electrodes formed by conducting organic polymers and electroactive inorganic species," Recent Research Development in Physical Chemistry", SG Pandalai Ed., Transworld Research Network, 379-401 (1997).

10. P. Judeinstein and C. Sanchez. "Hybrid organic–inorganic materials: a land of multidisciplinarity," Journal of Materials Chemistry, 6, 511-25 (1996).

11. C. Sanchez and F. Ribot. "Design of hybrid organic-inorganic materials synthesized via sol-gel chemistry," New Journal of Chemistry, 18, 1007-47 (1994).

12. J. Luan, S. Wang, Z. Hu and L. Zhang. "Synthesis techniques, properties and applications of polymer nanocomposites," Current Organic Synthesis, 9, 114-36 (2012).

13. I. Jeon and J. Baek. "Nanocomposites derived from polymers and inorganic nanoparticles," Materials, 3, 3654-74 (2010).

14. T. Krasia-Christoforou, "Organic–Inorganic Polymer Hybrids: Synthetic Strategies and Applications," pp. 11-63 in Hybrid and Hierarchical Composite Materials. Anonymous Springer, 2015.

15. S.S. Ray and M. Okamoto. "Polymer/layered silicate nanocomposites: a review from preparation to processing," Progress in polymer science, 28, 1539-641 (2003).

16. M. Albdiry, B. Yousif, H. Ku and K. Lau. "A critical review on the manufacturing processes in relation to the properties of nanoclay/polymer composites," J. Composite Mater., 47, 1093-115 (2013).

17. S. Lai, J. Chen, J. Han, Y. Yu and H. Lai. "Preparation and properties of melt-blended polylactic acid/polyethylene glycol-modified silica nanocomposites," J Appl Polym Sci, 130, 496-503 (2013).

18. X. Xia, S. Cai and C. Xie. "Preparation, structure and thermal stability of Cu/LDPE nanocomposites," Mater. Chem. Phys., 95, 122-9 (2006).

19. C. Decker, "The use of UV irradiation in polymerization," Polym. Int., 45, 133-41 (1998).

20. Y. Yagci, "New photoinitiating systems designed for polymer/inorganic hybrid nanocoatings," Journal of Coatings Technology and Research, 9, 125-34 (2012).

21. M. Alexandre and P. Dubois. "Polymer-layered silicate nanocomposites: preparation, properties and uses of a new class of materials," Materials Science and Engineering: R: Reports, 28, 1-63 (2000).

22. D. Bogdal, A. Prociak and S. Michalowski. "Synthesis of polymer nanocomposites under microwave irradiation," Current Organic Chemistry, 15, 178-88 (2011).

23. C. Janáky, C. Visy, O. Berkesi and E. Tombácz. "Conducting polymer-based electrode with magnetic behavior: electrochemical synthesis of poly (3-thiophene-acetic-acid)/magnetite nanocomposite thin layers," The Journal of Physical Chemistry C, 113, 1352-8 (2009).

24. G.L. Chakkalakal, S. Ramakrishnan and M.R. Bockstaller. "Polymer-Tethered Nanoparticle Materials—An Emerging Platform for Multifunctional Hybrid Materials," pp. 65-94 in Hybrid and Hierarchical Composite Materials. Anonymous Springer, 2015.

25. R. Barbey, L. Lavanant, D. Paripovic, et al. "Polymer brushes via surface-initiated controlled radical polymerization: synthesis, characterization, properties, and applications," Chem. Rev., 109, 5437-527 (2009).

26. B. Zhao and W.J. Brittain. "Polymer brushes: surface-immobilized macromolecules," Progress in Polymer Science, 25, 677-710 (2000).

27. H. Cong and S. Yu. "Self-assembly of functionalized inorganic–organic hybrids," Current Opinion in Colloid & Interface Science, 14, 71-80 (2009).

28. S. Förster and M. Antonietti. "Amphiphilic block copolymers in structure-controlled nanomaterial hybrids," Adv Mater, 10, 195-217 (1998).

29. C.J. Brinker and George W. Scherer. Sol-gel science: the physics and chemistry of sol-gel processing pp. 908. Academic Press, San Diego, 1990.

30. A.C. Pierre, Introduction to sol-gel processing pp. 394. Kluwer Academic Publishers, Boston, 1998.

31. L.C. Klein, "Sol-gel optics: processing and applications," The Kluwer International Series in Engineering and Computer Science, Boston: Kluwer Academic Publishers, edited by Klein, Lisa C., (1994).

32. Ebelmen, M. “Recherches sur les combinaisons des acides borique et silicique avec les ethers,” Ann. Chimie Phys. 1846, 16, 129.

33. T. Graham, "On the properties of silicic acid and other analogous colloidal substances," Proceedings of the Royal Society of London, 13, 335-41 (1863).

34. P.J. Flory, Principles of polymer chemistry; Cornell University Press, 1953; Chapter IX.

35. H.E. Bergna and W.O. Roberts. Colloidal silica: fundamentals and applications; CRC Press, 2005.

36. P. Hajji, L. David, J. Gerard, J. Pascault and G. Vigier. "Synthesis, structure, and morphology of polymer–silica hybrid nanocomposites based on hydroxyethyl methacrylate," Journal of Polymer Science Part B: Polymer Physics, 37, 3172-87 (1999).

37. J.D. Mackenzie and D.R. Ulrich. "Sol-gel optics, present status and future trends," 2-13 (1990).

38. J. Livage, M. Henry and C. Sanchez. "Sol-gel chemistry of transition metal oxides," Progress in solid-state chemistry, 18, 259-341 (1988).

39. J. Livage and C. Sanchez. "Sol-gel chemistry," J. Non Cryst. Solids, 145, 11-9 (1992).

40. R.K. Iler, "The chemistry of silica: solubility, polymerization, colloid and surface properties, and biochemistry. 1979," Canada: John Wiley &Sons Inc,

41. I. Artaki, T. Zerda and J. Jonas. "Solvent effects on the condensation stage of the sol-gel process," J. Non Cryst. Solids, 81, 381-95 (1986).

42. L.C. Klein, "Sol-Gel Coatings," pp. 501-520 in Vol. 2, Thin film processes II. Edited by W. Kern. Academic press, 2012.

43. N. Hüsing and U. Schubert. "Porous Inorganic-Organic Hybrid Materials," Functional Hybrid Materials, 86-121 (2004).

44. G.W. Scherer, "Aging and drying of gels," J. Non Cryst. Solids, 100, 77-92 (1988).

45. S.P. Watton, C.M. Taylor, G.M. Kloster and S.C. Bowman. "Coordination complexes in sol-gel silica materials," Progress in inorganic chemistry, 51, 333-420 (2003).

46. L.L. Hench and J.K. West. "The sol-gel process," Chem. Rev., 90, 33-72 (1990).

47. A.E. Gash, T.M. Tillotson, J.H. Satcher Jr, L.W. Hrubesh and R.L. Simpson. "New sol–gel synthetic route to transition and main-group metal oxide aerogels using inorganic salt precursors," J. Non Cryst. Solids, 285, 22-8 (2001).

48. J.D. Wright and N.A. Sommerdijk. Sol-gel materials: chemistry and applications; CRC press, 2000.

49. C. Sanchez, F. Ribot and S. Doeuff. "Transition metal oxo polymers synthesized via sol-gel chemistry," pp. 267-295 in Inorganic and Organometallic Polymers with Special Properties. R. M. Laine, ed., Nato ASI Series, vol 206, Kluwer Publishing, New York, (1992).

50. D. Levy and M. Zayat. The Sol-Gel Handbook: Synthesis, Characterization and Applications, 3-Volume Set; John Wiley & Sons, 2015.

51. D. Kundu and D. Ganguli. "Monolithic zirconia gels from metal—organic solutions," J. Mater. Sci. Lett., 5, 293-295 (1986).

52. R.C. Mehrotra, "Chemistry of metal β-diketonates," Pure and Applied Chemistry, 60, 1349-56 (1988).

53. H. Schmidt, "Organically modified silicates by the sol-gel process," 32, 327 (1984).

54. G. Wilkes, B. Orler and H. Huang. ""Ceramers": hybrid materials incorporating polymeric/oligomeric species into inorganic glasses utilizing a sol-gel approach," 26, 300-301 (1985).

55. G. Philipp and H. Schmidt. "New materials for contact lenses prepared from Si-and Ti-alkoxides by the sol-gel process," J. Non Cryst. Solids, 63, 283-92 (1984).

56. J. Livage, "Sol-gel processes," Current Opinion in Solid State and Materials Science, 2, 132-8 (1997).

57. K. Haas and H. Wolter. "Synthesis, properties and applications of inorganic–organic copolymers (ORMOCER®s)," Current Opinion in Solid State and Materials Science, 4, 571-80 (1999).

58. F. Mammeri, E. Le Bourhis, L. Rozes and C. Sanchez. "Mechanical properties of hybrid organic–inorganic materials," Journal of materials chemistry, 15, 3787-811 (2005).

59. K.J. Shea and D.A. Loy. "Bridged polysilsesquioxanes. Molecular-engineered hybrid organic− inorganic materials," Chemistry of materials, 13, 3306-19 (2001).

60. R.H. Baney, M. Itoh, A. Sakakibara and T. Suzuki. "Silsesquioxanes," Chem. Rev., 95, 1409-30 (1995).

61. M. Niederberger and N. Pinna. Metal oxide nanoparticles in organic solvents: synthesis, formation, assembly and application; Springer Science & Business Media, 2009.

62. . L.C. Klein and A. Jitianu. "Organic–inorganic hybrid melting gels " J. Sol Gel Sci. Technol., 55, 86-93 (2010).

63. A. Jitianu, J. Doyle, G. Amatucci and L.C. Klein. "Methyl-modified melting gels for hermetic barrier coatings," Proceedings MS&T, 2171-82 (2008).

64. A. Jitianu, J. Doyle, G. Amatucci and L.C. Klein. "Methyl modified siloxane melting gels for hydrophobic films " J. Sol Gel Sci. Technol., 53, 272 - 279 (2009).

65. L. Klein and A. Jitianu. "Synthesis of Melting Gels Using Mono-Substituted and Di-Substituted Alkoxysiloxanes," Material Matters, Volume 7, 8–14 (2012).

66. S. Wang, D.K. Wang, S. Smart and J.C. Diniz da Costa. "Ternary Phase-Separation Investigation of Sol-Gel Derived Silica from Ethyl Silicate 40 " Scientific Reports, 5, 14560 (2015).

67. K. Nakanishi, "Sol–Gel Process of Oxides Accompanied by Phase Separation " Bull. Chem. Soc. Jpn., 79, 10.1246/bcsj.79-691 (2010).

68. K. Nakanishi and N. Soga. "Phase separation in silica sol-gel system containing polyacrylic acid I. Gel formation behavior and effect of solvent composition " J. Non Cryst. Solids, 139, 1-13 (1992).

69. H. Kaji, K. Nakanishi and N. Soga. "Formation of porous gel morphology by phase separation in gelling alkoxy-derived silica. Phenomenological study " J. Non Cryst. Solids, 185, 18-30 (1995).

70. S. Sakka, Handbook of sol-gel science and technology. V.III Applications of Sol–Gel Technology; Springer Science & Business Media, 2005.

71. L.C. Klein, Sol-gel technology for thin films, fibers, preforms, electronics, and specialty shapes; William Andrew Publishing, 1988.

72. C. Sanchez, B. Julián, P. Belleville and M. Popall. "Applications of hybrid organic–inorganic nanocomposites," Journal of Materials Chemistry, 15, 3559-92 (2005).

73. D.R. Ulrich, "Prospects for sol-gel processes," J. Non Cryst. Solids, 121, 465-79 (1990).

74. J.D. Mackenzie, "Applications of the sol-gel process," J. Non Cryst. Solids, 100, 162-8 (1988).

75. M. Guglielmi, "Sol-gel coatings on metals," J. Sol Gel Sci. Technol., 8, 443-9 (1997).

76. G. Soula, "Ceramics from Organometallic Polymers: Industrial Perspectives," pp. 31-42 in Inorganic and Organometallic Polymers with Special Properties. R. M. Laine, ed., Nato ASI Series, vol 206, Kluwer Publishing, New York, (1992).

77. J.D. Mackenzie, "Glasses from melts and glasses from gels, a comparison," J. Non Cryst. Solids, 48, 1-10 (1982).

78. Y. Hasegawa, "Synthesis of continuous silicon carbide fiber," J. Mater. Sci., 24, 1177-90 (1989).

79. B.E. Yoldas, "Technological significance of sol-gel process and process-induced variations in sol-gel materials and coatings " J. Sol Gel Sci. Technol., 1, 65 - 77 (1993).

80. H. Dislich, "Glassy and crystalline systems from gels: Chemical basis and technical application " J. Non Cryst. Solids, 57, 371 - 388 (1983).

81. D.L. Segal, "Sol-gel processing: Routes to oxide ceramics using colloidal dispersions of hydrous oxides and alkoxide intermediates " J. Non Cryst. Solids, 63, 183 - 191 (1984).

82. F. wöhler, Ann. chim. phys., 28(3), 328 (1850); 29(3), 166 (1850).

83. A. Cossa, "Sull'Amalgama dell'Alluminio (On the Amalgam of Aluminum)," Il Nuovo Cimento, 3, 228 (1870).

84. S.S. Kistler, "Coherent Expanded Aerogels and Jellies." Nature, 127, 741 (1931).

85. T. Wood and H. Dislich. "Abbreviated History of Sol-Gel Technology," Ceram.Trans.Vol.55, 3-23 (1994).

86. W.A. Patrick, “Silica gel and process of making same”, U.S. Patent No. 1,297,724. 18 Mar. (1919).

87. W.A. Patrick, “Catalyst” British Patent 208,656 (1923).

88. (A selection) W.A. Patrick, “Adsorbent and catalyst oxides” U.S. Patent 1,520,305 (1924); “Porous catalytic gels” U.S. Patent 1,577,186 (1926); “Gels for catalytic and absorbent purposes” U.S. Patent 1.577,190 (1926); “Tungstic oxide gel” U.S. Patent 1,682,239 (1928); “Stannic oxide gel” U.S. Patent 1,682,240 (1928); “Aluminum oxide gel” U.S. Patent 1,682,241 (1928); “Titanium oxide gel” U.S. Patent 1,682,242 (1928); “Catalytic and absorbent gel” U.S. Patent 1,696,644 (1928); “Tungsten oxide gel” U.S. Patent 1,848,266 (1932).

89. W. Geffcken and E. Berger, "Method for producing layers on solid objects." U.S. Patent No. 2,366,516. 2 Jan. (1945).

90. W. Geffcken, "Dünne Schichten auf Glas," Glastechn.Ber, 24, 143-51 (1951).

91. J.D. Mackenzie, "Present and future directions in sol-gel science and technology," Ceram.Trans.Vol.55, 25-31 (1994).

92. R. Roy, "Aids in hydrothermal experimentation: II, Methods of making mixtures for both “Dry” and “Wet” phase equilibrium studies," J Am Ceram Soc, 39, 145-6 (1956).

93. D.M. Roy and R. Roy. "Synthesis and stability of minerals in the system MgO-Al_2O_3-SiO_2-H_2O," Am. Mineral., 40, 147-78 (1955).

94. R. Wymer, "Sol-gel Processes for Ceramic Nuclear Fuels," Proc.Panel on Sol-gel Processes for Ceramic Nuclear Fuels, Report STI/PUB–207, 131-72 (1968).

95. S. Hubert, Transparent, conductive, reflection-reducing coatings on non-conductive objects and method, (1963).

96. H. Dislich, "New Routes to Multicomponent Oxide Glasses " Angewandte Chemie International Edition in English, 10, 363-370 (1971).

97. Dimitriev, Y., Ivanova, Y., and Iordanova, R., "History of sol-gel science and technology," Journal of the University of Chemical Technology and Metallurgy, 43,2, 181-192 (2008).

98. H. Schmidt, "New type of non-crystalline solids between inorganic and organic materials," J. Non Cryst. Solids, 73, 681-91 (1985).

99. D. Avnir, D. Levy and R. Reisfeld. "The nature of the silica cage as reflected by spectral changes and enhanced photostability of trapped rhodamine 6G," J. Phys. Chem., 88, 5956-9 (1984).

100. Anonymous Method of preparing lead and alkaline earth titanates and niobates and coating method using the same to form a capacitor, (1967).

101. D. Ganguli and M. Chatterjee. Ceramic powder preparation: a handbook; Springer, 1997.

102. J. Wen and G.L. Wilkes. "Organic/inorganic hybrid network materials by the sol−gel approach," Chemistry of Materials, 8, 1667-81 (1996).

103. C. Sanchez, J. Galo, F. Ribot and D. Grosso. "Design of functional nano-structured materials through the use of controlled hybrid organic–inorganic interfaces," Comptes Rendus Chimie, 6, 1131-51 (2003).

104. H.S. Nalwa, Handbook of organic-inorganic hybrid materials and nanocomposites; American Scientific Publishers, 2003.

105. X. Guo, Q. Zhang, X. Ding, et al. "Synthesis and application of several sol–gel-derived materials via sol–gel process combining with other technologies: a review," J. Sol Gel Sci. Technol., 79, 328-58 (2016).

106. A. Jitianu, G. Amatucci and L.C. Klein. "Organic–inorganic sol-gel thick films for humidity barriers," J. Mater. Res., 23, 2084-90 (2008).

107. A. Jitianu, G. Amatucci and L.C. Klein. "Phenyl-Substituted Siloxane Hybrid Gels that Soften Below 140° C," J Am Ceram Soc, 92, 36-40 (2009).

108. A. Matsuda, Y. Matsuno, M. Tatsumisago and T. Minami. "Fine patterning and characterization of gel films derived from methyltriethoxysilane and tetraethoxysilane," J Am Ceram Soc, 81, 2849-52 (1998).

109. M. Kuniyoshi, M. Takahashi, Y. Tokuda and T. Yoko. "Hydrolysis and polycondensation of acid-catalyzed phenyltriethoxysilane (PhTES)," J. Sol Gel Sci. Technol., 39, 175-83 (2006).

110. Schmidt, H. and Popall, M., in Sol-Gel Optics I, edited by J.D. Mackenzie and D.R. Ulrich (Proc. SPIE1328, Washington, 1990), pp. 249.

111. H. Schmidt, H. Scholze and G. Tünker. "Hot melt adhesives for glass containers by the sol-gel process," J. Non Cryst. Solids, 80, 557-63 (1986).

112. K.J. Shea, D.A. Loy and O.W. Webster. "Aryl-bridged polysilsesquioxanes--new microporous materials," Chemistry of Materials, 1, 572-4 (1989).

113. K. Katagiri, K. Hasegawa, A. Matsuda, M. Tatsumisago and T. Minami. "Preparation of Transparent Thick Films by Electrophoretic Sol-Gel Deposition Using Phenyltriethoxysilane-Derived Particles," J Am Ceram Soc, 81, 2501-3 (1998).

114. A. Matsuda, T. Sasaki, K. Hasegawa, M. Tatsumisago and T. Minami. "Thermal softening behavior and application to transparent thick films of poly (benzylsilsesquioxane) particles prepared by the sol–gel process," J Am Ceram Soc, 84, 775-80 (2001).

115. A. Matsuda, T. Sasaki, K. Hasegawa, M. Tatsumisago and T. Minami. "Thermal softening behavior of poly (phenylsilsesquioxane) and poly (benzylsilsesquioxane) particles," Journal of the Ceramic Society of Japan, 108, 830-5 (2000).

116. H. Masai, M. Takahashi, Y. Tokuda and T. Yoko. "Gel-melting method for preparation of organically modified siloxane low-melting glasses," J. Mater. Res., 20, 1234-41 (2005).

117. H. Kakiuchida, M. Takahashi, Y. Tokuda, H. Masai, M. Kuniyoshi and T. Yoko. "Viscoelastic and structural properties of a phenyl-modified polysiloxane system with a three-dimensional structure," The Journal of Physical Chemistry B, 110, 7321-7 (2006).

118. H. Kakiuchida, M. Takahashi, Y. Tokuda, H. Masai and T. Yoko. "Effects of Organic Groups on Structure and Viscoelastic Properties of Organic− Inorganic Polysiloxane Hybrid System," The Journal of Physical Chemistry B, 111, 982-8 (2007).

119. L.C. Klein and A. Jitianu. "Encapsulating Battery Components with Melting Gels," Advances in Materials Science for Environmental and Energy Technologies III, Volume 250, 279-86 in Advances in Materials Science for Environmental and Energy Technologies III, Edited by T. Ohji, J. Matyas, N. J. Manjooran, G. Pickrell, and A. Jitianu. American Ceramic Soci- ety, Westerville, Ohio, 2014.

120. Y. Kamimura, K. Kurumada, K. Asaba, H. Ban-no, H. Kambara and M. Hiro. "Evaluation of activation energy of viscous flow of sol–gel derived phenyl-modified silica glass," J. Non Cryst. Solids, 352, 3175-8 (2006).

121. A. Jitianu, K. Lammers, G.A. Arbuckle-Kiel and L.C. Klein. "Thermal analysis of organically modified siloxane melting gels," Journal of thermal analysis and calorimetry, 107, 1039-45 (2011).

122. L.C. Klein, B. McClarren and A. Jitianu. "Silica-Containing Hybrid Nanocomposite" Melting Gels"," 783, 1432-7 (2014).

123. L. Gambino, A. Jitianu and L.C. Klein. "Dielectric behavior of organically modified siloxane melting gels," J. Non Cryst. Solids, 358, 3501-4 (2012).

124. A. Jitianu, G. Gonzalez and L.C. Klein. "Hybrid Sol–Gel Glasses with Glass-Transition Temperatures Below Room Temperature," J Am Ceram Soc, 98, 3673-9 (2015).

125. H. Ikeda, S. Fujino and T. Kajiwara. "Fabrication of Micropatterns on Silica Glass by a Room-Temperature Imprinting Method," J Am Ceram Soc, 94, 2319-22 (2011).

126. C. Fernández-Sánchez, V.J. Cadarso, M. Darder, C. Domínguez and A. Llobera. "Patterning high-aspect-ratio sol–gel structures by microtransfer molding," Chemistry of materials, 20, 2662-8 (2008).

127. M. Aparicio, A. Jitianu, G. Rodriguez, et al. "Corrosion Protection of 304 Stainless Steel with Melting Gels Coatings," (2015).

128. M. Aparicio, A. Jitianu, G. Rodriguez, et al. "Thickness-properties synergy in organic–inorganic consolidated melting-gel coatings for protection of 304 stainless steel in NaCl solutions," Surface and Coatings Technology, 315, 426-35 (2017).

129. L. Klein, A. Degnah, K. Al-Marzoki, et al. "Electrochemical Properties of Melting Gel Coatings," Advances in Materials Science for Environmental and Energy Technologies V: Ceramic Transactions, 260, 235 (2016).

130. A. Jitianu, S. Cadars, F. Zhang, et al. "29 Si NMR and SAXS investigation of the hybrid organic–inorganic glasses obtained by consolidation of the melting gels," Dalton Transactions, 46, 3729-41 (2017).

131. W.G. Klemperer, V.V. Mainz and D.M. Millar. "A Solid State Multinuclear Magnetic Resonance Study of the Sol-Gel Process using Polysilicate Precursors," MRS Proceedings, 73, (1986).

132. G. Webb, H. Kurosu and T. Yamanobe. "Synthetic macromolecules," pp. 415-70 in Nuclear Magnetic Resonance. The Royal Society of Chemistry, 2005.

133. A. Hunsche, U. Gorl, A. Muller, M. Knaack and T. Gobel. "Investigations concerning the reaction silica/organosilane and organosilane/polymer-Part 1: Reaction mechanism and reaction model for silica/organosilane," Kautschuk Gummi Kunststoffe, 50, 881-889 (1997).

134. H. Yasunaga, M. Kobayashi, S. Matsukawa, H. Kurosu and I. Ando. "Structures and dynamics of polymer gel systems viewed using NMR spectroscopy," Annual Reports on NMR Spectroscopy, 34, 39-104 (1997).

135. G. Höhne, W.F. Hemminger and H. Flammersheim. Differential scanning calorimetry; Springer Science & Business Media, 2013.

136. D. Lin-Vien, N.B. Colthup, W.G. Fateley and J.G. Grasselli. The handbook of infrared and Raman characteristic frequencies of organic molecules; Elsevier, 1991.

137. A.D. Chomel, P. Dempsey, J. Latournerie, D. Hourlier-Bahloul and U.A. Jayasooriya. "Gel to glass transformation of methyltriethoxysilane: A silicon oxycarbide glass precursor investigated using vibrational spectroscopy," Chemistry of materials, 17, 4468-73 (2005).

138. G. Das, P. Bettotti, L. Ferraioli, et al. "Study of the pyrolysis process of an hybrid CH 3 SiO 1.5 gel into a SiCO glass," Vibrational Spectroscopy, 45, 61-8 (2007).

139. A.V. Rao, R.R. Kalesh and G. Pajonk. "Hydrophobicity and physical properties of TEOS based silica aerogels using phenyltriethoxysilane as a synthesis component," J. Mater. Sci., 38, 4407-13 (2003).

140. X. Ren, R. Qiu and K. Li. "Modifications of kenaf fibers with N- methylol acrylamide for production of kenaf- unsaturated polyester composites," J Appl Polym Sci, 125, 2846-53 (2012).

141. R. Qiu, X. Ren and K. Li. "Effect of fiber modification with a novel compatibilizer on the mechanical properties and water absorption of hemp- fiber- reinforced unsaturated polyester composites," Polymer Engineering & Science, 52, 1342-7 (2012).

142. D.L. Ou and A.B. Seddon. "Near-and mid-infrared spectroscopy of sol–gel derived ormosils: vinyl and phenyl silicates," J. Non Cryst. Solids, 210, 187-203 (1997).

143. J. Coates, "Interpretation of infrared spectra, a practical approach," Encyclopedia of analytical chemistry, (2000).

144. A. Tunlert, P. Prasassarakich and S. Poompradub. "Effect of modified silica particles with phenyltriethoxysilane on mechanical and thermal properties of natural rubber composites," 354, 62-8 (2015).

145. M.D. Halls, C.P. Tripp and H.B. Schlegel. "Structure and infrared (IR) assignments for the OLED material: N, N′-diphenyl-N, N′-bis (1-naphthyl)-1, 1′-biphenyl-4, 4 ″-diamine (NPB)," Physical Chemistry Chemical Physics, 3, 2131-6 (2001).

146. A.V. Rao, R.R. Kalesh and G. Pajonk. "Hydrophobicity and physical properties of TEOS based silica aerogels using phenyltriethoxysilane as a synthesis component," J. Mater. Sci., 38, 4407-13 (2003).

147. C. Capozzi, L. Pye and R. Condrate. "Vibrational spectral/structural changes from the hydrolysis/polycondensation of methyl-modified silicates. I. Comparisons for single monomer condensates," Mater Lett, 15, 130-6 (1992).

148. K. Nakamoto," Infrared and Raman Spectra of Inorganic and Coordination Compounds" Part B, Applications in coordination, organometallic and bioinorganic chemistry, John Wiley & sons Inc., Hoboken, 2009, p283.

149. A. Bertoluzza, C. Fagnano, M.A. Morelli, V. Gottardi and M. Guglielmi. "Raman and infrared spectra on silica gel evolving toward glass," J. Non Cryst. Solids, 48, 117-28 (1982).

150. N. Colthup, "LH-Daly and SE Wiberley," Introduction to Infrared and Raman spectroscopy, (1964).

151. R. Al-Oweini and H. El-Rassy. "Synthesis and characterization by FTIR spectroscopy of silica aerogels prepared using several Si (OR) 4 and R″ Si (OR′) 3 precursors," J. Mol. Struct., 919, 140-5 (2009).

152. C. Tsai, H. Lin, H. Tsai, J. Hwang, S. Chang and Y. Chen-Yang. "Characterization and PEMFC application of a mesoporous sulfonated silica prepared from two precursors, tetraethoxysilane and phenyltriethoxysilane," Int J Hydrogen Energy, 36, 9831-41 (2011).

153. F. Rubio, J. Rubio and J. Oteo. "A DSC study of the drying process of TEOS derived wet silica gels," Thermochimica acta, 307, 51-6 (1997).

154. N.D. Hegde and A.V. Rao. "Organic modification of TEOS based silica aerogels using hexadecyltrimethoxysilane as a hydrophobic reagent," Appl. Surf. Sci., 253, 1566-72 (2006).

155. P. Innocenzi, "Infrared spectroscopy of sol–gel derived silica-based films: a spectra-microstructure overview," J. Non Cryst. Solids, 316, 309-19 (2003).

156. R.S. McDonald, "Surface functionality of amorphous silica by infrared spectroscopy," J. Phys. Chem., **62,** 1168-78 (1958).

157. A. Zecchina, S. Bordiga, G. Spoto, et al. "Silicalite characterization. 2. IR spectroscopy of the interaction of carbon monoxide with internal and external hydroxyl groups," J. Phys. Chem., **96,** 4991-7 (1992).

158. A. Fidalgo, T.G. Nunes and L.M. Ilharco. "The structure of hybrid gels by drift and NMR spectroscopies," J. Sol Gel Sci. Technol., **19,** 403-7 (2000).

159. L.L. Hench, Sol-gel silica: properties, processing and technology transfer; William Andrew, 1998.

160. C. Mutter, T. Bernards, M. Peeters, J. Lammers and M. Böhmer. "The effect of the solvent on the cross-link density of SiO 2 coatings," Thin Solid Films, 351, 95-8 (1999).

161. D. Marshall, B. Lawn and A. Evans. "Elastic/plastic indentation damage in ceramics: the lateral crack system," J Am Ceram Soc, 65, 561-6 (1982).

162. P. Innocenzi, "From the Precursor to a Sol," pp. 7-25 in The Sol to Gel Transition. Springer, 2016.

163. C. Alié, R. Pirard and J. Pirard. "Preparation of low-density xerogels from mixtures of TEOS with substituted alkoxysilanes. II. Viscosity study of the sol–gel transition," J. Non Cryst. Solids, 320, 31-9 (2003).

164. K. Nakanishi, "Pore structure control of silica gels based on phase separation," Journal of Porous Materials, 4, 67-112 (1997).

165. M. Nabavi, S. Doeuff, C. Sanchez and J. Livage. "Chemical modification of metal alkoxides by solvents: A way to control sol-gel chemistry," J. Non Cryst. Solids, 121, 31-4 (1990).

166. D. Niznansky and J. Rehspringer. "Infrared study of SiO2 sol to gel evolution and gel aging," J. Non Cryst. Solids, 180, 191-6 (1995).

167. P.A. Tick, "Water durable glasses with ultra-low melting temperatures," Physics and Chemistry of glasses, 25, 149-54 (1984).

168. R. Figueira, C.J. Silva and E. Pereira. "Organic–inorganic hybrid sol–gel coatings for metal corrosion protection: a review of recent progress," Journal of Coatings Technology and Research, 12, 1-35 (2015).